

AD-A061 450

EXXON RESEARCH AND ENGINEERING CO LINDEN N J
STATIC ELECTRICITY HAZARDS IN AIRCRAFT FUEL SYSTEMS.(U)
AUG 78 W G DUKEK, J M FERRARO, W F TAYLOR

F/G 21/4

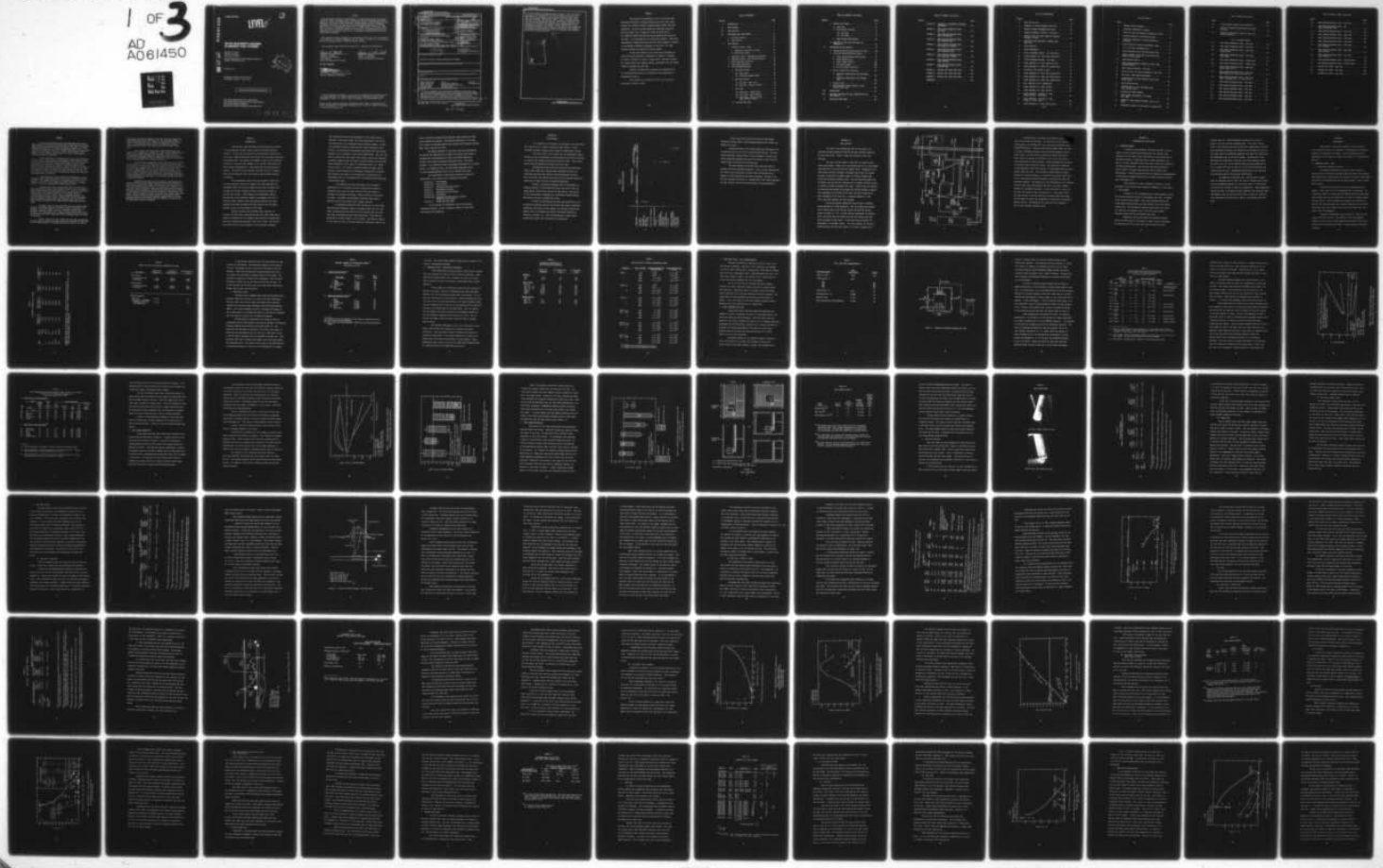
F33615-77-C-2046

EXXON/GRUS.1PEB.78 AFAPL-TR-78-56

NL

UNCLASSIFIED

1 OF 3
AD
A061450



AD A0 61450

AFAPL-TR-78-56

Q
B.S.

LEVEL II

STATIC ELECTRICITY HAZARDS IN AIRCRAFT FUEL SYSTEMS

WILLIAM G. DUKEK

JOHN M. FERRARO

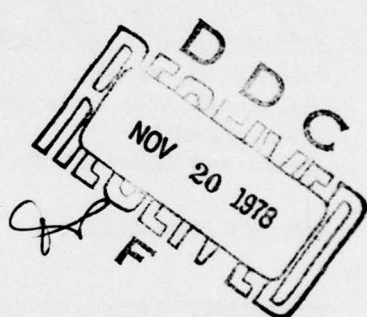
WILLIAM F. TAYLOR

EXXON RESEARCH AND ENGINEERING COMPANY

LINDEN, NEW JERSEY 07036

FILE COPY:
DDC

AUGUST 1978



TECHNICAL REPORT AFAPL-TR-78-56

Final Report: April 1977 — April 1978

Approved for public release; distribution unlimited.

AIR FORCE AERO PROPULSION LABORATORY
AIR FORCE WRIGHT AERONAUTICAL LABORATORIES
AIR FORCE SYSTEMS COMMAND
WRIGHT-PATTERSON AIR FORCE BASE, OHIO 45433

78 11 17 041

NOTICE

When Government drawings, specifications, or other data are used for any purpose other than in connection with a definitely related Government procurement operation, the United States Government thereby incurs no responsibility nor any obligation whatsoever; and the fact that the government may have formulated, furnished, or in any way supplied the said drawings, specifications, or other data, is not to be regarded by implication or otherwise as in any manner licensing the holder or any other person or corporation, or conveying any rights or permission to manufacture, use, or sell any patented invention that may in any way be related thereto.

This report has been reviewed by the Information Office (OI) and is releasable to the National Technical Information Service (NTIS). At NTIS, it will be available to the general public, including foreign nations.

This technical report has been reviewed and is approved for publication.

Charles R. Martel

CHARLES R. MARTEL
Technical Area Manager
Fuels Branch
Fuels and Lubrication Division

Arthur V. Churchill

ARTHUR V. CHURCHILL
Chief, Fuels Branch
Fuels and Lubrication Division

FOR THE COMMANDER

Blackwell C. Dunnam

BLACKWELL C. DUNNAM
Chief, Fuels and Lubrication Division
AF Aero Propulsion Laboratory

"If your address has changed, if you wish to be removed from our mailing list, or if the addressee is no longer employed by your organization please notify AFAPL/SFF, W-PAFB, OH 45433 to help us maintain a current mailing list".

Copies of this report should not be returned unless return is required by security considerations, contractual obligations, or notice on a specific document.

UNCLASSIFIED

SECURITY CLASSIFICATION OF THIS PAGE (When Data Entered)

(19) REPORT DOCUMENTATION PAGE		READ INSTRUCTIONS BEFORE COMPLETING FORM												
1. REPORT NUMBER AFAPL-TR-78-56	2. GOVT ACCESSION NO.	3. RECIPIENT'S CATALOG NUMBER EXXON/GRUS.1PEB.78												
4. TITLE (and Subtitle) STATIC ELECTRICITY HAZARDS IN AIRCRAFT FUEL SYSTEMS	5. TYPE OF REPORT & PERIOD COVERED Final Report. 27 April 1977 - April 1978													
6. AUTHOR(s) William G. Dukek John M. Ferraro William F. Taylor	7. CONTRACT OR GRANT NUMBER(s) F33615-77-C-2046	8. CONTRACT OR GRANT NUMBER(s) NW												
9. PERFORMING ORGANIZATION NAME AND ADDRESS Exxon Research and Engineering Company ✓ P.O. Box 8 Linden, New Jersey 07036	10. PROGRAM ELEMENT, PROJECT, TASK AREA & WORK UNIT NUMBERS Program Element 62203F 3048-05-86 1245													
11. CONTROLLING OFFICE NAME AND ADDRESS Air Force Aero Propulsion Laboratory (SFF) Air Force Systems Command Wright-Patterson Air Force Base, Ohio 45433	12. REPORT DATE August 1978													
13. MONITORING AGENCY NAME & ADDRESS (if different from Controlling Office) (12) 2046p. 7P	14. NUMBER OF PAGES 206													
15. SECURITY CLASS. (of this report) Unclassified														
16. DECLASSIFICATION/DOWNGRADING SCHEDULE														
17. DISTRIBUTION STATEMENT (of this Report) Approved for public release; distribution unlimited.														
18. SUPPLEMENTARY NOTES This program was initiated with FY77 Aero Propulsion Laboratory Director's Funds.														
19. KEY WORDS (Continue on reverse side if necessary and identify by block number) <table style="width: 100%; border-collapse: collapse;"> <tr> <td style="width: 33%;">Static Electricity</td> <td style="width: 33%;">Jet A</td> <td style="width: 33%;">Jet Fuel</td> </tr> <tr> <td>Charge Generation</td> <td>Conductivity Improver</td> <td>Fuel Additives</td> </tr> <tr> <td>Spark Discharge</td> <td>Reticulated (Open-Pore) Foam</td> <td></td> </tr> <tr> <td>Polyester Foam</td> <td>Polyether Foam</td> <td></td> </tr> </table>			Static Electricity	Jet A	Jet Fuel	Charge Generation	Conductivity Improver	Fuel Additives	Spark Discharge	Reticulated (Open-Pore) Foam		Polyester Foam	Polyether Foam	
Static Electricity	Jet A	Jet Fuel												
Charge Generation	Conductivity Improver	Fuel Additives												
Spark Discharge	Reticulated (Open-Pore) Foam													
Polyester Foam	Polyether Foam													
20. ABSTRACT (Continue on reverse side if necessary and identify by block number) <p>→ Static discharges that occurred during fueling in small-scale test rigs which simulated aircraft fuel tanks containing open-pore polyurethane foam were used to develop design criteria with respect to foam type, inlet configuration, and JP-4 conductivity. Blue polyether foam is more electrostatically active than red polyester foam; sparks can be eliminated only with a multiple orifice inlet and a minimum fuel conductivity level → over</p>														

DD FORM 1 JAN 73 EDITION OF 1 NOV 65 IS OBSOLETE

UNCLASSIFIED

SECURITY CLASSIFICATION OF THIS PAGE (When Data Entered)

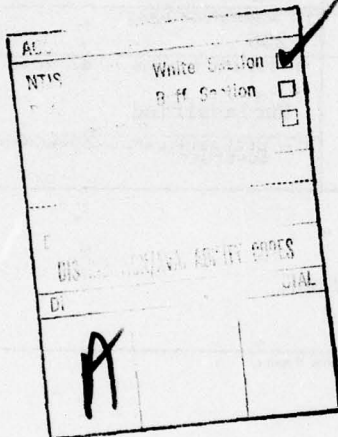
409 841

28 11 17 04 143

UNCLASSIFIED

SECURITY CLASSIFICATION OF THIS PAGE(When Data Entered)

of 50 pS/m, achieved by adding anti-static additive. With red polyester foam, either the multiple orifice inlet or minimum conductivity fuel suppresses static discharges. Spark energies from blue foam or from high velocity single orifice inlets appear to be 10-100 times greater than from red foam or from multiple orifice inlets. Variables such as flow rate, inlet type and exit velocity, metal charge collectors, fuel conductivity, foam dielectric properties, and other non-metallic fuel components were studied. For example, a rubber bladder cell is not significantly different from an empty tank in terms of static discharges. An aluminum mesh substitute for open-pore foam proved to be effective in minimizing static buildup but produced unacceptable metal fragments which acted as charge collectors.



UNCLASSIFIED

SECURITY CLASSIFICATION OF THIS PAGE(When Data Entered)

PREFACE

This project was sponsored by the U.S. Air Force Aero Propulsion Laboratory at Wright-Patterson Air Force Base, under Contract No. F33615-77-C-2046, Program Element 62203F, Work Unit 3048-05-86. The work reported herein was performed during the period 27 April 77 to 27 April 78, under the direction of Mr. Charles R. Martel who was the Project Engineer who monitored the work. For his guidance we are especially grateful. Many other individuals at Wright Field and other Air Force commands contributed to the numerous technical discussions of the work. For their valuable dialogue we express our special thanks.

We are also indebted to our other Exxon colleagues for their advice and assistance, especially Dr. Kenneth C. Bachman, Dr. Eric O. Forster, Mr. Dale A. Young, and Mr. William M. Bustin. Mr. William Davis also deserves special appreciation for his strong support in running the test rig.

Finally, we would like to express our appreciation to Ms. Corinne Barron and Ms. M. B. Hayes for their assistance in preparing the report.

This program was initiated with FY77 Aero Propulsion Laboratory Director's Funds.

TABLE OF CONTENTS

SECTION	PAGE
I INTRODUCTION	1
II TEST PROGRAM	4
III TEST FACILITY	7
IV LITERATURE AND FIELD SURVEY	10
1. Literature Survey	10
2. Field Survey.	10
V TEST RESULTS.	12
1. Laboratory Tests - Foam	12
a. Dielectric Properties of Foam	12
b. Mini-Static Tests	15
2. Laboratory Tests - Non-Metallic Materials	17
3. Laboratory Tests - Fuel Characteristics	20
4. Spark Discharge Test Unit	20
5. Foam Charge Generation.	28
6. Drum Charging/Sparking.	32
a. Base Case Studies	36
(1) Empty Drum	39
(2) Drum with Bladder Liner.	40
b. Red Foam Studies.	41
(1) Red Foam - Base Fuel	41
(2) Red Foam - Effect of ASA-3	48
c. Blue Foam	53
(1) Blue Foam - "Clean" Fuel	53
(2) Blue Foam - ASA-3 Effects.	61
(3) Blue Foam - Piccolo Versus High Velocity Inlets	66
d. Aluminum Mesh Foam.	71

TABLE OF CONTENTS (Continued)

SECTION		PAGE
7.	Bladder Cell Tests	73
a.	Base Case	75
b.	Piccolo-ASA-3 Studies	77
(1)	Red Foam	77
(2)	Blue Foam.	78
c.	Spark Energy Measurements	80
8.	Response of Test Fuel With ASA-3 to Temperature	85
VI	DISCUSSION OF TEST RESULTS	88
1.	Charge Generation and Retention of Foams.	88
2.	Localized Charge/Discharge Factors.	91
a.	Inlet Velocity/Charge Distribution.	91
b.	Input Charge Level.	97
c.	Input Charge Polarity	100
d.	Pro-Static Agents	100
e.	Role of Charge Collectors	102
3.	Role of Conductivity Improver	104
a.	Threshold Conductivity with Uncharged Fuel.	105
b.	Threshold Conductivity with Charged Fuel.	106
4.	Metallic Foam	108
5.	Relationship of Spark Energy to Input Charge Within Foam.	109
VII	CONCLUSIONS	111
VIII	SUGGESTED CRITERIA FOR FUEL SYSTEM DESIGN AND FUEL QUALITY.	114
IX	ADDITIONAL WORK NEEDS	118

TABLE OF CONTENTS (Continued)

SECTION		PAGE
APPENDIX A	ABSTRACTS OF PERTINENT LITERATURE REFERENCES	121
APPENDIX B	FOAM CHARGE GENERATING TESTS RAW DATA.	125
APPENDIX C	DRUM CHARGING/SPARKING TESTS BASE CASE STUDIES	133
APPENDIX D	DRUM CHARGING/SPARKING TESTS RED FOAM-BASE FUEL.	139
APPENDIX E	DRUM CHARGING/SPARKING TESTS RED FOAM-ASA-3 EFFECTS.	147
APPENDIX F	DRUM CHARGING/SPARKING TESTS BLUE FOAM-BASE FUEL	155
APPENDIX G	DRUM CHARGING/SPARKING TESTS BLUE FOAM-ASA-3 EFFECTS	163
APPENDIX H	DRUM CHARGING/SPARKING TESTS INLET STUDIES	169
APPENDIX I	DRUM CHARGING/SPARKING TESTS ALUMINUM MESH	177
APPENDIX J	BLADDER CELL TESTS BASE CASE.	181
APPENDIX K	BLADDER CELL TESTS RED FOAM	183
APPENDIX L	BLADDER CELL TESTS BLUE FOAM.	187
REFERENCES	192

LIST OF ILLUSTRATIONS

FIGURE		PAGE
1	DRUM FILLING RIG.	8
2	SCHEMATIC OF SPARK DISCHARGE TEST UNIT.	22
3	ENERGY IN SPARK DISCHARGES FROM FOAM.	26
4	CHARGING TENDENCY OF FOAM VS. FLOW RATE	30
5	EFFECT OF GAS AND INPUT CHARGE ON CHARGING TENDENCY OF FOAM.	31
6	SURFACE VOLTAGE PRODUCED BY CHARGED FUEL THRU FOAM	33
7	INLET LOCATION.	34
8	INLET PHOTOGRAPHS	37
9	TYPICAL RECORDER TRACING - RED FOAM TESTS	44
10	SPARK FREQUENCY VS. INPUT FUEL CONDUCTIVITY	52
11	TYPICAL RECORDER TRACING - BLUE FOAM.	57
12	SPARK FREQUENCY VS. INPUT CHARGE ON FUEL.	62
13	SPARK FREQUENCY VS. INPUT FUEL CONDUCTIVITY	63
14	RESPONSE OF TEST FUELS TO ASA-3	65
15	SPARK FREQUENCY VS. INPUT FUEL CONDUCTIVITY	69
16	SPARK FREQUENCY VS. INPUT FUEL CONDUCTIVITY	79
17	SPARK FREQUENCY VS. INPUT FUEL CONDUCTIVITY	81
18	FUEL CONDUCTIVITY VS. TEMPERATURE	86
19	SPARK FREQUENCY VS. INLET VELOCITY.	92
20	SPARK FREQUENCY VS. INLET VELOCITY.	94
21	SPARK FREQUENCY: BLADDER VS. DRUM SINGLE ORIFICE - BLUE FOAM.	96
22	SPARK FREQUENCY: BLADDER VS. DRUM PICCOLO 2 - BLUE FOAM	98
23	SPARK FREQUENCY VS. INPUT CHARGE LEVEL.	99

LIST OF TABLES

TABLE	PAGE
1 PROGRAM TESTING SEQUENCE.	5
2 DIELECTRIC PROPERTIES OF FOAMS.	13
3 EFFECT OF FUEL ON DIELECTRIC PROPERTIES OF FOAM . . .	14
4 CHARGING TENDENCY OF RETICULATED FOAMS.	16
5 DIELECTRIC PROPERTIES OF TANK NON-METALLIC MATERIALS	18
6 RESISTIVITIES OF VARIOUS IMPREGNATED LINERS	19
7 JET A TEST FUEL CHARACTERISTICS	21
8 SPARK DISCHARGE TESTS WITH RETICULATED FOAM	24
9 SPARK DISCHARGE TESTS WITH RETICULATED FOAM - EFFECT OF FOAM VOLUME	27
10 INLET DESIGN DETAILS.	35
11 DRUM CHARGING/SPARKING SUMMARY OF EMPTY DRUM/BLADDER TESTING	38
12 DRUM CHARGING/SPARKING - RED FOAM	42
13 EFFECT OF ASA-3 ON SPARK DISCHARGES IN RED FOAM . . .	50
14 BLUE FOAM - DRUM CHARGING/SPARKING.	55
15 LABORATORY DATA ON FUEL EXPOSED TO BLUE FOAM IN RIG TESTS.	58
16 INLET DESIGN DETAILS.	67
17 ALUMINUM MESH VS. BLUE FOAM DRUM TESTS (CLAY TREATED FUEL)	74
18 BLADDER CELL TESTS SUMMARY.	76
19 SPARK ENERGY MEASUREMENTS IN BLADDER CELL TESTS.	83
20 SUMMARY OF FOAM CHARGING TENDENCY LAB VS. RIG TESTS	90
21 GEOMETRICAL FACTORS IN TEST DRUM VS. BLADDER CELL . .	95

LIST OF TABLES (Continued)

TABLE		PAGE
22	FILTER SUMMARY ELEMENT SET UTILIZATION.	101
23	EFFECT OF CORROSION INHIBITOR/AIA ON SPARK FREQUENCY	103
24	THRESHOLD CONDUCTIVITY VALUES OF FUEL FOR SPARK ELIMINATION	107

LIST OF APPENDIX TABLES

B.1	FOAM CHARGE GENERATING TESTS - RED FOAM	126
B.2	FOAM CHARGE GENERATING TESTS - RED FOAM	127
B.3	FOAM CHARGE GENERATING TESTS - BLUE FOAM (COARSE PORE)	128
B.4	FOAM CHARGE GENERATING TESTS - BLUE FOAM (FINE PORE)	129
B.5	FOAM CHARGE GENERATING TESTS - YELLOW FOAM.	130
B.6	FOAM CHARGE GENERATING TESTS - ORANGE FOAM.	131
C.1	DRUM CHARGING/SPARKING TESTS - BASE CASE (EMPTY DRUM) JET A.	134
C.2	DRUM CHARGING/SPARKING TESTS - BASE CASE (EMPTY DRUM) JET A WITH ~4 PPM GA 178	135
C.3	DRUM CHARGING/SPARKING TESTS - BASE CASE (DRUM + BLADDER) JET A + 4 PPM GA 178	137
D.1	DRUM CHARGING/SPARKING TESTS - RED FOAM	140
D.2	DRUM CHARGING/SPARKING TESTS - RED FOAM	142
D.3	DRUM CHARGING/SPARKING TESTS - RED FOAM	143
D.4	DRUM CHARGING/SPARKING TESTS - RED FOAM	145
E.1	DRUM CHARGING/SPARKING TESTS - RED FOAM	148
E.2	DRUM CHARGING/SPARKING TESTS - RED FOAM	150

LIST OF APPENDIX TABLES (Continued)

TABLE		PAGE
E.3	DRUM CHARGING/SPARKING TESTS - RED FOAM	152
E.4	DRUM CHARGING/SPARKING TESTS - RED (WATER SATURATED) FOAM	154
F.1	DRUM CHARGING/SPARKING TESTS - BLUE FOAM	156
F.2	DRUM CHARGING/SPARKING TESTS - BLUE FOAM	158
F.3	DRUM CHARGING/SPARKING TESTS - BLUE FOAM	159
F.4	DRUM CHARGING/SPARKING TESTS - BLUE FOAM	161
G.1	DRUM CHARGING/SPARKING TESTS - BLUE FOAM - ASA-3 EFFECTS.	164
H.1	DRUM CHARGING/SPARKING TESTS - BLUE FOAM INLET STUDIES.	170
H.2	DRUM CHARGING/SPARKING TESTS - BLUE FOAM INLET STUDIES.	176
I.1	DRUM CHARGING/SPARKING TESTS - ALUMINUM MESH	178
I.2	DRUM CHARGING/SPARKING TESTS - ALUMINUM MESH	179
J.1	BLADDER CELL TESTS - BASE CASE	182
K.1	BLADDER CELL TESTS - RED FOAM.	184
L.1	BLADDER CELL TESTS - BLUE FOAM	188

SUMMARY

Static electrification and spark discharges which occur when fueling aircraft tanks containing reticulated plastic foam have been studied in two small-scale test tanks, a 208 liter (55 gallon) bladder-lined drum and a 341 liter (90 gallon) bladder cell. The dielectric properties and static charging tendencies of several foams were also investigated. The role of anti-static additive (ASA-3) added to fuel to improve conductivity as a means of eliminating spark discharges was assessed.

Inlet conditions for delivery of fuel into the foam filled tank in terms of fluid velocity and number of exit orifices proved to be crucial for minimizing spark discharges. When delivering fuel at maximum flow rates into foam through a single orifice, spark discharges were observed on a radio, by current measurements, as well as visually and photographically, under a variety of conditions. The number and energy of sparks was a function of the type of foam, the quantity of foam, the amount of charge carried by incoming fuel, the velocity of the fluid, the distribution of fluid into foam, and the conductivity of the fuel.

Spark frequency could be reduced or eliminated by using a multiple orifice type inlet (called a piccolo) to deliver fuel into the foam. The maximum velocity of fuel exiting each orifice also proved to be critical for eliminating spark discharges; a maximum value of 3 m/s is recommended for sizing each orifice.

Polyether type (blue) polyurethane foam is 10-100 times more active than polyester type (orange, yellow or red) polyurethane foam (charge generation, spark density, etc.). Even with a multiple orifice inlet the polyether foam will cause sparks unless the conductivity of the fuel is increased to a minimum value of 50 picosiemens per meter (pS/m). Spark energy measurements show that the multiple orifice inlet is helpful even in blue foam where with the multiple orifice inlet spark energies were only 2-5% as high as those resulting from a single orifice (high velocity) type inlet.

Polyester foam, on the other hand, does not produce sparks if fuel is introduced through a multiple orifice inlet below 3 m/s velocity. For this reason, it is not necessary to establish a minimum conductivity level in fuel if a multiple orifice inlet is provided. For continued use of a single orifice high velocity inlet, on the other hand, fuel conductivity with a minimum value of 50 pS/m is necessary.

Design criteria for fuel systems and fuel quality suggested by these tests in small-scale rigs include the avoidance of blue foam and the establishment of a minimum conductivity level of 50 pS/m in

JP-4 fuel by the use of additive. The test data also support the modification of aircraft tank inlets to use a multiple orifice type to distribute fuel into a tank at a maximum exit velocity of 3 m/s. If the multiple orifice inlet is installed, the more electrostatically active blue foam can be used in place of red foam.

Test results with the bladder liner indicate that the presence of a non-metallic bladder in a tank does not significantly affect static charge generation or discharge. Tests with an aluminum mesh type replacement for reticulated foam show that it is effective in minimizing static buildup but produces unacceptable metal fragments which act as charge collectors.

The conclusions supporting these design criteria are based on data specific to the test materials and facilities used during this project. In some cases, data were limited in scope or incomplete for particular configurations. As with most static electricity studies, a high degree of data scatter sometimes occurred. This is to be expected when the end result sought is the frequency and energy content of static spark discharges. Although the test rigs sought realistically to simulate actual aircraft fueling operations, a direct extension of these data to a full-scale aircraft tank must be done with caution.

Considerable progress has been made in understanding the complex problem of static charge generation and spark discharge in foam-filled aircraft fuel tanks. We feel that the results of this study will expand the state-of-the-art in this area. However, it is clear from our work (and the work of others) that certain technical questions remain unanswered. Additional experimental work is needed to adequately fill the technical gaps remaining. Specifically, the areas of spark incendivity, scale up effects, inlet type, fuel system design, and fuel quality criteria should be investigated further. The work effort on this project strongly suggests that the static problems associated with these areas are amenable to solution, and that additional study is warranted.

SECTION I
INTRODUCTION

Electrostatic spark discharges during fueling are believed to be responsible for eight recent incidents involving military aircraft. In each case the aircraft was being fueled, usually with JP-4, into a bladder-lined fuel tank packed with reticulated (open-pore) polyurethane foam. The ignition of flammable vapors by the discharge resulted in relatively minor damage to the aircraft tank because the foam prevented propagation of a detonation wave and rapid pressure buildup. The foam is used in military aircraft in fact to suppress fires and overpressures that could develop from incendiary bullets or shrapnel.

The circumstances under which each incident occurred led to strong suspicion that static charges were being generated and discharged within the foam and caused the Air Force to support both in-house and contract research on static electricity hazards in aircraft fuel systems. Exxon Research and Engineering Company participated in this research program to investigate the role of different foams, bladder cells, and fueling conditions in static generation and spark discharge utilizing special test facilities modified to meet the requirements of the study.

Previous research that followed static ignitions in aircraft and tank trucks identified factors that create high static charges in flowing fuel, for example, high velocities through filter media and splashing and spraying of fuel into a tank. Both factors were involved in previous accidents to fuel systems containing

only liquid fuel and are also applicable to the current group of incidents. With filter media, the volume downstream of the filter case was found to be an important charge relaxation regime. Without this relaxation volume the potential for static discharge is much greater. The reticulated polyurethane foam-filled fuel tank problem appears to be an extension of the filter observations. With the foam, which in effect acts like coarse filter media, there is no downstream relaxation regime because the foam is contained within the fuel tank. Charge separation occurs right at the delivery point (i.e. inside the fuel tank). As a result, localized pockets of charge tend to build up and the potential for discharge is dramatically increased. Exxon Research has drawn on this background of theoretical and experimental work to investigate static electrification and discharge in foam-filled tanks.

The mechanism of static discharge is not thoroughly understood but it is probable that for enough static charges to concentrate and create the high localized field that leads to breakdown and energetic discharge a charge collector of some kind is needed. The polymer (polyurethane) open-pore foams used in military aircraft may provide such a charge collector.

Considerable research has been carried out to study static electrification phenomena related to pumping liquid fuels into open tanks, including aircraft tanks but very little work has been done with tanks containing open-pore reticulated foam. This study was undertaken to provide insight on this problem. The foams of concern to this study are made of polymers similar to dielectrics such as are

used in electrical insulation and represent large surfaces on which static charges can separate. The military application of the foam is to reduce the explosion hazard from shrapnel and incendiary bullets which could strike the aircraft.

The general approach on the project has been experimental. The project was organized into a series of discrete tasks aimed at systematically investigating the static electricity hazards in aircraft fuel systems containing reticulated foams. The tasks included: (a) Literature Survey and Equipment Modification, (b) Field Survey, (c) Laboratory Tests, (d) Foam Charge Generation Tests, (e) Drum Charging/Sparking Tests, and (f) Bladder Cell Tests.

The organization of this report basically follows the organization of the project and is presented as follows:

- Section II Test Program
- Section III Test Facility
- Section IV Literature and Field Survey
- Section V Experimental Results
- Section VI Discussion of Test Results
- Section VII Conclusions
- Section VIII Suggested Criteria for Fuel System Design and Fuel Quality
- Section IX Additional Work Needs

In the interest of readability, much of the general background material, as well as specific details of data, have been placed into appendices.

SECTION II

TEST PROGRAM

To accomplish the objectives of the project, the work effort was organized into a series of discrete tasks (Table 1), which included preliminary support work followed by experimental testing.

The basic thrust of the project was an experimental investigation into the various modes of charge generation and spark discharge in aircraft fuel systems containing reticulated foams. This investigation included laboratory and small scale test work.

The laboratory work involved testing with the Exxon Mini-Static Tester (MST) and a special Spark Discharge Test Unit for evaluating the nature and energy of spark discharges from foam. Other electrical test devices were also used for measuring dielectric properties of foams and other non-metallic materials.

The MST, a laboratory apparatus used for evaluating the charging tendency of filter media and fuels, was used to test the foams against various fuels used in our Rig testing. One purpose of this testing was to determine if a correlation existed between MST results and Drum or Bladder Cell tests.

In order to characterize the electrical properties of the non-metallic materials used in the aircraft fuel system, laboratory measurements were made on foam samples, top coatings, sealants and bladder cells to determine both surface and volume resistivity, dielectric strength, etc. Fuel characterization, using routine specification tests, was also done in the laboratory.

TABLE 1
PROGRAM TESTING SEQUENCE

Task Work	Testing Facilities		Exxon Filling Rig	
	Lab	Spark Discharge Unit	Drum Testing	Bladder Cell Tests
Lab Tests				
Foam Prop.	X			
Non-Metal Mat.	X			
Fuel Char	X			
MST Testing	X			
Spark Disch. Testing		X		
Foam Charge Generation Testing			X	
Drum/Charging/ Sparking Testing			X	
● Base Case			X	
● Foam Type			X	
● Fuel Additives			X	
● Al Mesh			X	
Bladder Charging/ Sparking Testing				X
● Base Case				X
● Foam Type				X
● Additives				X

A small scale test facility was used for Foam Charge Generation Testing (FCGT), Drum Charging/Sparking Tests (DCST), and Bladder Cell Tests.

Charge generation on the foam surface was considered to be an important part of the static electrification problem. The Foam Charge Generation Testing (Table 1) was an attempt to isolate this charge generating mechanism and study the effects of fuel velocity, charge levels, two-phase flow and foam type.

The Drum Charging and Bladder Cell tests (see Table 1) simulated aircraft refueling operations. Here, we were investigating the effects and interactions of foams, fuels and fueling inlet designs on charge generation and static discharge. Details of the work are discussed in Section V. Section III of this report describes the test facility used for drum and bladder cell experimentation.

SECTION III

TEST FACILITY

The bulk of the experimental work on the project was conducted in Exxon Research's Drum Filling Rig, specially modified for the study needs. Figure 1 shows the schematic of the test facility.

The test fuel was stored in 208 liter (55 gallon) epoxy-lined supply drums. During tests the fueling pump (10 hp, centrifugal) delivered fuel to the Test Drum (or Bladder Cell). Depending on the tests being conducted (charged, uncharged, mixed flow) fuel passed through a filter-monitor (Bendix Gage) or through a bypass line. Valves and flowmeters regulated flow. The test drum was purged with N₂ between runs and was also equipped with a separate nitrogen system to conduct two phase (fuel/gas) flow tests. Liquid level was measured by observing back pressure as nitrogen was bubbled through a separate tube extending to the bottom of the tank; this device retained an inert atmosphere in the test rig. A complete bypass to a clay filter was also available for fuel cleanup.

During the initial testing the rig was used to evaluate charge generation in foam separately. The test system was equipped with a special add-on test section called the Foam Test Section (shown in Figure 1). The Foam Test Section represented an enlarged inlet line which could be packed with foam and through which fuel could be pumped at high rates. It was electrically isolated for measurement of streaming current. (In later testing, the foam was packed directly into the test vessel, i.e. drum or bladder cell.)

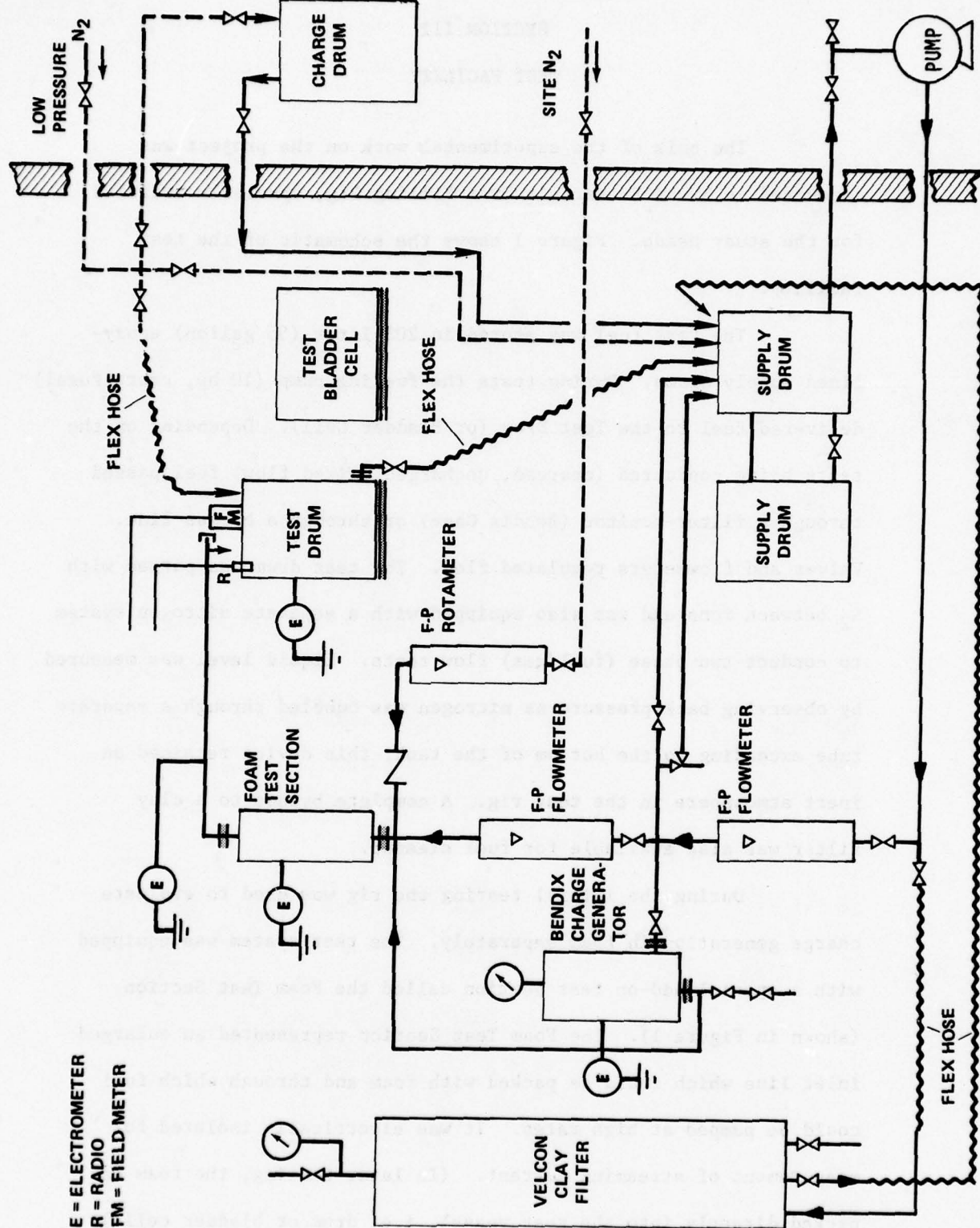


Figure 1. Drum Filling Rig

Instrumentation to measure charge density, static and field strength was provided. The test drum, filter-monitor (Bendix gage), and fueling inlet were electrically isolated using Teflon® connectors. Keithley Electrometers (Model 600B) were used to measure streaming currents from the isolated equipment (filter, inlet, drum). An electrostatic voltmeter (Comstock and Wescott Model 12009) was placed on a platform on top of the test drum to allow measurement of field strength. Spark discharges were detected by specially tuned transistor radios. The radios were calibrated at the beginning of each test sequence by discharging sparks of known energy inside the drum. They provided a rough measure of energy content of a static discharge. An external and internal radio were used to discriminate between discharges occurring in the drum and extraneous signals. The signals from the Electrometers, the voltmeter, and the radios were simultaneously fed into a six point recorder (SOLIEC) for permanent recording. At the completion of a test run, the fuel was allowed to flow by gravity back to the supply drums. The vapor spaces in the test drum and the supply drums were purged with nitrogen to prevent the possibility of explosion if incendiary sparks occurred. The piping in the system was 3.81 centimeter (1 1/2 inch) diameter stainless steel.

SECTION IV
LITERATURE AND FIELD SURVEY

1. LITERATURE SURVEY

A survey of the scientific literature was made to get an update on recent publications dealing with the technical areas pertinent to this study (static electricity in fuel systems and on insulating surfaces, charge generation, charge relaxation, etc.). Most of the work identified dealt with static electricity generation in flowing hydrocarbons. Less work has been done relating the static effects of polymer type materials which interact with hydrocarbons. The CRC Literature Survey on "Generation and Dissipation of Electrostatic Charge During Aircraft Fueling" provided important basic information.(1)

Brief abstracts of other references we found to be most pertinent to the current project appear as Appendix A to this report.

2. FIELD SURVEY

On April 27, 1977 representatives of Exxon Research visited the Fairchild Republic factory at Farmingdale, New York, to examine actual aircraft fuel systems. This visit provided valuable and useful familiarization with an actual aircraft (A-10) fuel system construction. The information obtained during this visit served as a basis for the design of one of the fuel inlet systems evaluated during the Drum and Bladder Cell tests.

Additional contacts were made with Fairchild Republic during the early part of the program to assist them in increasing the charging level of the test fuel used in their full-scale

aircraft tank rig. These discussions culminated in a visit to inspect their rig and make recommendations. The primary factors noted in the Fairchild rig were the high fuel temperatures ($\sim 35\text{--}38^\circ\text{C}$) and considerable residence time between the filter-separator and the test tank, which in combination suggested that high fuel conductivity was dissipating most of the filter charge. Confirmation of this hypothesis was found when a test with the filters bypassed showed that most if not all of the observed charge was being generated in the 7.2 meters (22 feet) of 3.81 cm (1 1/2") hose used between the flowmeter and the tank. Subsequent modifications to the Fairchild rig alleviated some of their earlier difficulties.

We suggested to Fairchild that a filter monitor (Bendix Gage) be installed close to their test tank to increase input charge. We also recommended addition of a pro-static agent to clay-treated fuel and use of cooling to lower fuel temperatures. These suggestions helped Fairchild to establish fueling conditions that generated spark discharges in both red and blue foams under a variety of conditions that complimented the work done at Exxon in our smaller sized test rigs.

SECTION V

TEST RESULTS

This section of the report describes the test results of the different tasks of the program. The discussion is presented primarily as observation of results. The interpretation of the significance of the results is taken up in Section VI, "Discussion of Results."

1. LABORATORY TESTS - FOAM

a. Dielectric Properties of Foam

As baseline information on the foam, and in order to characterize the electrical properties which may affect electrostatic charge generation, accumulation, and discharge, laboratory measurements were made of reticulated foam (new and used) samples. Table 2 shows these results.

The dielectric properties of all six samples are quite similar. There seems to be no outstanding good or bad sample. AC conductivity which is derived when determining dielectric loss index shows similar data for all foams except red which is slightly higher than the others. The AC breakdown data suggests that perhaps the smaller cell structure might have a slight advantage over the foams with larger hole size (compare the Fine pore and Coarse pore blue foams, under "AC Breakdown").

Laboratory measurements were also made on foams that had been wet with fuel (Jet A). The results of this investigation (Table 3) on the two blue foams showed that dielectric values were different from those reported (Table 2) using standard calibrating materials.

TABLE 2
DIELECTRIC PROPERTIES OF FOAMS

Type	Color	Dielectric*, Constant, E'	Dielectric*, Loss Index, E''	AC Cond.* PS/m	AC Breakdown** V/mil
I	Orange	3.574	.00453	2400	669
II	Yellow	3.932	.00437	2400	728
III	Red	3.158	.00155	8550	532
Fine	Blue	3.323	.00247	1360	641
Coarse	Blue	3.483	.00399	2200	369
Used	Orange	3.543	.00539	2910	778

*ASTM D150 using air and silicone oil. 1000 HZ across 0.5" plates at 25°C.

**ASTM D149 using two 1" diameter brass electrodes. Breakdown is defined as the voltage when current exceeded 5 milliamperes.

TABLE 3
EFFECT OF FUEL ON DIELECTRIC PROPERTIES OF FOAM

<u>Foam Type</u>	<u>Dielectric Constant, E'</u>	<u>Dielectric Loss Index, E''</u>	<u>AC Conductivity pS/m</u>
Blue (Fine)			
- Air/Silicone Oil	3.323	.00247	1360
- Air/Fuel*	3.468	.00503	4200
Blue (Coarse)			
- Air/Silicone Oil	3.483	.00399	2200
- Air/Fuel*	3.876	.00767	2800

***Fuel Properties:**

Base Fuel	2.138	3.3
Base Fuel + Corrosion Inhibitor and Anti-Icing Additives	2.140	3.7

In the initial laboratory work, air and silicone oil were used as the fluid media. The dielectric constant of the silicone oil was 2.736 whereas the Jet A fuel was 2.138 (both at 25°C and 1000 Hz). ASTM D-150 involving two liquids requires that one of the liquids has a dielectric constant similar to the sample. The silicone oil appeared to fulfill this requirement. The jet fuel's dielectric constant was too far from the value for the foam. It is also possible but not very likely that there was an interaction between the jet fuel and the polymer.

b. Mini-Static Tests

Laboratory scale charging tests using the Mini-Static Test procedure (MST) were carried out on each of the test foams using both Jet A base fuel and Jet A base containing DCI-4A corrosion inhibitor and ethylene glycol monomethyl ether anti-icing additive (EGME). The results presented in Table 4 represent the average of two or three runs on an uncompressed sample of foam 20 mm in diameter and 23 mm high in a special cell of similar dimensions.

The MST results on foams which are listed in order of increasing pores per inch rating do not show any pattern of increasing charging tendency with porosity as was found by NRL (2). The reason for the difference is probably to be found in the method of installing the foam samples into the test cell. NRL used a 12 mm x 12 mm foam sample compressed into the standard 13 mm MST cell. This technique would tend to produce much higher local velocities within the compressed pores. The linear velocity used in the Exxon MST test on uncompressed foams at a flow rate of 100 mL/minute is a uniform

TABLE 4

CHARGING TENDENCY OF RETICULATED FOAMS⁽¹⁾
(MST Tests at 25°C)

A. TESTS WITH BASE FUEL⁽²⁾

	Foam Type	Sample Wt. g	MST $\mu\text{C}/\text{m}^3$
	None	---	18
I	Orange	0.2860	18
	Coarse Blue	0.2254	30
II	Yellow	0.1950	22
	Red	0.1851	7
	Fine Blue	0.2320	26

B. TESTS WITH ADDITIVE FUEL⁽³⁾

	None	---	35
I	Orange	0.2645	27
	Coarse Blue	0.2575	66
II	Yellow	0.1914	36
	Red	0.1878	25
	Fine Blue	0.2420	36

(1) Samples were 20 mm Diameter X 23 mm high in similar-size cell.

(2) Jet A fuel with no additives.

(3) Jet A with corrosion inhibitor (DCI4A) and anti-icing additive (EGME).

0.53 cm/s. Blue foams charge slightly higher than the orange or red foams of corresponding porosity.

2. LABORATORY TESTS - NON-METALLIC MATERIALS

Other non-metallic materials found in USAF aircraft systems were also evaluated in terms of their electrical properties. These materials included bladder cells, sealants, and tank inner liners. Table 5 shows the results of laboratory measurements made on these materials.

Eleven samples of non-metallic materials were received for dielectric testing. Dielectric measurements were made using ASTM Method D 150, the two fluids technique used in foam tests. For the most part the results are fairly similar. Where differences do exist it is due in part to the uncertainties of the sample thickness under the test pressures, and in part due to the mismatch of the dielectric constant of the fluids used in the ASTM method. Note for example that the Bladder Cells show relatively low breakdown strength per mil (of thickness) compared with the tank inner liners. This is because the Bladder Cells are fairly thick but tend to compress under pressure.

Six different impregnated inner liners described by MIL-T-6396D or MIL-T-5578C were studied for dc surface and volume resistivity. The data shown in Table 6 indicate the existence of significant differences in the surface resistivity of some of the samples while the volume resistivities are quite similar. These measurements were carried out with an HP 4329A High Resistance Meter in conjunction with an HP 16008A Resistivity Cell.

TABLE 5
DIELECTRIC PROPERTIES OF
TANK NON-METALLIC MATERIALS

	<u>Dielectric Constant</u>	<u>AC Conductivity nS/m</u>	<u>AC Breakdown v/mil</u>
<u>Sealants</u>			
899	7.17	12	232
PR	9.94	38	340
<u>Inner liners</u>			
BTL 69	5.27	11	705
BTL 17.4 '76	6.75	19	489
BTL 17.4 '60	5.50	15	568
1105-3	10.84	39	477
1367-2	12.67	38	346
1389	12.31	46	431
<u>Bladder Cells</u>			
63A '76	4.2	27	171
63A '74	4.6	88	109
63B-1 '75	4.36	4	172

TABLE 6
RESISTIVITIES OF VARIOUS IMPREGNATED LINERS

<u>Sample #</u>	<u>Appl. Voltage</u>	<u>Surface Resistivity</u> ohm/unit area	<u>Volume Resistivity</u> ohm cm
1389 A	500	$>10^{15}$	6.1×10^{13}
	1000	$>10^{15}$	3.3×10^{13}
B	500	3.2×10^{11}	3×10^{14}
	1000	3.1×10^{11}	0.86×10^{14}
1367-2 A	500	$>10^{15}$	3.0×10^{13}
	1000	$>10^{15}$	3.0×10^{13}
B	500	9.8×10^{11}	1.6×10^{14}
	1000	10.5×10^{11}	0.6×10^{14}
1105-3 A	500	1.7×10^{15}	3.6×10^{13}
	1000	1.5×10^{15}	3.3×10^{13}
B	500	7.5×10^{11}	1.3×10^{14}
	1000	7.5×10^{11}	0.5×10^{14}
BTC-17-4 A Jan., 1976	500	3×10^{15}	9.2×10^{13}
	1000	3×10^{15}	4.4×10^{13}
B	500	1.7×10^{15}	1.2×10^{14}
	1000	1.7×10^{15}	0.7×10^{14}
BTC 69 A April, 1976	500	2.8×10^{15}	1.1×10^{14}
	1000	2.8×10^{15}	0.3×10^{14}
B	500	3.0×10^{15}	6.5×10^{13}
	1000	3.0×10^{15}	4.0×10^{13}
BTC 17-4 A Jan., 1968	500	6.0×10^{15}	6.6×10^{13}
	1000	6.1×10^{15}	3.3×10^{13}
B	500	5.6×10^{14}	1.2×10^{14}
	1000	5.6×10^{14}	0.6×10^{14}

A = Cloth side facing measuring electrode

B = Rubbery side facing measuring electrode

3. LABORATORY TESTS - FUEL CHARACTERISTICS

Physical and chemical properties of the fuel used in the Test Rig were evaluated. The fuel, a Jet A material, was analyzed for Gravity (API), Flash Point, Freezing Point, Distillation, Saybolt Color, and Water Separometer Index. ASTM procedures were used. The test results shown in Table 7 are typical of Jet A grade fuel and as such was judged acceptable for our test program.

The Jet A test fuel was obtained from Exxon's Bayway refinery as typical commercial product and used to prepare blends with additives. During the course of testing in Drum and Bladder Cells, additional Jet A fuel was obtained on several occasions. The inspections of these additional batches gave results similar to Table 7. Thus, the results of this test program represent several different Jet A fuel batches and not a single fuel.

4. SPARK DISCHARGE TEST UNIT

A small-scale spark discharge laboratory apparatus was assembled in order to evaluate the effect of reticulated foam on the nature and energy of spark discharges. This test unit, which was similar to that used by Leonard and Carhart (3) for studying electrical discharges from a fuel surface, appeared to be a useful and practical technique for making measurements on the extent to which spark energies might be influenced by substituting foam for a liquid surface as one of the electrodes.

A schematic drawing of the apparatus appears in Figure 2. Fuel is recirculated at constant rate through an electrically isolated small filter which imposes a charge. The charged fuel is

TABLE 7
JET A TEST FUEL CHARACTERISTICS

<u>Test Description</u>	<u>ASTM Test Method</u>	<u>Result</u>
Gravity, °API	D-287	43.4
Distillation, °F	D-86	
IBP		314
10%		376
50%		428
FBP		521
Flash Point, °F	D-56	130
Freezing Point, °F	D-2386	-46
Saybolt Color	D-156	28
Water Separometer Index-Modified	D-2550	98

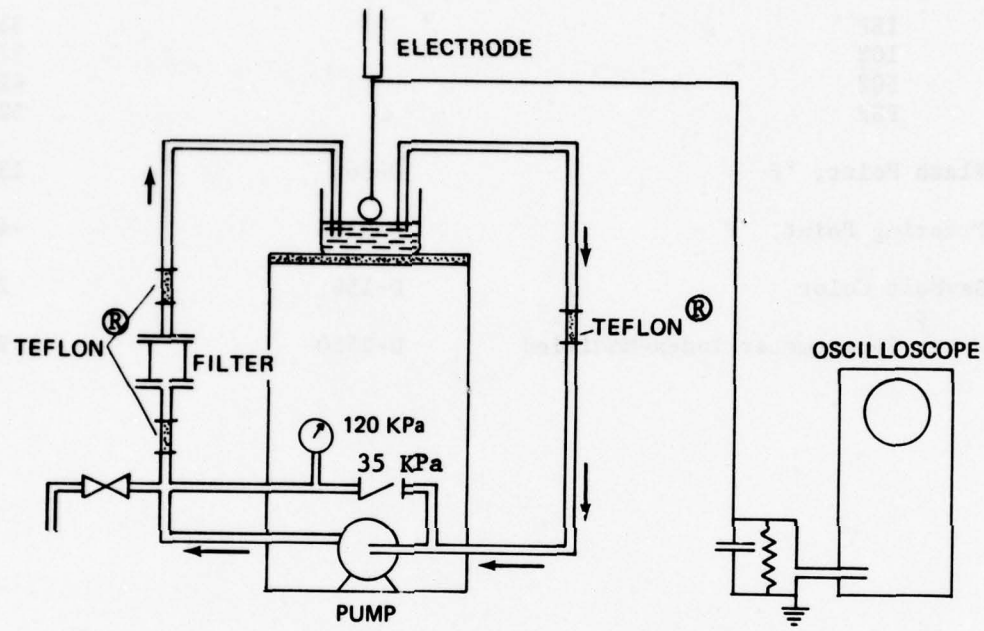


Figure 2. Schematic of Spark Discharge Test Unit

held at a constant level in a lucite container which is also electrically isolated. The electrode above the surface is a 25 mm (1") sphere (or smaller); the measuring circuit for the charge transferred during a spark discharge between surface and sphere contains a 1000 pF capacitor and a 10000 Ω resistor. Voltage rise, spark duration, and discharge frequency are observed and recorded on an oscilloscope.

In order to generate enough charge from the filter to observe discharges, it was necessary to add pro-static agent to the fuel. For these tests, Jet A containing 100 ppm of GA 178 pro-static additive (a corrosion inhibitor) was used. Base fuel of 1.16 pS/m conductivity had produced a filter charge of only $-1100 \mu\text{C}/\text{m}^3$ and no signals -- static discharges -- could be detected from liquid, fine blue (polyether) foam or orange (polyester) foam at a gap setting of 13 mm. However, with additive fuel, each of the foams was tested at two different gap settings with the results shown in Table 8.

Spark energies were calculated as in Ref. (3) using the expression $E = 1/2 QV$ where Q is the quantity of charge transferred in a single discharge and V is the breakdown potential. Q is measured by recording the voltage rise across the calibrated capacitor. The value of breakdown potential was taken from Figure 7.16 of the book "Gaseous Conductors" by J. D. Cobine where the gradient of spark breakdown in air for plane-parallel electrodes is plotted against gap dimensions. At a 13 mm gap, the breakdown potential of air is 30 KV/cm. Gibson and Lloyd (4) argue that the above equation cannot be used in the case of electrically insulating

TABLE 8

SPARK DISCHARGE TESTS WITH RETICULATED FOAM
 (All tests with Jet A containing 100 ppm GA 178
 Pro-static additive at 36°C) (1)

Run No.	Foam (3)		Spark Gap to Surface	Spark Discharges (2)				Polarity of Signal	Remarks
	Type	Height Above Fuel mm		Peak Energy v	Duration μ s	No./Min	Calc E mJ		
25	None		38	0.7	25	17	0.04	-	38 mm Gap to avoid liquid bridging
26-1	Fine Blue	25	13	0.85	25	7	0.016	-	Peak estimated
26-2	Fine Blue	25	5	1.9	25	200	0.017	-	Peak estimated
27-1	Red	25	13	2.5	90	20	0.049	+	
27-2	Red	25	5	1.7	60	40	0.015	+	
28-1	Orange	25	13	9.0	80	30	0.176	+	Peak estimated
28-2	Orange	25	5	~2.0	80	200	0.018	+	Peak estimated
29-1	Coarse Blue	25	13	2.0	50	45	0.039	-	Peak estimated
29-2	Coarse Blue	25	5	>2.0	50	130	0.022	-	Peak estimated
30-1	Yellow	25	13	2.5-7	80	45	0.098	+	Variable signals
30-2	Yellow	25	5	1.6-3	80	18	0.020	+	Variable signals

(1) Fuel of 4.3 pS/m conductivity recirculated at 2.2 L/min constant rate through a fiberglass filter media. Charge density averaged $-3800 \mu\text{C}/\text{m}^3$. Fuel level constant at 50 mm. At end of test 30, $K = 14.3 \text{ pS}/\text{m}$.

(2) Spark voltage, duration and frequency observed on oscilloscope. Probe is 25 mm diameter sphere. Calculated energy represents theoretical maximum.

(3) Foam blocks 76 mm high placed in container, fuel introduced below foam.

materials such as foam (or a fuel surface) to estimate spark energies because the high surface and volume resistance impedes the flow of charge to the point of discharge. Nevertheless, it can be argued that the calculated value using the peak voltage rise gives an upper limit for spark energy.

The spark energies observed with a gap setting of 13 mm showed a difference among the foams that disappeared at smaller gap settings. The orange foam displayed the highest spark energy, the red foam the lowest. We also observed that the polarity of the spark signals reversed with the two blue (polyether) foams compared with the others. These results are summarized in the graph of Figure 3. To verify these findings, repeat tests were carried out.

Using fresh batches of additive fuel, spark discharge tests were repeated on each foam at the same gap setting using two different foam levels but the same fuel level to insure that foam was exposed to the same quantity of charge. Results are summarized in Table 9. The foams, listed in order of increasing spark discharge energy, show a similar pattern as in Table 8, red and blue foam the lowest, orange foam the highest. While the spark energies observed in Table 9 were higher for each of the foams than with liquid fuel alone and generally higher when more foam was in place above the charged liquid, none of the calculated spark discharge energies reached the minimum level (0.2mJ) considered necessary for an incendiary discharge. The total amount of charge transferred in the spark gap could be estimated by integrating the voltage rise vs. time curve but this is not necessarily a better measure of spark energy than

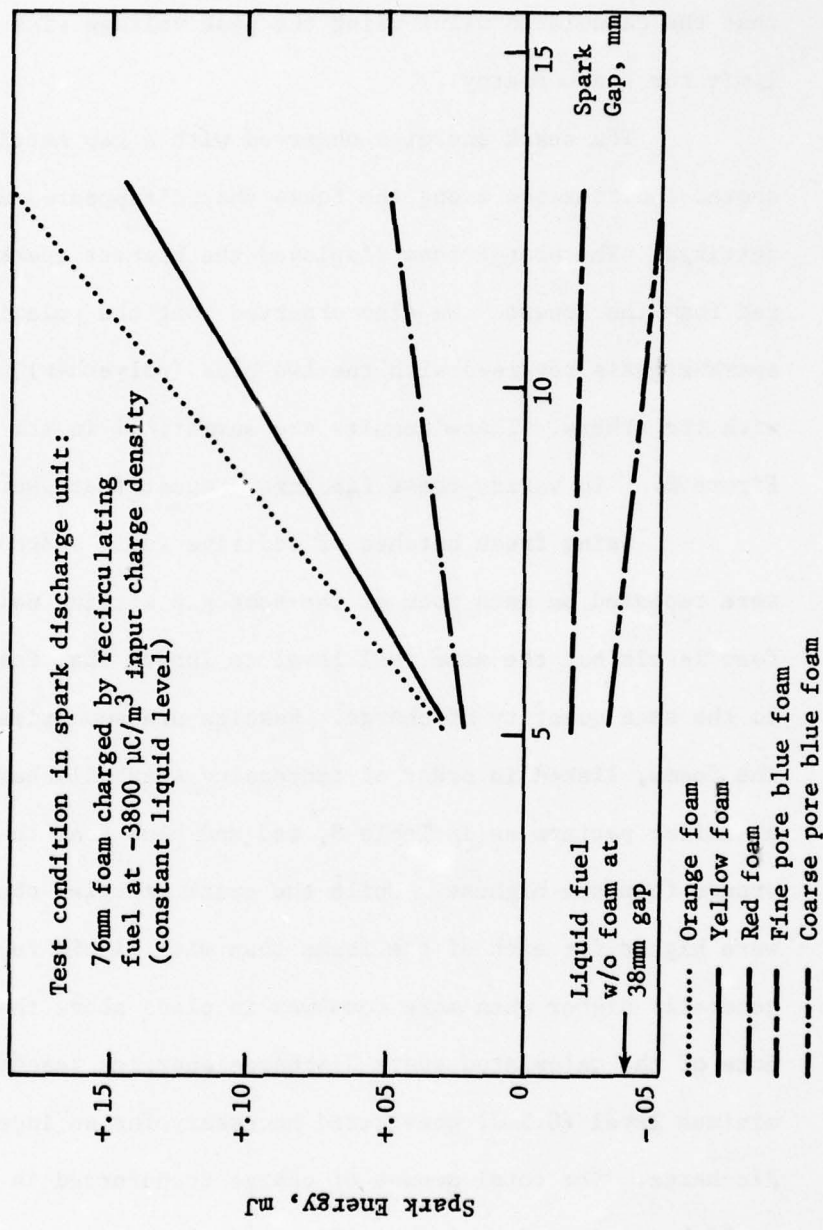


Figure 3. Energy in Spark Discharges from Foam
 (Spark Gap from 25 mm Probe to Foam Surface)

TABLE 9

SPARK DISCHARGE TESTS WITH RETICULATED FOAM - EFFECT OF FOAM VOLUME
 (Tests with Jet A containing 100 ppm GA 178
 Pro-static additive at 36°C) (1)

A: TESTS WITH 76 mm FOAM BLOCKS⁽²⁾

Run No.	Foam		Spark Gap To Surface	Spark Discharges			Polarity of Spark Signal
	Type	Height Above Fuel mm		Peak Energy v	Duration μ s	No/min	
32	-----None-----		38	0.1	20	30	0.006
35	Red	26	13	0.7	20	56	0.014
33	Fine Blue	26	13	1.5	25	190	0.029
37	Yellow	26	13	1.7	25	192	0.033
36	Coarse Blue	26	13	1.8	25	160	0.035
34	Orange	26	13	4.0	50	70	0.08

B: TESTS WITH 127 mm FOAM BLOCKS⁽³⁾

43	Fine Blue	77	13	0.43	35	22	0.008	-
39	Coarse Blue	77	13	1.7	45	200	0.033	-
40	Red	77	13	2.4	90	18	0.047	+
42	Yellow	77	13	7.5	50	18	0.146	+
41	Orange	77	13	8.0	50	24	0.156	+
44	Orange (Used)	77	13	0.48	45	36	0.009	-

(1) Fuel recirculated at constant 2.2 L/min; liquid level constant 50 mm.

(2) Fuel conductivity = 3.73 pS/m at start, 13.9 pS/m after test 37. Charge density varied from -3550 to -4500 μ C/m³ at filter.

(3) Fuel conductivity = 3.73 pS/m at start, 18.7 pS/m after test 44. Charge density varied from -1640 to -4370 μ C/m³ at filter.

the calculated values from the voltage peak across the gap. It is perhaps noteworthy that the duration of positive spark signals was considerably longer than negative spark signals.

The data in Tables 8 and 9 show a consistent pattern of higher energy spark discharges from new orange or yellow foams than from the higher porosity red foam. (The used orange foam, on the other hand, produced low energy sparks.) The blue (polyether) foams show lower energy sparks than the red or orange (polyester) foams of equivalent porosity suggesting that the difference in chemical nature of the blue foams may play a role in charge separation.

However, as experimentation expanded to the larger test units the differences in charge separation of the foams took on quite a different flavor. Sections V-5 and V-6 describe these test results.

5. FOAM CHARGE GENERATION

Foam Charge Generation Tests (FCST) were conducted in the Drum Filling Rig identified in Figure 1. A special section of the Rig ("Foam Test Section" of Figure 1) was used to evaluate the charge generation effects of the foam as fuel passed through its open-pore structure. The Foam Test Section represented, in effect, an enlarged section of the inlet fueling line into which foam could be packed without compression and through which fuel could be pumped at high rates. The diameter of the Test Section was chosen to represent an average section in a typical aircraft tank through which fuel would flow at high velocities during filling.

The experimental plan for Foam Charge Generation Testing investigated various fuel flow rates and different charging conditions, as well as the effect of two phase flow (fuel + N₂) on foam charge generation. Base fuel (Jet A), fuel containing the JP-4 additive package and fuel containing different levels of anti-static additive (ASA-3) were tested. (Individual details of all the Foam Charge Generation test runs appear as Appendix B to this report. The major observations are discussed below.)

Figure 4 identifies the effect of flow rate on each foam. The charging tendencies for blue foams are two orders of magnitude higher and of opposite polarity to the red, orange, and yellow foams using uncharged fuel. This effect is most dramatic at high velocity.

Figure 5 shows the combined effects of gas and input fuel charge on charging tendency of the foams.

With positively charged fuel, red, orange, and yellow foams switch polarity from positive to negative. Blue foams show increased negative values. When two phase flow takes place through foam (by mixing N₂ gas with fuel) charge levels increase in the same direction compared with all liquid flow for each of the foams regardless of whether input fuel was charged or uncharged (dotted lines of Figure 5).

The addition of JP-4 additives (Corrosion Inhibitor, Anti-icing Additive) to the base fuel had no major effect on these results. The charging tendency of the foams followed the same format. However, the addition of anti-static additives showed reduced foam charging tendency.

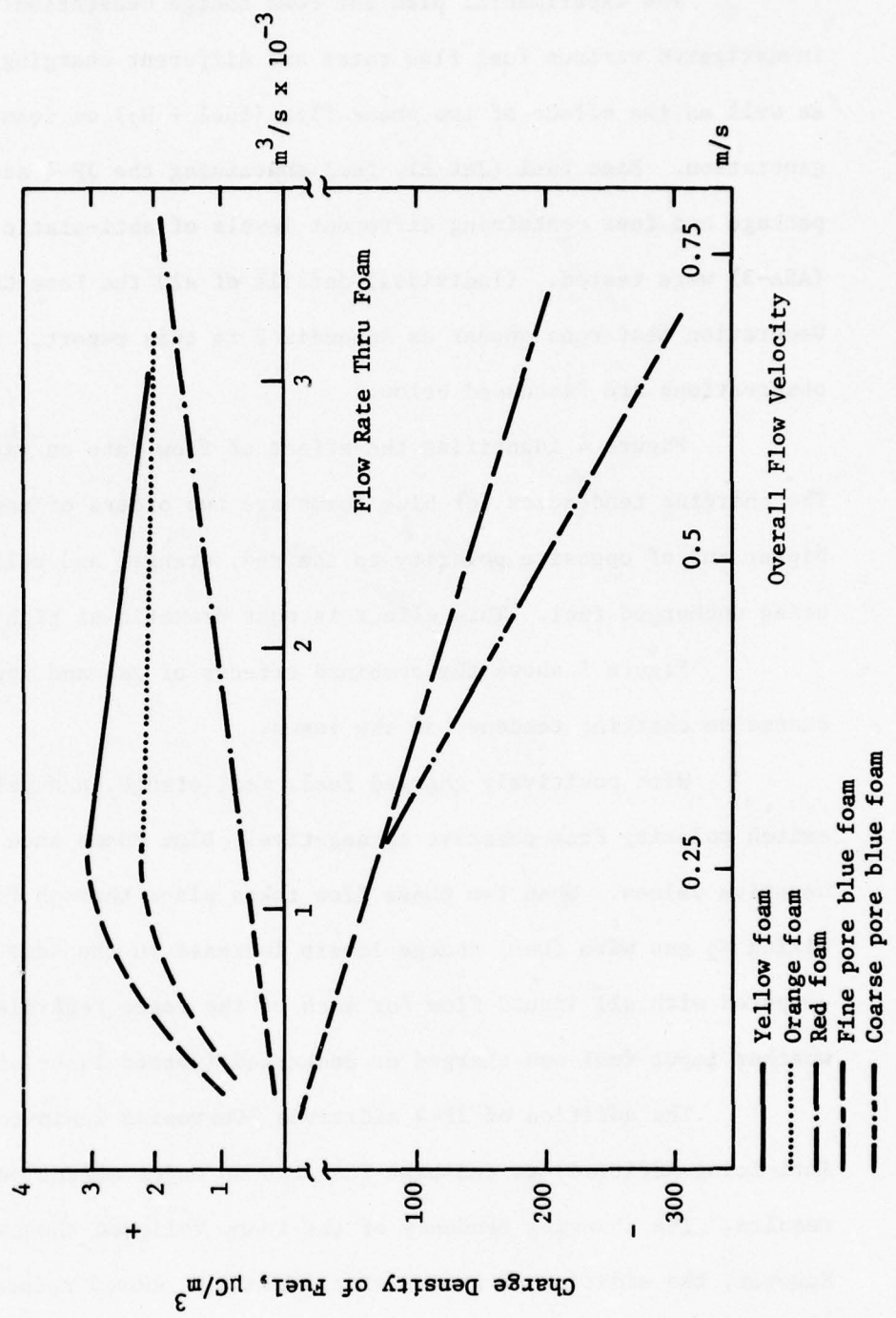


Figure 4. Charging Tendency of Foam vs. Flow Rate
(Uncharged Base Fuel Thru Foam Test Section)

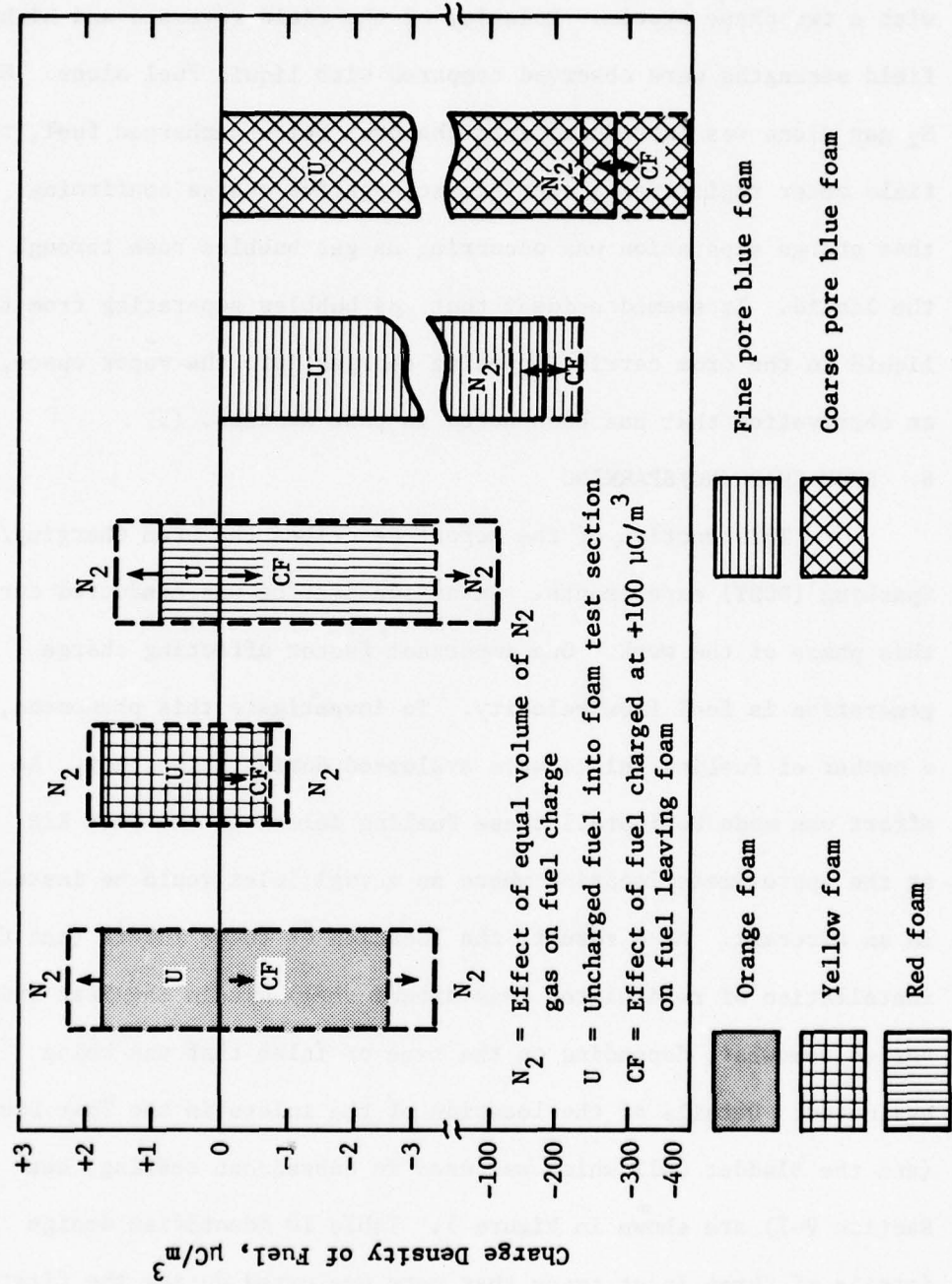


Figure 5. Effect of Gas and Input Charge on Charging Tendency of Foam
(Base Fuel at $.003 \text{ m}^3/\text{s}$ Thru Foam Test Section)

Figure 6 illustrates the Surface Voltage produced by charged fuel flowing through the test foams into the Drum. The field meter readings that were observed showed a significant change with a two-phase system. Polarity of the field reversed and higher field strengths were observed compared with liquid fuel alone. When N₂ gas alone was introduced into the drum below uncharged fuel, the field meter registered a significant negative charge confirming that charge separation was occurring as gas bubbles rose through the liquid. It seemed evident that gas bubbles separating from the liquid in the drum carried opposite charges into the vapor space, an observation that has been noted in past studies. (5)

6. DRUM CHARGING/SPARKING

This section of the report describes the Drum Charging/Sparking (DCST) experiments. Extensive testing was conducted during this phase of the work. One important factor affecting charge generation is fuel flow velocity. To investigate this phenomena, a number of fueling inlets were evaluated during this study. An effort was made to install these fueling inlets in the Test Rig at the approximate location where an actual inlet would be installed in an aircraft. As a result, the location of these inlets (and the installation of reticulated foam around them) within the Test Drum varied somewhat, depending on the type of inlet that was being evaluated. Details of the location of the inlets in the Test Drum (and the Bladder Cell which was used in subsequent testing, see Section V-7) are shown in Figure 7. Table 10 identifies design details of three inlet types that were evaluated during the first

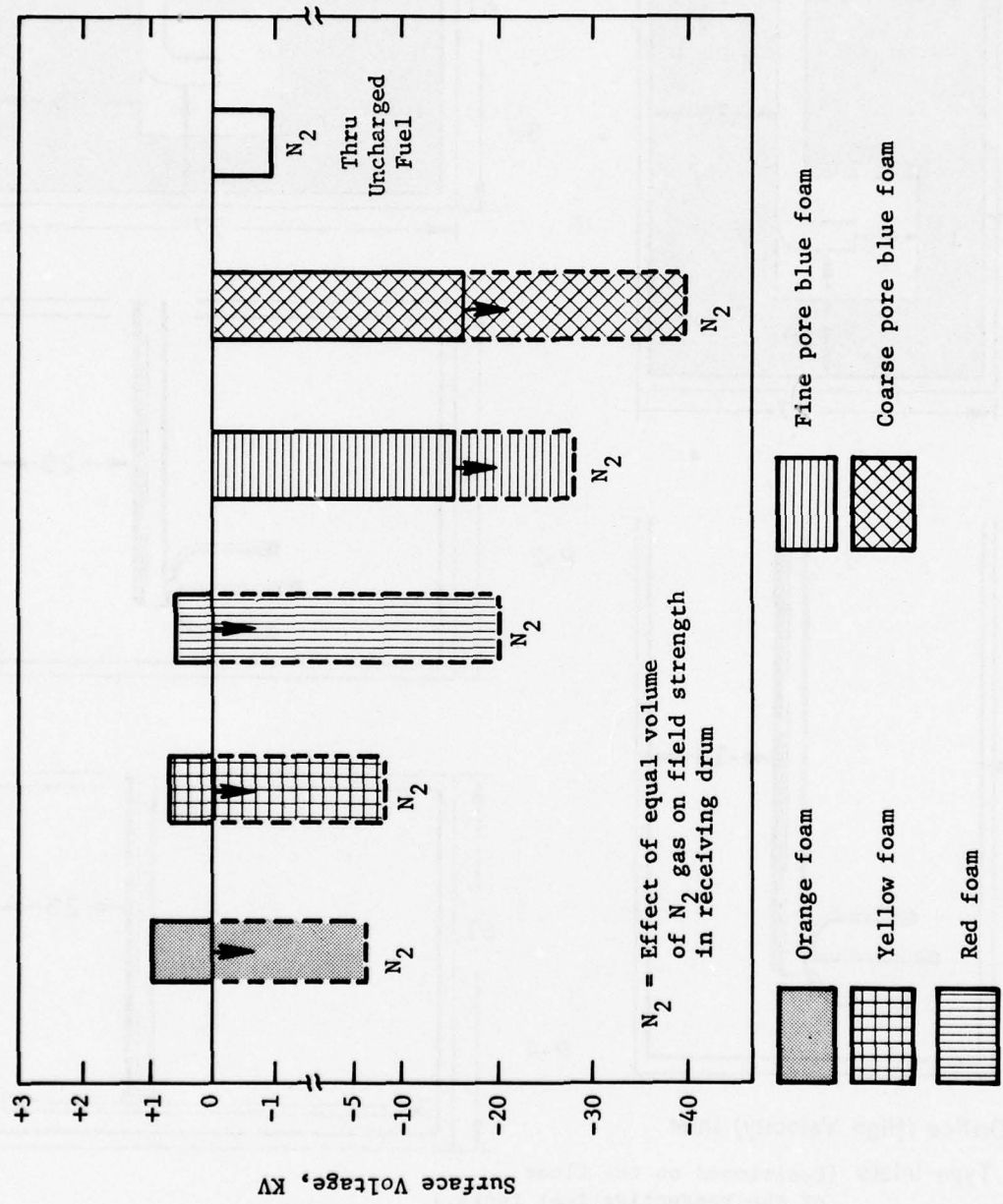
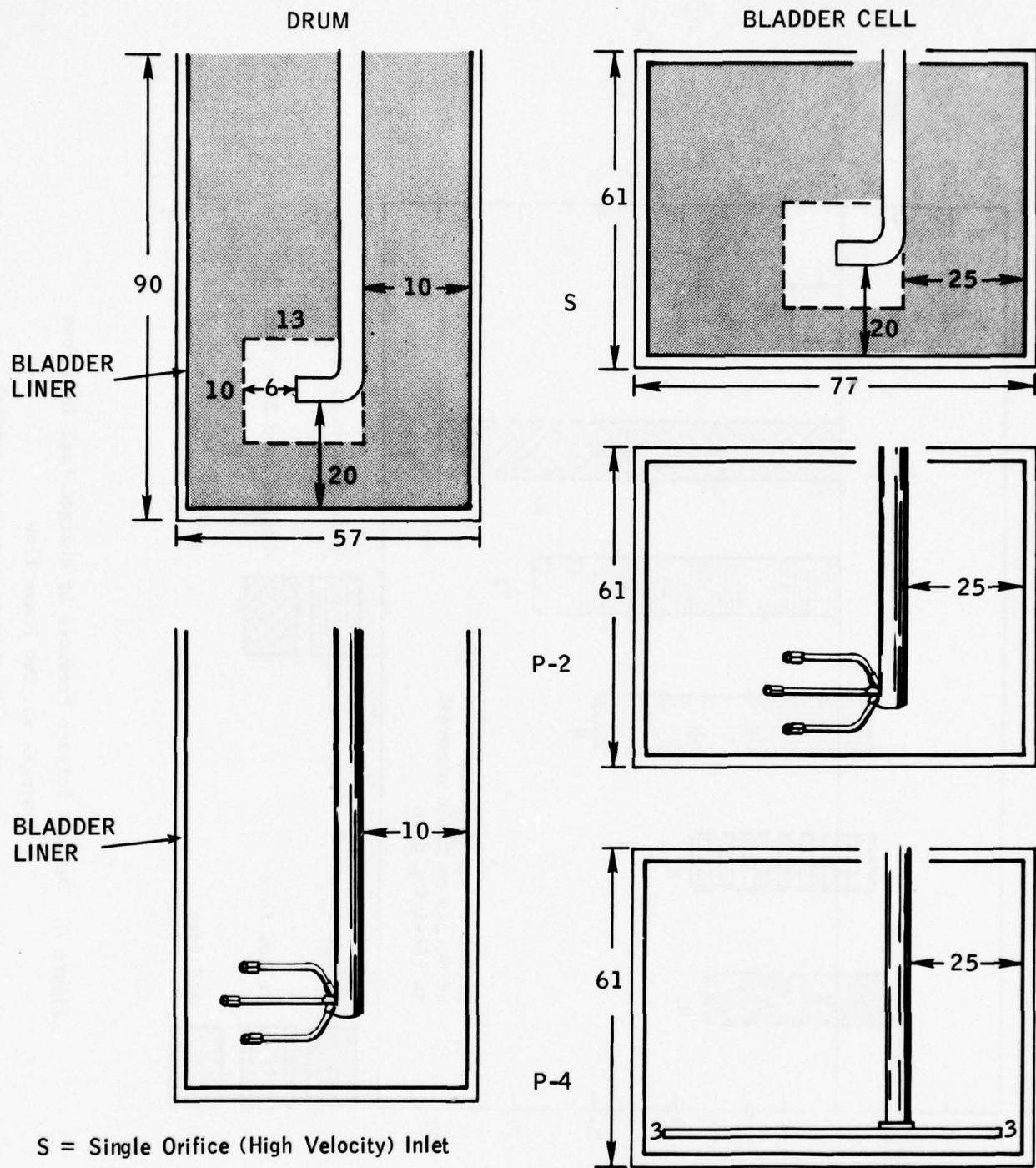


Figure 6. Surface Voltage Produced by Charged Fuel Thru Foam
Single vs. Two Phase Flow
(Base fuel at .003 m³/s thru foam test selection)



S = Single Orifice (High Velocity) Inlet

P = Piccolo Type Inlets (Positioned on the floor
of the respective test tanks.)

Dimensions in Centimeters

FIGURE 7
INLET LOCATIONS

TABLE 10
INLET DESIGN DETAILS

Inlet Type	No. of Holes	Hole Diameter, cm	Maximum Exit Velocity m/s (fps)	Distance Inlet Extends Into Test Vessel cm
Splash Plate ⁽¹⁾	1	3.8	3.3 (10)	60
Drop Tube ⁽²⁾	1	1.5	21 (68)	20
High Velocity Ell ⁽³⁾	1	1.5	21 (68)	60

(1) The splash plate inlet was an open tube (3.8 cm diameter stainless steel) with a plate located about 4 cm from the end of the tube. Exiting fuel impinged on the plate and was distributed into the test vessel in a circular fashion.

(2) The "drop tube" was a short inlet fitted with an orifice for creating high flow velocities. Fuel exited from the inlet and was delivered vertically into the test vessel.

(3) The high velocity ell was a tube fitted with a 90° elbow and an orifice. The ell provide horizontal flow and the orifice was used for creating the high flow velocities.

part of the Drum Charging/Sparking Tests (DCST). The photo of Figure 8 shows that basic differences between the inlets is in the fuel velocity exiting from the inlet, the orifice being the high velocity and the open tube with splash plate being low velocity. In order to investigate the "worst case" charging effects, the bulk of initial DCST work involved primarily the high velocity inlets. Later testing (with Drum and Bladder Cell) investigated several low velocity inlets (see Section V-6-C and V-7). The data appendices contain relevant details about inlet utilization.

Several tests involved insertion of a charge collector into the Drum to evaluate the tendency of unbonded metal to accumulate charge. The charge collector used was a marriage clamp of the type used in the A-10 aircraft tank fixed to the grounded inlet. The rubber gasket around the metal electrically separated the clamp from the inlet. Discharges would be expected to occur in the gap between clamp and inlet.

a. Base Case Studies

Base case tests for drum charging were conducted with the empty drum (of the Drum Filling Rig - Figure 1) and with the empty drum fitted with a bladder liner. Various input fuel charge levels and fueling inlets were tested. Table 11 summarizes the testing conditions during the base case studies. (The detailed data for the base case experiments are presented in Appendix C of this report.) Details are discussed below.

It was observed from the first set of tests flowing fuel at high velocities into the Drum that recorder signals fluctuated wildly

FIGURE 8
INLET PHOTOGRAPHS



High Velocity (Single Orifice) Inlet



Splash Plate (Low Velocity) Inlet

TABLE 11
DRUM CHARGING/SPARKING
SUMMARY OF EMPTY DRUM/BLADDER TESTING (1)

Fuel	Flow Velocity m/s	Fuel(3) Charge Density $\mu\text{C}/\text{m}^3$	Inlet(4) Charge Density $\mu\text{C}/\text{m}^3$	Drum(4)	
				Field(5) Strength KV/m	
Empty Drum	Base Jet A (2)	3 to 15	-22 to +619	-3.8 to +85.7	-9.5 to +412.7
Drum with Bladder	Jet A (+ GA178)	3 to 12	+61 to +201	+7.9 to +26.5	+51.1 to +137.6

(1) For the raw data concerning individual test runs the reader is referred to the tables of Appendix C of this report.

(2) Also includes Jet A doped with about 4 ppm GA-178, a prostatic agent.

(3) Fuel charge represents the current density measured from the filter but of opposite polarity.

(4) All current readings were made about 8 seconds after flow started.

(5) Field Strength observed when the drum was about 90% full.

at startup and for several seconds thereafter. By about 8 seconds, i.e. after 5-8 gallons of flow with the drum about 10% full, recorder signals had settled down. It was decided to standardize on readings at this specific time in the run so that tests could be compared at equivalent conditions.

In the case of field strength readings, it was observed that recorder signals reached their maximum value as the fuel approached the 90% full mark and just covered the foam. Again in order to compare tests at equivalent conditions, it was decided to standardize all field strength readings at this mark.

(1) Empty Drum

For the initial empty drum tests input charge levels with base fuel were quite low (see Run Nos. 201-212, Appendix C) varying from about $4 \mu\text{C}/\text{m}^3$ to about $30 \mu\text{C}/\text{m}^3$. With this material no discharge signals were observed in the drum. In order to produce a higher input charge on the fuel, the base fuel was doped with GA 178, a pro-static additive (a corrosion inhibitor). With resulting input charge levels of $500-600 \mu\text{C}/\text{m}^3$ (Run Nos. 213-214, Appendix C) internal radio signals were observed. This was with a low velocity inlet (linear velocity $\sim 3\text{m/sec.}$). However, when the input fuel charge level was reduced to the neighborhood of $250 \mu\text{C}/\text{m}^3$ these radio signals disappeared. Even with a charge collector present, at the lower charge level, no internal radio signals were detected. This seemed to indicate that some threshold level of charge was required before electrical discharges could occur. Testing with the high velocity inlet was limited to a "drop tube" type arrangement (Run Nos. 313-322, Appendix C). Fluid velocities of about 12 m/sec were the

maximum attainable for reliable operation. Higher flow velocity interfered with the operation of the field strength meter. Test runs with this inlet were conducted at input fuel charge levels between 125-300 $\mu\text{C}/\text{m}^3$. Discharge signals were not observed.

(2) Drum with Bladder Liner

Test Runs with a bladder liner (Run Nos. 401-413, Appendix C) fitted in the Test Drum were similar to the empty drum studies noted above. Three bladder liners were provided by the Air Force for use in this program. One was specially fabricated to fit inside our Test Drum. (There was no cover with this liner.) The other two were standard Test Bladder Cells (dimensions 76 cm L x 76 cm W x 61 cm H), as identified in MIL-T-5578 and MIL-T-6396. These bladder liners were reported as materials meeting MIL-T-6396 and MIL-T-5578. The liners were manufactured by Uniroyal (US 180 Construction, under Contract F33615-77-M-3119). Internal radio signals were not detected with the low velocity inlet or with the ("drop tube") high velocity inlet. Input charge levels varied from 60 $\mu\text{C}/\text{m}^3$ to 200 $\mu\text{C}/\text{m}^3$.

The one major difference between the empty drum tests and the drum/bladder tests was observed in the field strength rate of decay. Initially the field strength decay was similar for both test configurations. However, at a surface voltage of about 0.23 Kv the field strength rate of decay for the drum/bladder configuration became much slower than that of the empty drum. This indicated that a slight charge retention mechanism was present when the bladder was used.

b. Red Foam Studies

Red foam testing in the drum was conducted under a variety of fuel and flow conditions. The breakdown of testing, for the purposes of discussion in the next two subsections, relates to the fuel condition. For the most part two general fuel conditions were examined -- (1) fuel without antistatic additive and (2) fuel containing various doses of antistatic additive. The objective in this series of testing was to establish, under a variety of flow and charge conditions, the discharge threshold for red foam, first with fuel in the unadditized condition. Then, having established this discharge threshold for the red foam/fuel configuration, the next step was to add antistatic additive to the fuel in incremental amounts to determine the fuel conductivity additive requirement for the elimination of discharges. Sections V-6-b (1) and V-6-b (2) below discuss the experimental tests associated with these test series.

(1) Red Foam - Base Fuel

Table 12 summarizes the test results for the red foam test series. Several fuel charge and flow conditions were evaluated.

Initial Drum Charging/Sparking testing was conducted with base fuel (Jet A) and the red (polyester) foam (see Run Nos. 501-511, Appendix D). Testing was carried out with an ell-shaped, high velocity inlet. Fluid velocities of about 50 ft/sec (17 m/s) were the maximum attainable for reliable operation. (Higher fluid velocities interfered with the operation of the field strength meter.) No internal discharge signals were detected. This we feel was due to a relatively low

TABLE 12
DRUM CHARGING/SPARKING - RED FOAM⁽¹⁾

Fuel	Flow Velocity m/s	Range of Test Results			Drum (3) Charge Density μC/m ³	Field (4) Strength KV/m
		Input Fuel (2)		Inlet (3)		
		Charge Density μC/m ³	Charge Density μC/m ³	Charge Density μC/m ³		
Jet A + GA 178 (2 to 4.5 ppm)	15	+19.8 to +107.1	-95.2 to +10.3	+17.9 to +198.4	+0.2 to +60	
Jet A (Clay treated)	15 to 20	-2882 to +21.8	-317 to +11.9	-576 to +21.8	-500 to -130	

(1) For details of individual test runs the reader is referred to Appendix D of this report.

(2) Fuel charge represents the current density measured from the filter but of opposite polarity.

(3) All current readings were made about 8 seconds after flow started.

(4) Field Strength observed at about 90% full when fuel reached the top of the foam.

(5) The field meter used for this study was limited in the maximum value it could sense (500 KV/m). Thus, a reading of 500 KV/m could indicate that the field strength was 500 KV/m or more.

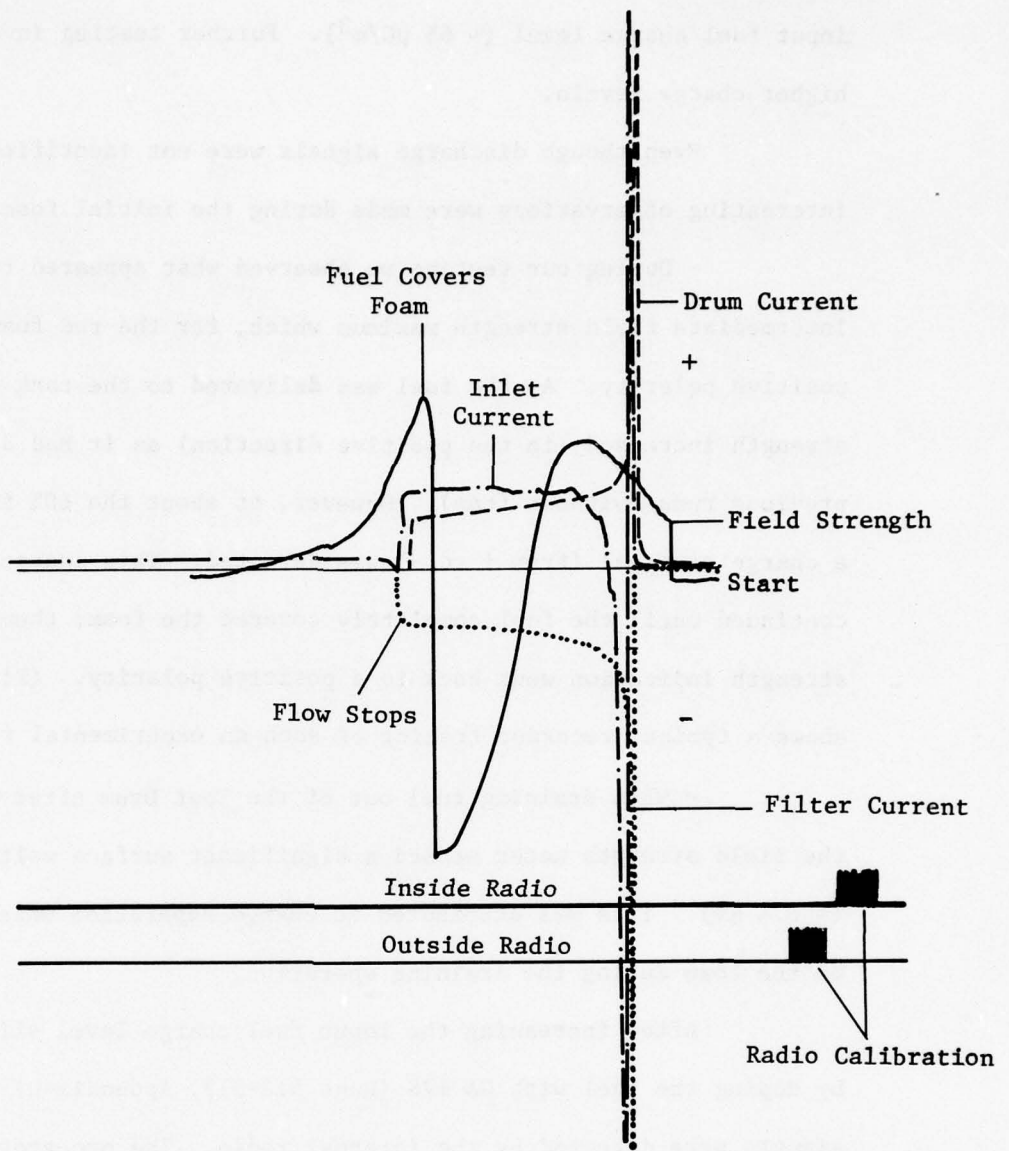
input fuel charge level ($\sim 65 \mu\text{C}/\text{m}^3$). Further testing investigated higher charge levels.

Even though discharge signals were not identified, several interesting observations were made during the initial foam studies:

- During our testing we observed what appeared to be an intermediate field strength maximum which, for the red foam, was of positive polarity. As the fuel was delivered to the tank the field strength increased (in the positive direction) as it had done in previous runs (without foam). However, at about the 60% fill point a charge reversal (from + to -) was detected. This charge reversal continued until the fuel completely covered the foam; then the field strength indication went back to a positive polarity. (Figure 9 shows a typical recorder tracing of such an experimental run.)

- When draining fuel out of the Test Drum after a run, the field strength meter sensed a significant surface voltage ($\sim 0.4 \text{ Kv}$). This was attributed to charge separation which occurs on the foam during the draining operation.

After increasing the input fuel charge level slightly by doping the fuel with GA 178 (Runs 512-517, Appendix D) discharge signals were detected by the internal radio. The pro-static activity of the GA 178 had influenced the charge generation at the filter, raising the charge level to about $100 \mu\text{C}/\text{m}^3$, and consequently fuel containing significant charge was delivered to the Test Drum. The result, as sensed by the internal radio, was electrostatic discharge. The radio signals were also accompanied by current spikes on the inlet and drum recorder tracing.



Test Run No. 504
 (Jet A w 2 ppm GA 178)
 Fuel CD, $\mu\text{C}/\text{m}^3$ +19.8
 Inlet CD, $\mu\text{C}/\text{m}^3$ +2.6
 Drum CD, $\mu\text{C}/\text{m}^3$ +17.9
 (Max) Field Strength KV/m -7
 +1.2

Figure 9. Typical Recorder Tracing - Red Foam Tests

Uncharged fuel was also tested with the drum/bladder/foam configuration. The field meter readings were about the same as with charged fuel. Discharge signals were also recorded during this experiment, indicating perhaps, residual effects of the pro-static agent (GA 178). This was further indication of charge separation on the foam, as sensed by the field meter.

Subsequent experimental runs at lower initial fuel velocities did not cause discharges. This was an initial indication of the importance of flow velocity on static discharge (see Section V-6-c (3)).

Current signals received from the drum were considerably higher than those from the filter (Bendix Gage) with the fuel containing the pro-static agent (GA 178). This seemed to indicate that an additional charge generating mechanism was at work. In order to systematically investigate these observations, signal leads from the drum and the inlet were combined and sent to the recorder as one signal. Several runs were made in this fashion. The signals from the filter and the combined leads (drum and inlet) were then comparable, indicating in an indirect way that "what was going in was what was coming out." The logical conclusion then was that the inlet was contributing to charge separation. During this investigation no discharge signals were identified by the internal radio.

Radio signals had previously been detected at the same input charge level before the leads were combined. To facilitate the collection of charge from the foam or the fuel, a metal clamp

of the type used in the A-10 aircraft tank as a "marriage" clamp between fuel lines and structure was placed on the inlet. The metal is covered by a rubber sheath which effectively isolates it from the inlet. To increase its capacitance for charge, a small brass plate was added. No radio signals were observed with the collector in place (Runs 528-530).

Additional red foam testing was conducted with clay treated fuel. In order to obtain higher input charge levels new filter elements (Set No. 2) were installed. These had the immediate effect of raising fuel charge off the filter to $-1700 \mu\text{C}/\text{m}^3$ -- a reverse polarity compared with older filter elements. No discharges were noted (Runs 531-532, see Appendix D) but when fuel that had been exposed to the new elements was pumped through foam uncharged, radio discharge signals were observed. This surprising result was confirmed by subsequent runs in which blends of charged and uncharged fuel were tested (Appendix D has raw data details). When the blend contained more than 75% of uncharged fuel, radio signals were again observed.

During this testing phase, the critical importance of inlet velocity was confirmed. When initial flow velocity was cut back from 21 to 17 meters per second, radio discharges ceased (see Runs 537 vs. 538, Appendix D).

Because the new elements (Set No. 2) had produced negatively charged fuel and the unexpected effect of radio discharges, it was decided to check the old elements (Set No. 1) with the same fuel since they had previously produced charge up to $+300 \mu\text{C}/\text{m}^3$. Upon reinstallation, a very low negative charge level was observed but

no radio signals. After three runs, the old elements were again producing positive charge on the fuel but no radio discharges were noted until a charge collector was inserted. It is interesting to note that the marriage clamp used as a charge collector on the inlet did produce a single radio signal (Runs 551-552) despite the low input charge level. The timing of this signal coincided with the approaching fuel level and therefore tended to confirm that the metal clamp was indeed concentrating charge from the fuel and discharging to the inlet. At this point it was noted that fuel conductivity had dropped from 3.7 to about 1.9 pS/m suggesting that the elements were removing the pro-static agent that had entered the system with the new elements. It was decided to clay treat the fuel and recheck the "new element" effect.

After clay treating the fuel to 1.5 pS/m conductivity and re-installing the new elements (Set No. 2), testing was resumed. This time the "pro-static" effect was dramatic. A run with uncharged fuel produced no radio signals but the runs through the filter showed almost continuous discharges. The residual effect on the foam was seen by an uncharged run following the charged runs. This also produced radio signals. These tests would appear to confirm that a pro-static agent is picked up from new filter elements. It was interesting to note that these radio signals coincided with sharp spikes on the recorder traces of current flow from the inlet and from the drum which suggests that discharges are of considerable intensity. It was also noteworthy that current traces from the drum and the inlet show great fluctuations at high inlet velocities but when flow was cut back to 17 mps (50 fps), the traces became very smooth.

The discharge situation is much more pronounced at the higher inlet charge levels which resulted when new filter elements were first installed. Having established base discharge conditions in non-additive fuel, the next step was to add anti-static additive in incremental amounts to determine the additive threshold for the disappearance of these discharges. (This is discussed in Section V-6-b (2), "Red Foam - Effect of ASA-3".)

It is noteworthy that the maximum field meter readings - all negative in polarity - were about the same regardless of whether fuel entered the drum charged or uncharged and regardless of the polarity of the input charge. This finding tends to support the hypothesis that the field meter senses charged fuel droplets and charged froth rising to the top through the foam. The field meter frequently reached its maximum value of 500 KV/meter, at which point the input signal was saturated.

(2) Red Foam - Effect of ASA-3

The combination of new filter elements (Set No. 2) and clay treated fuel had produced spark discharges in red foam under a variety of conditions (see Section V-6-b (1)). There appeared to be a carryover or residual "pro-static" effect of the active ingredient extracted from the filter elements on the foam since sparks were detected even with uncharged fuel.

Following this test series, where discharges were consistently noted at an input charge of about $-600 \mu\text{C}/\text{m}^3$, increments of ASA-3 were added to the fuel in order to determine at what concentration, i.e. fuel conductivity level, spark signals were extinguished. Details of these experiments (Runs 559-599) appear in Appendix E of the report.

A summary of the effect of anti-static additive (ASA-3) on spark discharges in the red foam is shown in Table 13. A number of important points were illustrated during this test series:

- Discharge signals were observed with the first two increments of ASA-3 and then disappeared. Installing the marriage clamp charge collector (Run 566) immediately restored discharge signals but again they disappeared as input charge levels decreased.

- Spark discharges at least on an initial run became more frequent as ASA-3 increased to 17 pS/m conductivity. However, discharges disappeared at a concentration of 0.125 ppm ASA-3 equivalent to 33 pS/m conductivity using both old and new elements.

- With the first increments of ASA-3, additive depletion was noted by a drop in conductivity. Also the input charge would drop and the sparks would disappear on repeat runs.

- An interesting observation during this stage of testing was the discovery that pro-static activity and sparking would be restored merely by a two-hour break or an overnight shutdown of the test rig that permitted fuel to drain from the foam.

- The pro-static activity of ASA-3 was seen in the increased charge levels in fuel from the filter up to about 33 pS/m. On the other hand, the drum current and field meter readings decreased as conductivity increased.

- At several more incremental ASA-3 additions, the charge collector was reinstalled but after a conductivity of 9 pS/m no discharges were noted. The relatively low drum and inlet current readings combined with the increasing fuel conductivity indicated that very little charge was reaching the metal clamp.

TABLE 13

EFFECT OF ASA-3 ON SPARK DISCHARGES IN RED FOAM
(Drum Charging Tests) at Max Flow Velocity

Run (1) No.	ASA Conc. PPM	C.U. PS/m @ °C	C.D. $\mu\text{C}/\text{m}^3$			Radio Signals	Remarks
			Fuel (2) ex Filter*	Drum (3)	F _S (4) KV/m (5)		
558	--	1.3/-2	-576	-317	-500 (5)	4	Base Case
559	0.01	4.0/5	-865	-288	-180	40	
563	0.015	9.2/15	-1153	-375	-19	4	Partially opened by-pass line caused low field strength
565	0.015	5.7/12	-404	-202	-70	None	Additive Depletion?
566	0.015	5.7/12	-346	-144	+60	43	After 2 hours
569	0.015	5.7/12	-576	-144	+150	49	Overtight
572	0.02	9.7/17	-375	-115	+26	35	
573	0.02	9.7/17	-288	-115	-45	None	Reduced initial flow velocity
577	0.044	17.2/19	-403	-144	+25	21	
580	0.125	32.7/18	-634	-127	-6	None	
584	0.125	32.7/18	+576	+202	+7	None	Element Set #3 New
586	0.285	74.6/15	+461	+4.3	-2	None	
588	0.285	74.6/15	-288	-4.3	-3	None	Element Set #3 New

*All tests with Element Set #2 except as noted.

(1) Details of all the experimental runs associated with ASA-3 testing in Red Foam can be found in Appendix E of this report.

(2) Fuel charge represents current density measured from the filter but of opposite polarity.

(3) All current readings were made about 8 seconds after flow started.

(4) Field Strength observed at about 90% full, when fuel reached the top of the foam.

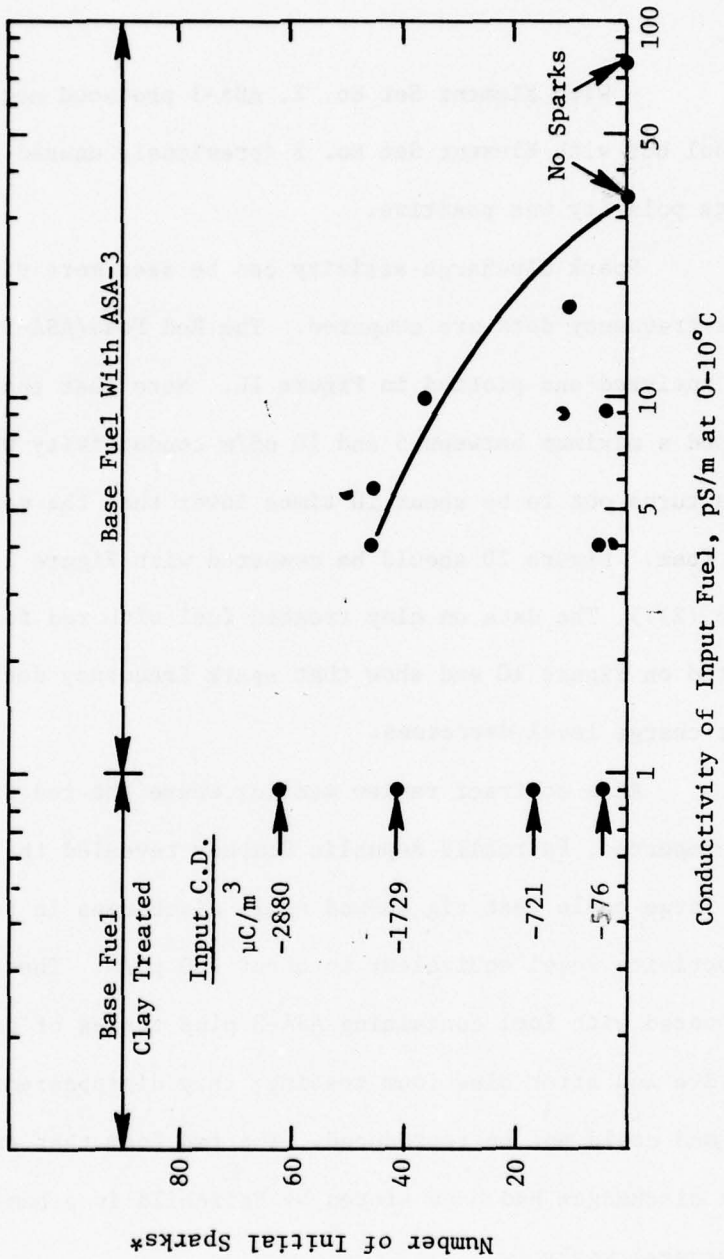
(5) The field meter used for this study was limited in the maximum value it could sense (500 KV/m). Thus, a reading of 500 KV/m could indicate that the field strength was 500 KV/m or more.

- Confirming the effects of initial flow velocity on spark discharges noted with clay treated fuel, a small reduction (22 to 20 m/sec) also eliminated sparks with fuel plus ASA-3 (Run 573 vs. 572).

- With Element Set No. 2, ASA-3 produced negative charge in fuel but with Element Set No. 3 (previously unused filters) the charge polarity was positive.

Spark discharge activity can be seen more vividly if the spark frequency data are compared. The Red Foam/ASA-3 test runs were analyzed and plotted in Figure 10. Note that spark frequency reached a maximum between 5 and 10 pS/m conductivity with red foam. (This turns out to be about 10 times lower than the maximum with blue foam. Figure 10 should be compared with Figure 13 of Section V-6-c (2).) The data on clay treated fuel with red foam are also plotted on Figure 10 and show that spark frequency decreases as inlet charge level decreases.

At a contract review meeting, where the red foam/ASA-3 data were reported, Fairchild Republic Company revealed that their tests in a large scale test rig showed spark discharges in red foam at a conductivity level equivalent to about 200 pS/m. These discharges were noted with fuel containing ASA-3 plus traces of pro-static additive and after blue foam testing; they disappeared after a few runs and could not be reproduced. The red foam that exhibited spark discharges had been stored by Fairchild in a humid atmosphere for several weeks.



* Sparks observed by radio during first 30% fill.

Figure 10. Spark Frequency vs. Input Fuel Conductivity
Drum Filling Tests in Red Foam at Maximum Flow Rate
(High Velocity Inlet)

Our testing plan to explore ASA-3 effects on blue foam made it possible to determine whether the Fairchild results could be explained by the testing sequence. A suggestion was advanced that Fairchild's results might also have been influenced by the pickup of moisture in red foam. To explore this point, the red foam was removed from the Drum Test Rig and placed in a plastic bag and water saturated air was passed through it during the testing period on blue foam.

At the point in the blue foam testing when the fuel reached a conductivity of 166 pS/m, the blue foam was removed and the red foam which had been water saturated by exposure to humid air was inserted into the test drum. On several test runs no sparks were observed on red foam with the fuel that had been exposed to blue foam. (See Appendix E for run details.) Presumably some other factor than water in fuel or in the test system accounted for the Fairchild spark discharges at this ASA-3 level. It is perhaps important to note that Fairchild fuel contained GA 178 pro-static additive at this point while Exxon Research's test fuel contained only ASA-3.

c. Blue Foam

The testing sequence for the blue foam studies was similar to the red foam series (Section V-6-b) -- base fuel under various flow and charge conditions followed by additive fuel testing. The subsections below describe the experimental results.

(1) Blue Foam - "Clean" Fuel

Initial tests with blue foam and fuel containing pro-static agent (GA 178) produced many discharges sensed by the internal radio.

(The raw data for this testing series are presented in Appendix F of this report.) Table 14 summarizes the test sequence. Discharges were noted during the first six seconds (i.e. first five gallons), as the fuel reached the inlet (i.e. after 12 gallons), as the fuel reached an installed charge collector and at the very end of the run a few seconds before shutdown (i.e. after 40 gallons). Radio signals were usually but not always accompanied by spikes in the current signal from the inlet and from the drum.

The fuel used for initial tests with blue foam had been producing charge levels of about $+90 \mu\text{C}/\text{m}^3$ off the filter during red foam testing (Runs 519-530). As the test runs continued, with the same fuel, but with blue foam in place, the charge produced on fuel by the filter increased to $-337 \mu\text{C}/\text{m}^3$. The inlet also proved to be adding high levels of negative charge to fuel entering the foam. In fact with uncharged fuel (see Run 606, Appendix F) the inlet contributed about $-400 \mu\text{C}/\text{m}^3$ charge to the fuel entering the foam.

The observed increase in pro-static activity of the fuel was accompanied by a rise in conductivity from about 2 to 13 pS/m after only three runs, indicating that the blue foam contained a pro-static agent that was being picked up by the fuel.

It was also interesting to note that regardless of input charge, the field meter, initially at a low positive value due to residual charge on blue foam, always reversed polarity midway in the run and produced the same high maximum reading ($-500 \text{ KV}/\text{m}$) at about 90% full. The particular Comstock and Wescott meter, Model No. 12009-2 being used is extremely sensitive but is limited in the maximum value it can sense to $500 \text{ KV}/\text{meter}$. Inasmuch as almost every run with blue foam using non-additive fuel saturated

TABLE 14
BLUE FOAM - DRUM CHARGING /SPARKING

Fuel	Range of Test Conditions			Range of Test Results		
	Flow Velocity (1) m/s	Input Fuel (2)		Inlet (3)		Field (4) Strength KV/m
		Charge Density $\mu\text{C}/\text{m}^3$	Charge Density $\mu\text{C}/\text{m}^3$	Charge Density $\mu\text{C}/\text{m}^3$		
Jet A + GA 178 (2 ppm)	13 to 18	-337 to +71	+183 to +397	+183 to +397	-500 (5)	
Jet A (Clay treated)	13 to 18	-864 to +309	-72 to +43.2	-72 to +43.2	-500 (5)	

- (1) The flow velocity into the test drum was regulated by controlling flow rates through the system and by changing fueling inlets.
- (2) Different filter elements affected the polarity and magnitude of charge on the fuel. In this series of tests Element Sets number 1, 2, and 4 were used. Fuel charge represents the current density measured from the filter but of opposite polarity.
- (3) Current density readings were made about 8 seconds after flow started.
- (4) Field Strength observed at about 90% full, when fuel reached the top of the foam.
- (5) The field meter used for this study was limited in the maximum value it could sense (500 KV/m). Thus, a reading of 500 KV/m could indicate that the field strength was 500 KV/m or more.

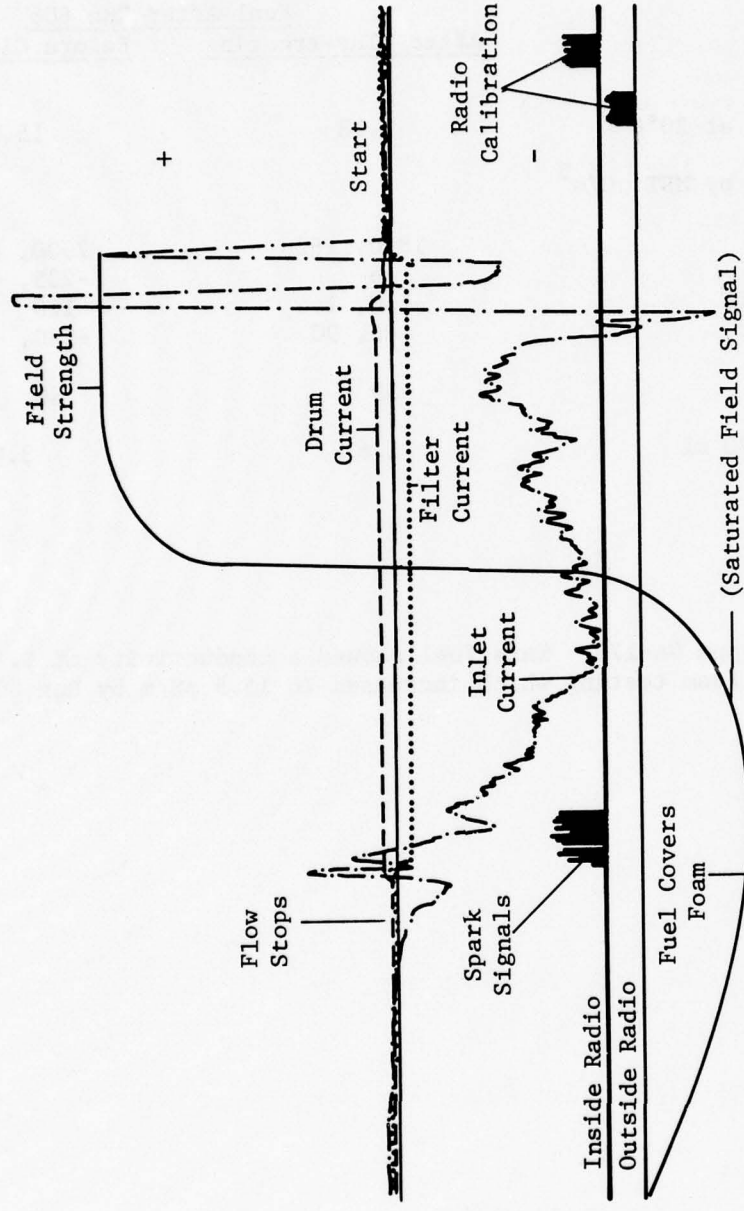
the field meter, the maximum value must be considered to be greater than 500 KV/meter. The maximum reading usually coincided with a final group of radio discharges. Figure 11, a recorder tracing for a blue foam test run, illustrates these observations.

In some experiments when the fuel reached the top of the foam with a froth on its surface the field meter reversed polarity from negative to positive as the froth collapsed. The residual positive charge sensed by the meter remained even after fuel was drained and relaxed very slowly to about 0.300 KV/meter.

In contrast with runs in red foam, the field meter readings with blue foam were negative in polarity; in fact regardless of the polarity of incoming fuel the field meter always registered negative charge on blue foam.

Because the initial tests with blue foam showed increased pro-static activity of the fuel compared with the preceding red foam tests, the next series with blue foam was made after clay-treating to a conductivity of 2 pS/m. Samples of the clay-treated fuel were then compared with the active fuel in laboratory tests. The data in Table 15 show the results. These MST tests showed that the more conductive fuel containing GA-178 and exposed to both red and blue foam was four times more active than clay-treated fuel with Type 10 paper and reversed in polarity with two of the other three separator papers tested.

Other observations made with clay-treated fuel on the blue foam were significantly different than with pro-static fuel.



Test Run No. 621
 (Jet A - Clay Treated)
 Fuel CD, $\mu\text{C}/\text{m}^3$ +238.1
 Inlet CD, $\mu\text{C}/\text{m}^3$ -10
 Drum CD, $\mu\text{C}/\text{m}^3$ +59.5
 Field Strength, KV/m - 500

Figure 11. Typical Recorder Tracing - Blue Foam

TABLE 15

LABORATORY DATA ON FUEL
EXPOSED TO BLUE FOAM IN RIG TESTS

	<u>Fuel After Run 606</u>	
	<u>After Clay-treating</u>	<u>Before Clay-treating</u>
Conductivity pS/m at 20°C	2.18	15.5
Charging Tendency by MST $\mu\text{C}/\text{m}^3$		
SP-10 Paper	1830, 1620	7500, 6600
C-709 Paper	48	-235, -300
V-614 Separator	150, 144	120
V-616 Separator	66, 90	-180, -78
Total Water, ppm	39	40
Existent Gum mg/100 mL	1.6	3.0

*Fuel contained 2 ppm GA-178. This fuel showed a conductivity of 1.75 pS/m @ 17°C after red foam testing which increased to 15.5 pS/m by Run 606.

- Discharges that were noted were far fewer but were also seen at the beginning of the run, where a charge collector was located and also at the end of the run. Radio signals were noted even when fuel entered uncharged. Removing the charge collector (after Run 613) eliminated the signals associated with its location as well as beginning signals.

- With clay-treated fuel, the filter placed a $+200 \mu\text{C}/\text{m}^3$ charge on fuel while the inlet itself added only a $+12 \mu\text{C}/\text{m}^3$ charge to fuel. The contribution of the blue foam itself to fuel as judged by drum current readings is about $+20 \mu\text{C}/\text{m}^3$.

- The field meter produced the same maximum negative readings of -500 KV/m at about 90% full with clay-treated fuel and showed the identical pattern of a sudden shift from positive to negative at the mid-point of filling as before.

- Increasing the initial inlet velocity to about 65 fps (most tests had been run at about 50 fps to prevent surging fuel from flooding the field meter and from overflowing the drum) did not produce any beginning radio signals even though the input charge reached over $+300 \mu\text{C}/\text{m}^3$.

- The persistent radio signals as fuel reached the top of the blue foam indicated that even with clay-treated fuel, the blue foam is much more active in charge accumulation and discharge than red foam.

Other clay-treated fuel tests (for purposes of comparison to red foam results) were made to evaluate the effect of inlet fuel velocity, and new filter elements.

Experiments with a short inlet containing a high velocity orifice which jetted fuel into a cavity in the top of the foam produced so much turbulence and rebound fuel that the drum could not be filled beyond 70% without splashing over the top (see Appendix F, Runs 625-630). Inlet charging was low ($-6 \mu\text{C}/\text{m}^3$) and the foam itself generated a charge density of about $20 \mu\text{C}/\text{m}^3$. A few sparks were noted.

Subsequent tests were made with a longer inlet containing the high velocity orifice. This inlet permitted high flow operations. Charging with Element Set #2, which had previously been used with red foam was low (see Section V-6-b (1), Runs 631-636, Appendix F) and few sparks were noted. In contrast to red foam tests, fuel became positively charged.

When the original filter elements (Set #1) were used, results similar to the first blue foam test series were obtained, i.e. spark discharges with both charged and uncharged fuels (Runs 637-642, Appendix F). Charging levels were low, however ($\sim 65 \mu\text{C}/\text{m}^3$ input fuel charge). (Element Set No. 3 proved to be unlike Set No. 2 and placed a low positive charge on fuel.)

A new set of filter elements (Set #4) raised charging levels ten-fold (i.e. from $-80 \mu\text{C}/\text{m}^3$ input fuel charge to about $-800 \mu\text{C}/\text{m}^3$) and increased spark discharge frequency (Runs 643-647, Appendix F). At the end of five tests, fuel conductivity had increased from 1.3 to 8 pS/m due to exposure to the new elements or to the blue foam. The fuel was again clay filtered to 0.5 pS/m conductivity.

To aid in analysis of inlet current measurements, the foam cavity around the inlet was widened to insure that the inlet

would not touch the foam (Runs 648-654, Appendix F). No significant changes were observed. The charge generated at the inlet was relatively low ($\sim 20 \mu\text{C}/\text{m}^3$). Radio discharges were noted with clay treated fuel (Runs 648-654) even when fuel was uncharged. When they disappeared installing the charge collector produced a signal once again.

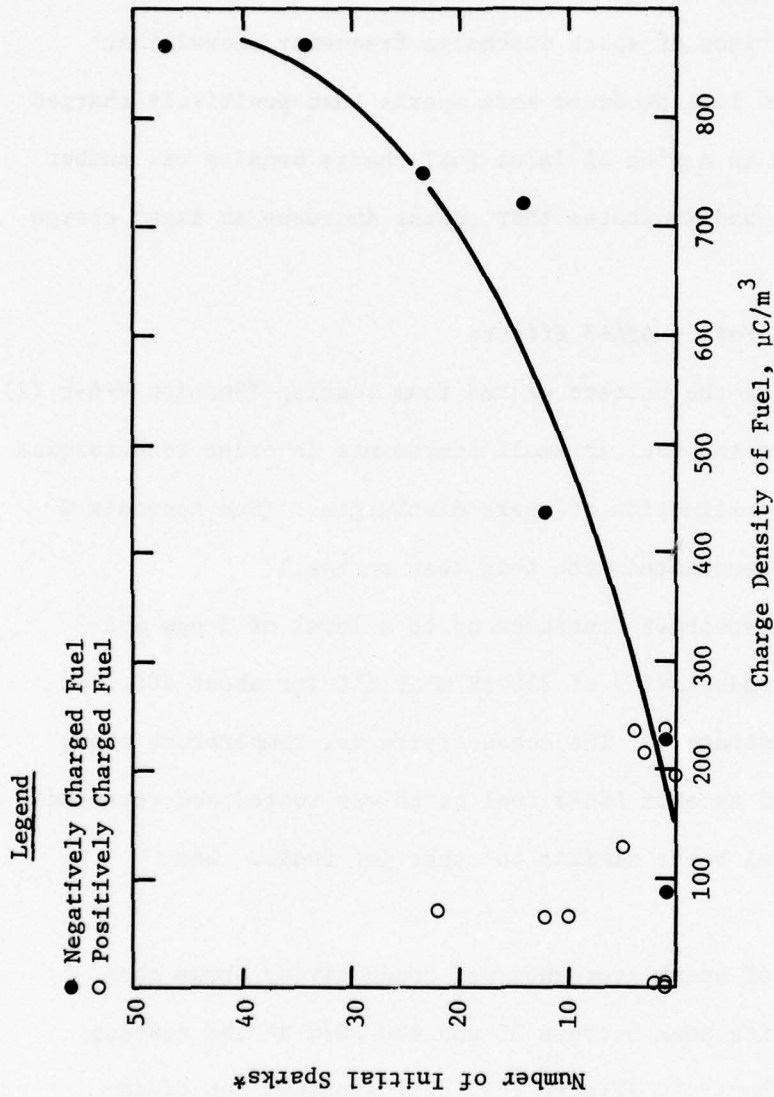
A comparison of spark discharge frequency showed that negatively charged fuel produced more sparks than positively charged fuel. (Figure 12 is a plot of inlet fuel charge density vs. number of initial sparks and indicates that sparks increase as input charge rises.)

(2) Blue Foam - ASA-3 Effects

Following the pattern of red foam testing (Section V-6-b (2)), ASA-3 was added to the fuel in small increments in order to determine the threshold for extinction of spark discharges. (See Appendix G for the raw data associated with this test series.)

Spark discharges continued up to a level of 3 ppm ASA-3 equivalent to a conductivity of 258 pS/m at 6°C (or about 800 pS/m at laboratory temperature. The conductivity vs. temperature chart that was developed as each ASA-3 fuel batch was tested and retested shows our test fuel to be similar to other jet fuels. See Section V-8).

A plot of spark frequency vs. conductivity shows that sparking reaches its peak between 50 and 100 pS/m at the testing temperatures of about 5°C (Figure 13), approximately ten times higher than the maximum with red foam (see Figure 9 for comparison).



* Sparks observed on radio during first 30% fill.

Figure 12. Spark Frequency vs. Input Charge on Fuel
Effect of Charge Polarity
Drum Filling Tests in Blue Foam
With Clay Treated Fuel
(Conductivity $\approx 1 \text{ pS/m}$)

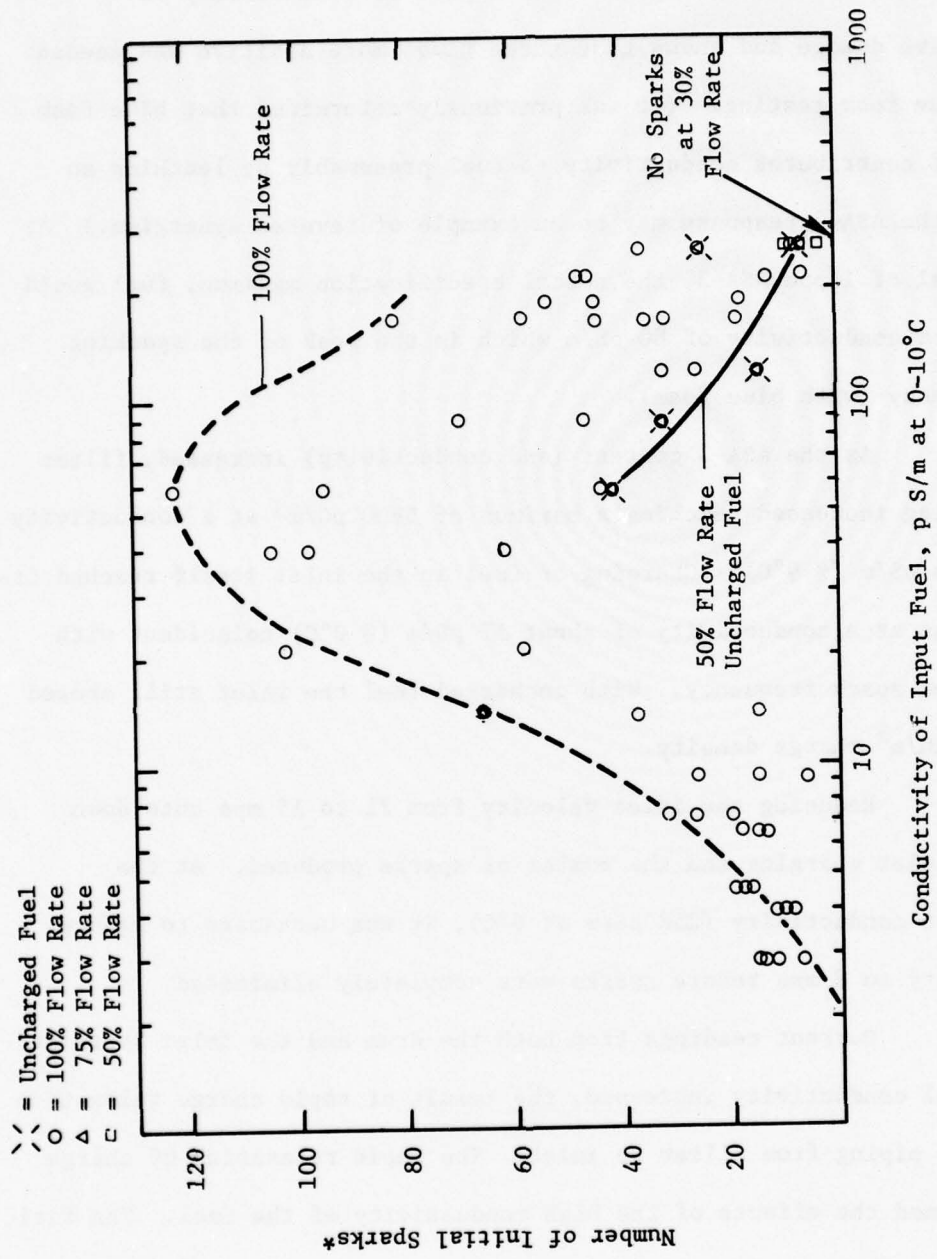


Figure 13. Spark Frequency vs. Input Fuel Conductivity
Drum Filling Tests in Blue Foam (Fuel 1 + ASA-3)
(High Velocity Inlet at Various Flow Rates)

* Sparks observed by radio during first 30% fill.

The additive response of clay-treated fuel exposed to blue foam was significantly less than the same clay-treated fuel exposed to red foam. Figure 14 is a plot of conductivity vs. additive dosage and shows that three times more additive was needed in blue foam testing. (It was previously determined that blue foam itself contributes conductivity to fuel presumably by leaching so that the ASA-3 response may be an example of reverse synergism.) At a level of 1 ppm ASA-3, the normal specification maximum, fuel would reach a conductivity of 80 pS/m which is the peak of the sparking frequency (with blue foam).

As the ASA-3 content (and conductivity) increased, filter charging increased reaching a maximum of $5800 \mu\text{C}/\text{m}^3$ at a conductivity of 166 pS/m (@ 9°C). Charging of fuel in the inlet itself reached its maximum at a conductivity of about 57 pS/m (@ 0°C) coincident with maximum spark frequency. With uncharged fuel the inlet still showed $2900 \mu\text{C}/\text{m}^3$ charge density.

Reducing the inlet velocity from 21 to 15 mps cuts down both inlet charging and the number of sparks produced. At the highest conductivity (258 pS/m at 6°C), it was necessary to reduce velocity to 8 mps before sparks were completely eliminated.

Current readings from both the drum and the inlet decreased as fuel conductivity increased, the result of rapid charge relaxation in the piping from filter to inlet. The rapid relaxation of charge confirmed the effects of the high conductivity of the fuel. The field meter readings continued to produce maximum (saturated) signals equivalent to -500 KV/m until a conductivity of 14 pS/m (@ 15°C) was

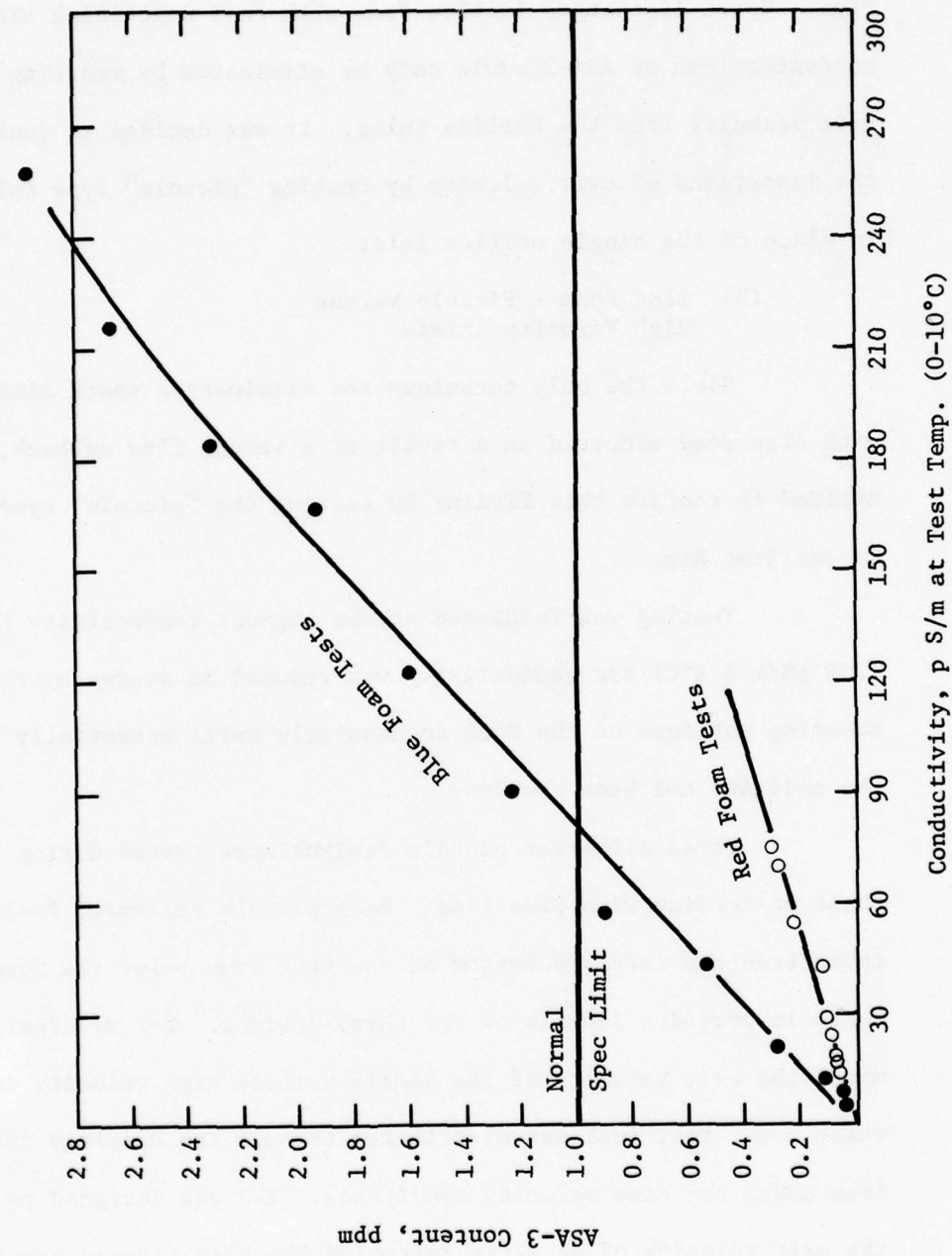


Figure 14. Response of Test Fuels to ASA-3
(Blue vs. Red Foam Tests)

attained. After that, maximum field meter readings dropped but still registered significant field strengths with fuel of high conductivity.

This series of experiments brought out one very important fact: Spark discharges in blue foam with fuel containing high concentrations of ASA-3 could only be eliminated by reducing the exit velocity from the fueling inlet. It was decided to confirm the importance of exit velocity by testing "piccolo" type inlets in place of the single orifice inlet.

(3) Blue Foam - Piccolo Versus
High Velocity Inlets

Since the only technique for eliminating spark discharges with blue foam occurred as a result of a severe flow cutback, we decided to confirm this finding by testing the "piccolo" type inlet in our Test Rig.

Testing was initiated at the highest conductivity level (258 pS/m @ 6°C) and conductivity was reduced in stages by clay treating portions of the fuel successively until essentially all of the additive had been removed.

Three different piccolo designs were tested during this phase of testing with blue foam. Each piccolo delivered fuel through three branches into the bottom of the test drum below the foam. Table 16 provides details of the three designs. P-1 was designed to match the exit velocity of the single orifice high velocity inlet which meant that fuel was distributed through ten openings into the foam under the same velocity conditions. P-2 was designed to match the exit velocity of an early Fairchild Republic piccolo specification for the A-10 aircraft. (The current production inlet design for the

TABLE 16
INLET DESIGN DETAILS

<u>Inlet Type</u>	<u>Code</u>	<u>No. of Holes</u>	<u>Hole Diameter cm</u>	<u>Max. Exit Velocity⁽²⁾ m/s(fps)</u>	<u>Tested in Drum</u>	<u>Cell⁽³⁾</u>
Single Orifice	S	1	1.5	21 (68)	X	X
Multiple Orifice	P-1 ⁽¹⁾	10	0.46	22 (72)	X	
	P-2	19	0.51	9.4 (30)	X	X
	P-3	19	0.71	4.8 (15)	X	
	P-4	23	0.86	3.3 (10)		X

- (1) P-1, P-2, P-3 are three-branched with 5 cm orifice spacing.
P-4 is straight pipe with 5 cm orifice spacing (used only in the Bladder Cell Tests).
- (2) The actual discharge velocities from each of the holes may differ slightly since all orifices for any one piccolo had identically sized holes and since some holes are further downstream. The exit velocities reported are the average exit velocities at maximum flow conditions neglecting flow coefficient effects and based on the number and sizes of the orifices.
- (3) Bladder Cell Tests are described in Section 5.7 of this report.

A-10 will have much lower velocities than that which was originally tested in their small-scale test rig.) P-3 represented the same type of piccolo with enlarged holes to cut the exit velocity to half that of the Fairchild design. Note that the range of fuel conductivities tested varied with each piccolo that was evaluated. (Experimental details are presented in Appendix H.)

• P-1 Piccolo

With the P-1 piccolo, sparks were reduced in frequency but not completely eliminated by introducing charged fuel into blue foam at maximum flow rates. Figure 15 is a plot of spark frequency vs. input fuel conductivity. For the range of conductivities 130 to 260 pS/m at about 5°C, one to three sparks were observed compared with 36 to 80 for the single high velocity orifice (see Figure 15). Uncharged fuel also produced sparks through the P-1 piccolo. The comparison between Figure 13 and 15 suggests that distribution of charged fuel has a greater effect on sparks than velocity into the foam.

• P-2 Piccolo

With the P-2 piccolo (less than half the exit velocity of the P-1) sparks could only be eliminated at a conductivity of about 100 pS/m at 5°C by operating at 50% flow rate. With uncharged fuel, sparks disappeared at about 27 pS/m.

Spark frequency increased as additive was removed and reached a maximum (30-40 sparks) at a conductivity of 5-10 pS/m. Under these conditions a flow cutback to 30% of normal was needed to eliminate sparks.

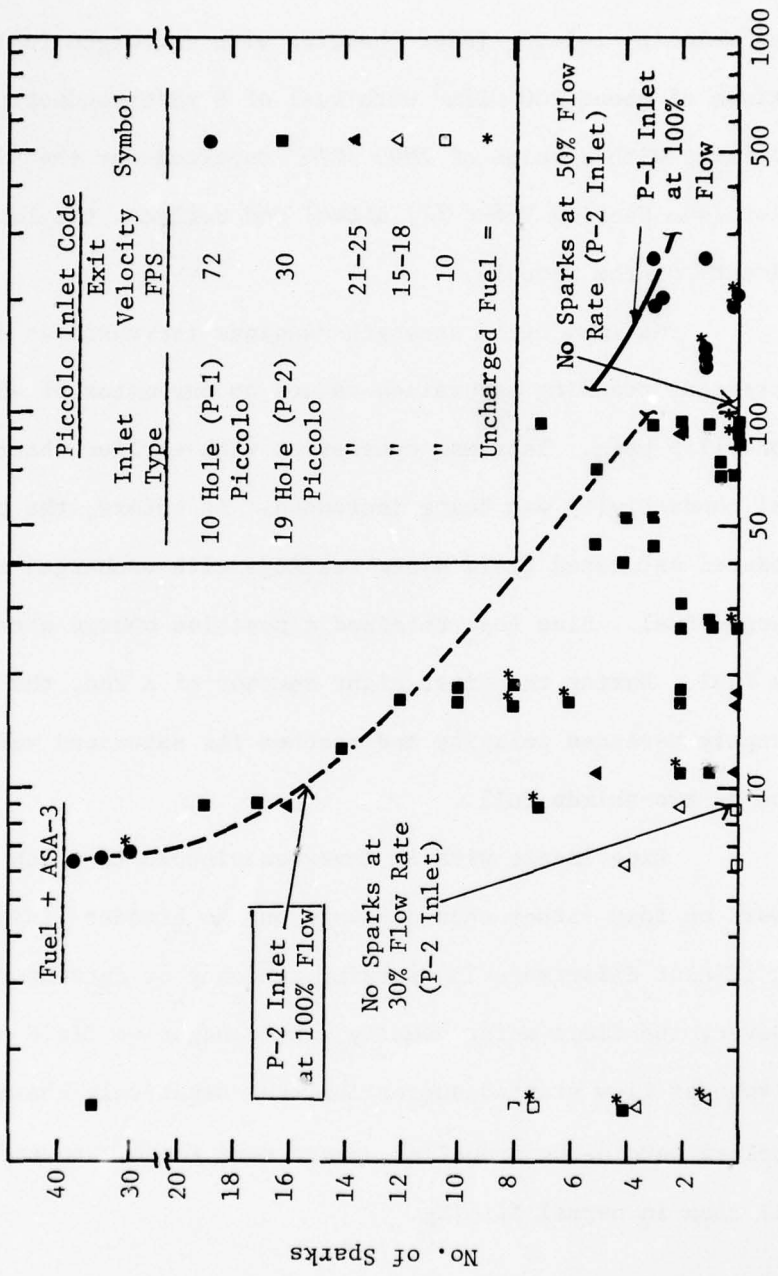


Figure 15. Spark Frequency vs. Input Fuel Conductivity
Drum Filling Tests in Blue Foam
(Piccolo Type Inlets)

Filter charging (with Piccolo P-2) reached a maximum between 50 and 100 pS/m conductivity. The same observation was made as additive concentration was increased in earlier tests with the high velocity inlet. Inlet charging with uncharged fuel showed a maximum of about $200 \mu\text{C}/\text{m}^3$ with fuel of 8 pS/m conductivity. This contrasts with a value of $2900 \mu\text{C}/\text{m}^3$ reported for the high velocity inlet (see Section V-6-c (2) above) and reflects the lower exit velocity of the piccolo.

Maximum field strength readings increased as conductivity decreased, reaching saturation values on our meter of -500 KV/m at about 17.5 pS/m. This was consistent with earlier observations when fuel conductivity was being increased. As before, the blue foam produced saturated field meter readings with uncharged as well as charged fuel. Blue foam retained a positive charge after draining the fuel. During the first eight seconds of a run, the field abruptly reverses polarity and reaches its saturated value when the drum is two-thirds full.

Experiments with an inverted piccolo in which fuel impinges upward on foam rather than downward on the bladder lining showed no significant difference in sparking tendency or current readings. However, the field meter usually sensed negative field momentarily as soon as flow started suggesting that negatively charged fuel droplets were being propelled upward more rapidly toward the field mill than in normal filling.

- Blue Foam Testing with Piccolo Inlet -
Clay Treated Fuel

Final cleanup of fuel to remove all traces of ASA-3 proved to be very difficult but a combination of clay filtering and fresh fuel addition eventually flushed additive residues from the system. Since tests with low concentrations of ASA-3 had shown that only reduced flow rate eliminated sparks, a new piccolo (P-3) was built (see Table 16) to produce a maximum exit velocity of 4.8 m/s (15 ft. per second). Tests of the P-2 and P-3 piccolo produced the following results with clay treated fuel of about 1 pS/m conductivity. (Details of test runs appear in Appendix H, Table H.2.)

The lower velocity inlet (p-3) reduced sparks from 62 to 22 at maximum flow rate. Uncharged fuel also produced a few sparks and even a flow cutback to 50% of maximum still showed one discharge signal (Run 6104).

Unlike the tests with the high velocity inlet using clay treated fuel (Figure 13) none of these sparks occurred during initial filling through the piccolos but throughout the filling cycle and also at the end of the run as fuel reached the top of the foam.

In most other respects--filter charge level, inlet current, drum current and field strength--the tests with clay treated fuel using the piccolo were comparable to the earlier tests with similar fuel using the high velocity orifice.

d. Aluminum Mesh Foam

"Explosafe", an aluminum mesh tank filling material produced by Vulcan Industrial Packaging of Canada, was evaluated in the Drum Filling Rig using clay-treated fuel.

Following tests using both the P-3 type piccolo inlet and the high velocity single orifice inlet, the same fuel was tested with both inlets in an empty drum containing only the bladder so that results with the aluminum mesh could be compared under identical conditions with and without polyurethane foam. Details of test runs appear in Appendix I. Several significant observations were made from the resulting test data:

- No sparks were detected in "Explosafe" when flowing at maximum rate through either the high velocity inlet or the P-3 piccolo inlet.

- Testing the same fuel in the empty drum plus bladder liner after removing the aluminum mesh produced unexpected sparks. These signals were found to result from very small pieces of mesh which broke off during removal and acted as unbonded metallic charge collectors. When these pieces were removed from the drum, sparks ceased. The turbulence produced by the high velocity orifice evidently sweeps the metal chips from the bottom of the drum and they make contact with the grounded inlet, causing discharge.

- With the aluminum mesh in the drum in contact with the inlet, it was not possible to separate signals from the drum and the inlet. However, good charge balances were observed (see Runs 700-706, Appendix I). Therefore, it was necessary to compare field meter readings to define the role of the aluminum mesh in charge generation.

- With the aluminum mesh in the drum, the field meter is looking at grounded metal. The field meter did not sense charged fuel until it approached the top of the aluminum mesh, then in the

last six seconds the meter reading increased from zero to a maximum value as fuel covered the mesh. When these maximum values -- all at the same percent full -- are compared as in Table 17, it is interesting to note that when the drum is filled with aluminum mesh the field strength is less than the value measured with either an empty drum or a drum filled with blue polyurethane foam. This suggests that the metal mesh is conducting charge to ground to a significant extent. However, the data on uncharged fuel (shown in parentheses in Table 17) show no difference with the aluminum mesh while the empty drum readings are much lower as expected. It would appear that the aluminum mesh behaves to a small degree like the plastic foam in providing a large charge separating surface.

- The advantages of the piccolo inlet in reducing field strength can be seen in Table 17 for both the empty drum and the aluminum mesh. However, the blue foam is unique. Regardless of charge or inlet velocity, it produces field strengths which saturate our meter at about 60% full.

7. BLADDER CELL TESTS

In order to evaluate a geometry somewhat closer to that of an actual aircraft fuel tank, our program provided for testing in a 90 gallon bladder cell. (The cell was modified with a viewing window in order to observe spark discharges, but otherwise was instrumented similarly to the drum; for measuring field strength, streaming current (i.e. charge density), and static discharges.)

Both red and blue foams were tested with various inlets in the Bladder Cell, starting with clay-treated fuel. A new,

TABLE 17

ALUMINUM MESH VS BLUE FOAM
DRUM TESTS (CLAY TREATED FUEL)

Inlet Type ⁽²⁾ Inlet Velocity, m/s	Max Field Strength (90% full) KV/m ⁽¹⁾		
	S 22	S 10	P-3 5
Empty Drum	>500 (45)	200 (11)	150 (20)
Al. Mesh	200 (180)	--	20 (15)
Blue Foam	>500 (>500)	>500	>500 (>500)

(1) All values in the table are negative. The field meter used for this study was limited in the maximum value it could sense (500 KV/m). Thus, a reading of 500 KV/m could indicate that the field strength was 500 KV/m or more.

(2) S = single orifice (High Velocity)
P = multiple orifice (Piccolo)

straight pipe piccolo (P-4) containing 23 holes and providing a maximum exit velocity of 3 meters per second was tested for comparison with P-2 and P-3. Since sparks were detected at maximum flow rates, increments of ASA-3 were added to the fuel until signals were eliminated. Table 18 summarizes the experimental sequence, as it occurred, for the entire Bladder Cell test series. The subsections below discuss the base case tests (empty cell, fuel without ASA-3), and the testing with red and blue foams.

a. Base Case

In order to provide a baseline for our observations, initial Bladder Cell experiments were performed with clay-treated fuel and the empty bladder. Two piccolo inlets (P-2 and P-4) were tested. (Appendix J has individual test details.)

With input fuel charge levels of about $400 \mu\text{C}/\text{m}^3$ and the P-4 (3 m/s) inlet, there were no discharges. Uncharged fuel also produced no discharges. The corresponding field strengths were low (-100 KV/m, charged; -12 KV/m, uncharged). It appeared as though the distribution of charge through multiple orifices coupled with the reduction of inlet flow velocity was effective in reducing discharges in the empty cell.

However, when the P-2 (10 m/s) inlet was installed in the empty cell spark discharge signals were recorded. The input fuel charge during these experiments measured about $300 \mu\text{C}/\text{m}^3$. The corresponding field strength measurements showed maximum readings (-500 KV/m). The effect of increased flow velocity seemed apparent. With uncharged fuel spark signals disappeared.

TABLE 18
BLADDER CELL TESTS SUMMARY

<u>Sequence</u>	<u>Foam</u>	<u>Additives</u>	<u>pS/m</u>	Spark Occurrence ⁽¹⁾ <u>Inlet</u>		
				<u>HV</u>	<u>PIC 2</u>	<u>PIC 4</u>
<u>1000-1013</u>		<u>None (Clay treated)</u>	<u>1.4</u>		<u>Y</u>	<u>N</u>
2000-2012	Red	CI + AIA	1.4	Y		Y
3000-3008	Blue	CI + AIA	4.4		Y	Y
2013-2017	Red	CI + AIA	3.3		N	
2018-2023	Red	CI + AIA + ASA-3	6.8		Y	
3009-3023	Blue	CI + AIA + ASA-3	6.8	Y	Y	
2024-2041	Red	CI + AIA + ASA-3	7.3	Y	N	
3024-3027	Blue	CI + AIA + ASA-3	8.7		Y	
3028-3037	Blue	None (Clay treated)	2.5		Y	Y
2042-2047	Red	None (Clay treated)	3.1	Y		
2048	Red	ASA-3	12.4	N		
2049-2050	Red	ASA-3	6.8	N		
3038-3039	Blue	ASA-3	6.8	Y		
3040-3057	Blue	CI + AIA + ASA-3	9.9	Y	Y	
2051-2057	Red	CI + AIA + ASA-3	9.6	Y	N	
2058-2060	Red	CI + AIA + ASA-3	33	N	N	
3058-3069	Blue	CI + AIA + ASA-3	33	Y	Y	N
3070-3075	Blue	CI + AIA + ASA-3	65		Y	N
3076-3080	Blue	CI + AIA + ASA-3	127		Y	
3081-3084	Blue	CI + AIA + ASA-3	180		Y	
3085-3087	Blue	CI + AIA + ASA-3	250		N	
3088-3089	Blue	CI + AIA + ASA-3 + GA 178	293		N	
3090-3094	Blue	CI + AIA + ASA-3 + GA 178		Y		

Threshold values

(1) Y = Yes
N = No

(2) Inlet Code: HV = high velocity; PIC 2 = Piccolo #2 (10 m/s velocity);
PIC 4 = Piccolo #4 (3 m/s velocity)

The field meter readings were also significantly lower (-35 KV/m versus -500 KV/m for the charged fuel).

b. Piccolo-ASA-3 Studies

Following base case testing in the bladder cell, the investigation into foam/inlet/additive effects proceeded with red and blue foams. The objective of the testing was to determine the additive concentration required for elimination of discharges with each foam and inlet configuration.

(1) Red Foam

With the high velocity inlet and non-additive fuel, discharge signals were observed at the same input charge level as drum tests ($\sim 700 \mu\text{C}/\text{m}^3$). With fuel containing the JP-4 additive package (corrosion inhibitor and anti-icing additive) more sparks were produced. (Appendix K has the raw data for the bladder cell/red foam tests.) Some were even visible through the viewing window.

When ASA-3 was added to the fuel, discharges continued with the high velocity inlet until the fuel conductivity reached 33 pS/m, the same value noted in earlier drum testing (Section V-6-b (2)).

Energy measurements of the discharges were made using an oscilloscope, as discussed in Section V-7-c below.

Two piccolo inlets (P-2 and P-4) were tested in this series. With the P-2 (10 m/s velocity) no sparks were detected with non-additive fuel (containing C.I. + A.I.A.) at input charge levels of $1000 \mu\text{C}/\text{m}^3$. The addition of ASA-3 to the fuel did not change these observations. (Although field strength and charge levels decreased as the conductivity improver began to show its effect.) In the case of the P-4 inlet (3 m/s velocity), a few

sparks were recorded with fuel containing the JP-4 additive package (see Runs 2005-2006, Appendix K). These signals occurred at an input charge level greater than $2000 \mu\text{C}/\text{m}^3$.

A comparison of the spark frequency for the conductivity range studied shows, as expected, that the P-4 multiple orifice inlet is non-critical at a much lower fuel conductivity than the single orifice high velocity inlet. Figure 16 illustrates these observations.

(2) Blue Foam

The blue foam testing in the bladder cell followed the same general sequence as that of the red foam: All three inlets (high velocity, P-2, P-4) exposed to the same fuel quality until discharge signals were eliminated. (Appendix L contains the raw data for this test series.)

The high velocity inlet was quite active. Experiments in the cell were similar to those performed in the drum (see Section V-6-c (2)). Sparks were still being recorded at a fuel conductivity of 293 pS/m. (Spark energy measurements were made and, at lower conductivities, time-exposure photos were made. Section V-7-c describes these energy measurements.)

With the P-2 (10 m/s velocity) inlet sparks were eliminated at 250 pS/m fuel conductivity. With uncharged fuel passing through this inlet, sparks were recorded at a conductivity of 65 pS/m. The P-4 inlet was somewhat more effective. Sparks were eliminated at 33 pS/m conductivity.

With uncharged fuel there were no discharges with the P-4 inlet. P-2, on the other hand, required a conductivity of 10 pS/m to eliminate discharges with uncharged fuel.

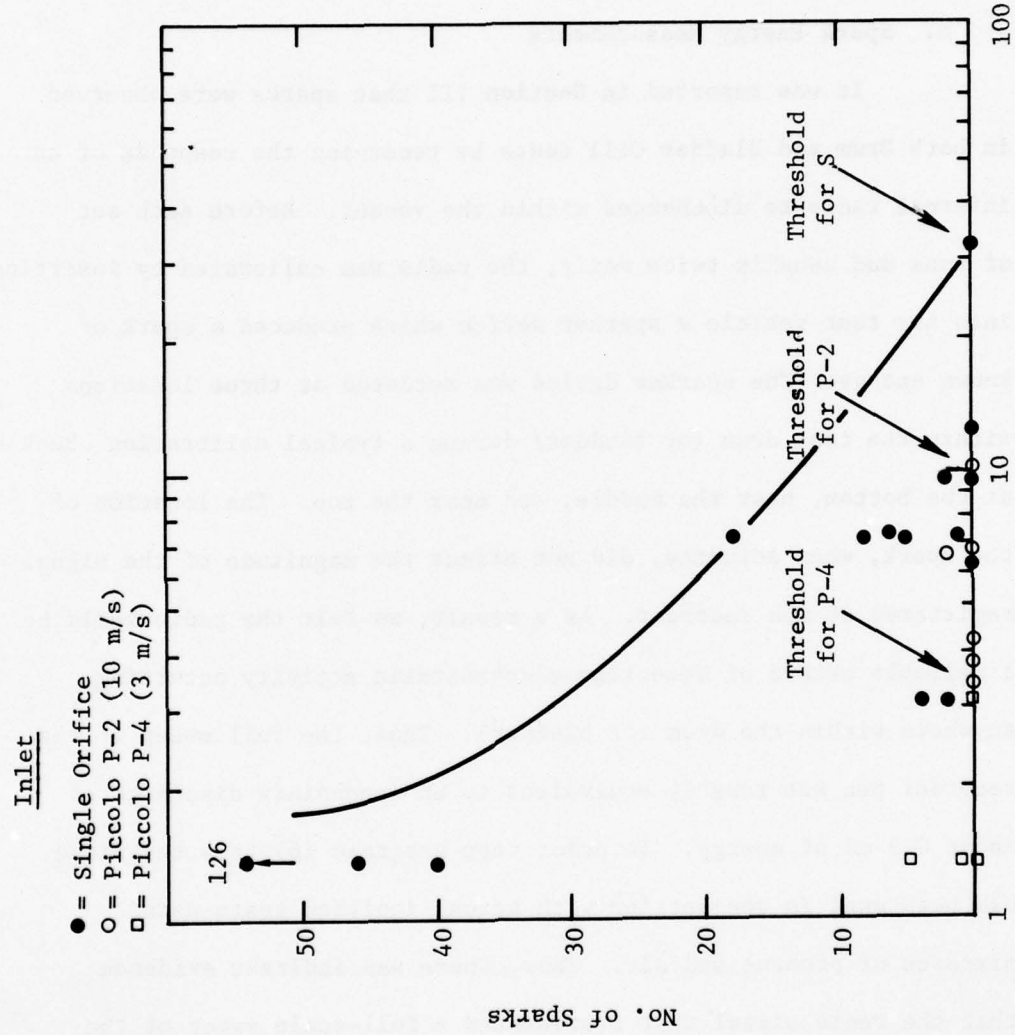


Figure 16. Spark Frequency vs. Input Fuel Conductivity
 Bladder Cell Tests - Red Foam
 Fuel + ASA-3

A plot of spark frequency versus fuel conductivity (Figure 17) for the inlets tested shows the effect of inlet fuel velocity on spark discharge. As predicted, the higher the flow velocity (for a given conductivity) the more frequent are the discharges.

c. Spark Energy Measurements

It was reported in Section III that sparks were observed in both Drum and Bladder Cell tests by recording the response of an internal radio to discharges within the vessel. Before each set of runs and usually twice daily, the radio was calibrated by inserting into the test vehicle a sparker device which produced a spark of known energy. The sparker device was actuated at three locations within the test drum (or bladder) during a typical calibration check -- at the bottom, near the middle, and near the top. The location of the spark, when actuated, did not affect the magnitude of the signal registered at the recorder. As a result, we felt the radio would be a reliable method of detecting electrostatic activity occurring anywhere within the drum (or bladder). Thus, the full sweep of the recorder pen was roughly equivalent to an incendiary discharge of about 0.3 mJ of energy. In prior test programs (6) this technique had been used in conjunction with actual ignition tests using mixtures of propane and air. Thus, there was indirect evidence that the radio signal that represented a full-scale sweep of the pen was detecting a potentially incendive spark. It should be pointed out, however, that the radio signals were not intended to quantify the energy from any discharge. Rather, the radio signal

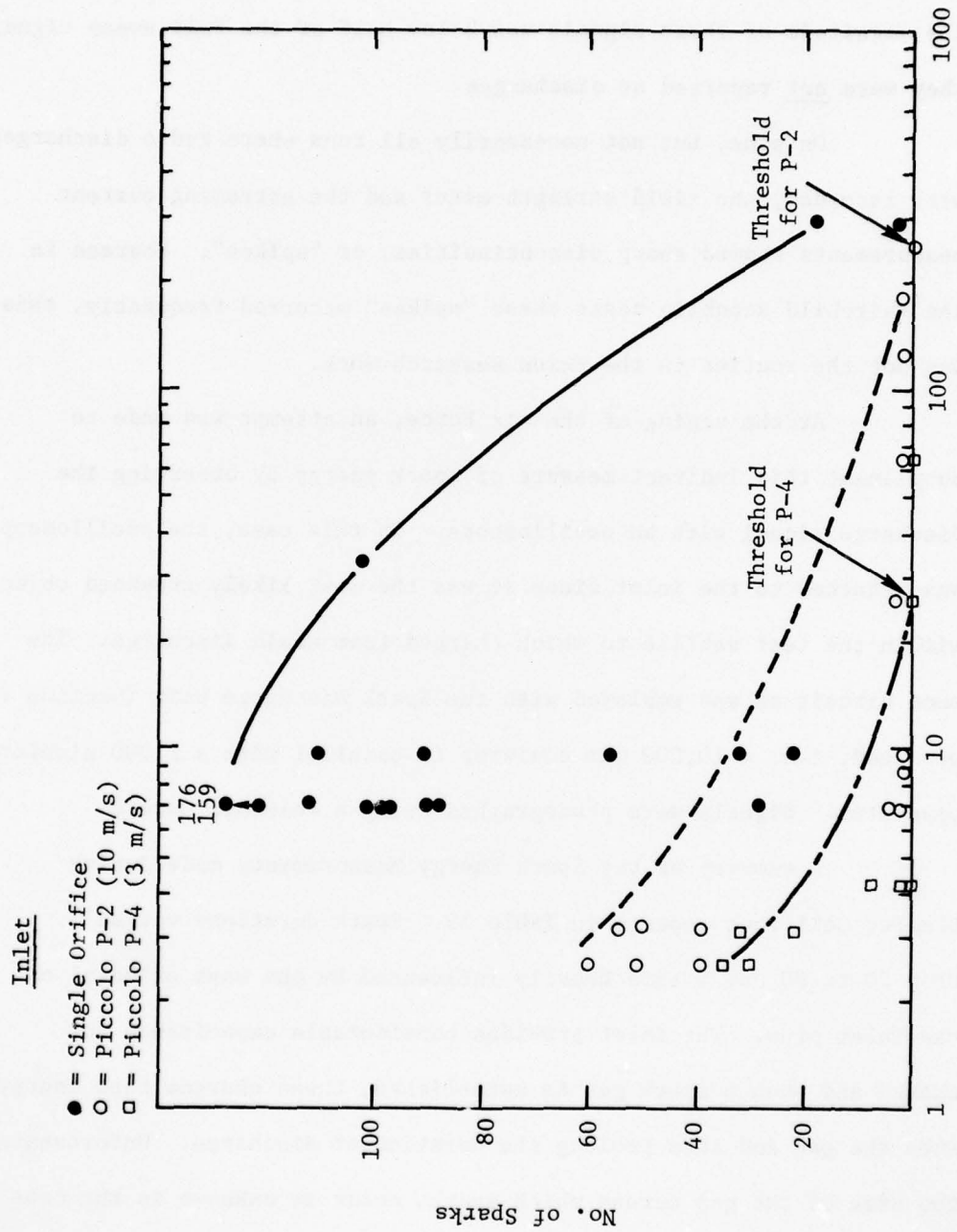


Figure 17. Spark Frequency vs. Input Fuel Conductivity
Bladder Cell Tests - Blue Foam
Fuel + ASA-3

was used to record the occurrence of discharge, on a simple "Yes" or "No" basis. The fact is, however, that we did record radio signals of different magnitude on the recorder during the test runs. Where the magnitude of these signals was below half of the full sweep signal they were not reported as discharges.

On some, but not necessarily all runs where radio discharges were recorded, the field strength meter and the streaming current measurements showed sharp discontinuities, or "spikes". Whereas in the Fairchild Republic tests these "spikes" occurred frequently, this was not the routine in the Exxon Research work.

At the urging of the Air Force, an attempt was made to supplement this indirect measure of spark energy by observing the discharge signal with an oscilloscope. In this case, the oscilloscope was attached to the inlet since it was the most likely grounded object within the test vehicle to which charged foam would discharge. The same circuit as was employed with the Spark Discharge Unit (Section V-4) was used, i.e. a 10,000 ohm resistor in parallel with a 1,000 picofarad capacitor. Signals were photographed using a Polaroid Camera.

A summary of the Spark Energy Measurements made during Bladder Cell runs appears in Table 19. Spark durations varied from 20 to 80 μ s, a time heavily influenced by the mass of metal of the inlet pipe. The inlet provides considerable capacitance for charge and when a spark gap is established, these charges feed energy into the gap and thus prolong the duration of discharge. Unfortunately, the size of the gap across which sparks occur is unknown in the case of the Bladder Cell configuration (unlike the Spark Discharge Unit tested in Section V-4) and hence the breakdown voltage cannot be determined.

AD-A061 450

EXXON RESEARCH AND ENGINEERING CO LINDEN N J
STATIC ELECTRICITY HAZARDS IN AIRCRAFT FUEL SYSTEMS.(U)

F/G 21/4

AUG 78 W G DUKEK, J M FERRARO, W F TAYLOR
EXXON/GRUS.1PEB.78 AFAPL-TR-78-56

F33615-77-C-2046

NL

UNCLASSIFIED

2 OF 3
AD
A061450

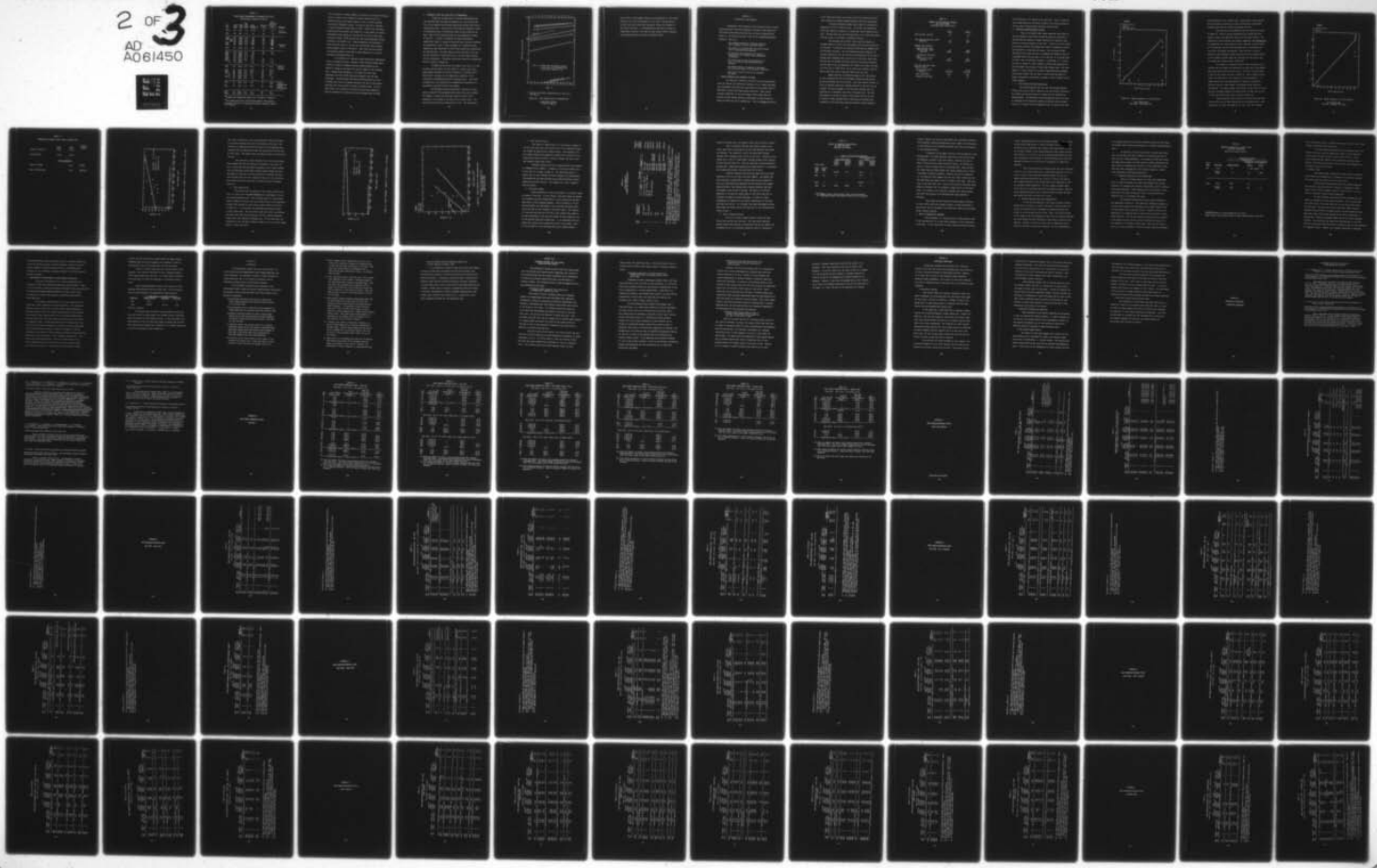


TABLE 19

SPARK ENERGY MEASUREMENTS IN BLADDER CELL TESTS
(Oscilloscope reading from inlet)

Run No.	Inlet Type	Foam Type	Fuel Cond pS/m	Peak Energy, V	Duration μ s	Transfer, nC	Calc. Charge ⁽¹⁾	Remarks
2026	HV	Red	7.3	(2.3)	80	(2.3)		() = Estimated
2027	HV	Red	7.3	10	60	10		
3018	HV	Blue	6.8	50	50	50		
3019 init	HV	Blue	6.8	170	20	<u>170</u>		
mid	HV	Blue	6.8	200	30	<u>200</u>		
3020	HV	Blue	6.8	200	25	<u>200</u>		
3021	HV	Blue	6.8	180	25	<u>180</u>		Uncharged fuel
3023	HV	Blue	6.8	600	40	<u>600</u>		
3029	P-2	Blue	2.5	10	20	10		
3030	P-2	Blue	2.5	10	20	10		
3031	P-4	Blue	2.5	(2)				
3033	P-4	Blue	2.5	(2)				
3036	P-4	Blue	3.1	0.7	50	0.7		
3037-1	P-4	Blue	3.1	2	30	2		
-2	P-4	Blue		0.8	20	0.8		
3041	HV	Blue	9.9	>0.4	40	>0.4		Additive package
3042	HV	Blue	9.9	>0.25	30	>0.25		
3043	HV	Blue	9.9	>0.5	25	>0.5		
3044-1	HV	Blue	9.9	>1.5	35	>1.5		
-2	HV	Blue	9.9	>4	40	>4		
3045-1	HV	Blue	9.9	75	20	75		
-2	HV	Blue	9.9	75	20	75		
3049	HV	Blue	9.9	150	25	<u>150</u>		Sparks photographed
3051	HV	Blue	9.9	200	30	<u>200</u>		Sparks photographed
3055	P-2	Blue	9.9	0.1	35	0.1		
3056	P-2	Blue	9.9	0.15	30	0.15		

(1) Charge (Q) transferred based on $Q = CV$ where $C = 1000 \text{ pF}$.

(2) No sparks detected by oscilloscope despite radio signals.

Underlined values of Q represent potentially incendive sparks,
i.e. $>140 \text{ nC}$.

For this reason, it seemed logical to calculate the energy of discharge merely in terms of the coloumbs of charge transferred from the observed voltage rise without regard to time or without assuming a particular breakdown voltage. In only two runs was it possible to obtain measurable sparks with red foam. However with blue foam, signals were both numerous and energetic; it was possible to clearly distinguish energy levels as a function of the type of inlet used. During one series, visible sparks were seen and photographed through a window in the Bladder Cell. These photographs show pinpoints of light around the inlet at the time the oscilloscope was recording charge transfer levels of 150-200 nC. This level has been related to incendiary sparks in work done by Shell Thornton in a test rig containing polyurethane foam (7).

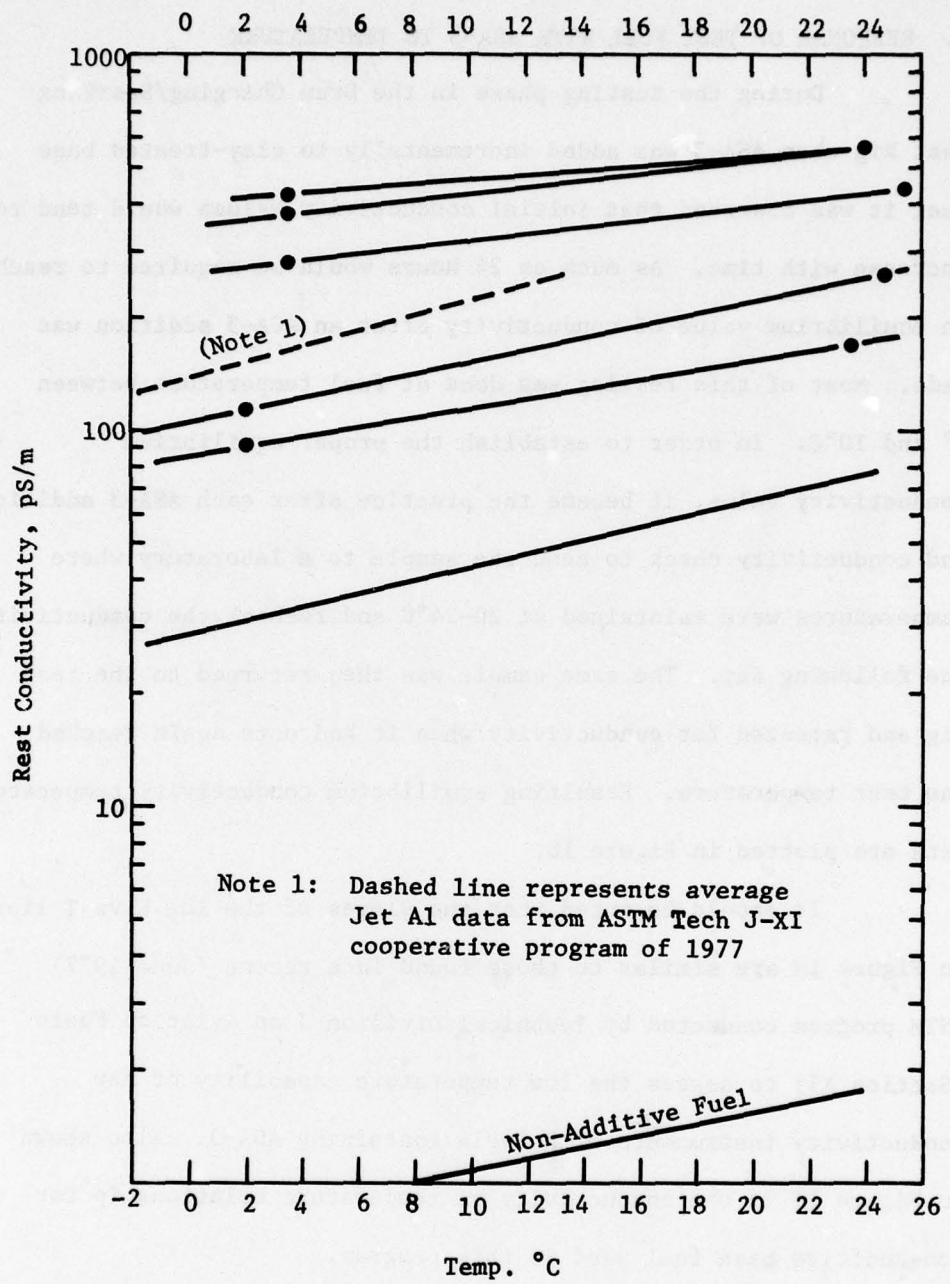
It is difficult to interpret these oscilloscope measurements except in comparative terms. Whether a spark contains enough energy actually to ignite a flammable fuel/air mixture depends on the density of energy in the spark core and the length of the discharge path. Comparatively speaking, it is evident that blue foam discharges are about 10-100 times more energetic than red foam discharges. The measurement that shows red foam sparks to be low in energy should not be accepted literally; the fact is that several ignitions have occurred with red foam in aircraft tanks. On this basis alone, one is bound to conclude that blue foam represents a greater probability of ignition by static discharge than red foam.

8. RESPONSE OF TEST FUEL WITH ASA-3 TO TEMPERATURE

During the testing phase in the Drum Charging/Sparking Test Rig when ASA-3 was added incrementally to clay-treated base fuel it was observed that initial conductivity values would tend to increase with time. As much as 24 hours would be required to reach an equilibrium value of conductivity after an ASA-3 addition was made. Most of this testing was done at fuel temperature between 0° and 10°C. In order to establish the proper equilibrium conductivity value, it became the practice after each ASA-3 addition and conductivity check to send the sample to a laboratory where temperatures were maintained at 20-24°C and recheck the conductivity the following day. The same sample was then returned to the test rig and retested for conductivity when it had once again reached the test temperature. Resulting equilibrium conductivity temperature data are plotted in Figure 18.

It should be noted that the slopes of the log K vs T line on Figure 18 are similar to those found in a recent (June 1977) ASTM program conducted by Technical Division J on Aviation Fuels (Section XI) to assess the low temperature capability of new conductivity instruments with fuels containing ASA-3. Also shown in Figure 18 is the conductivity vs temperature relationship for non-additive base fuel used in this program.

The difference between equilibrium conductivity values shown in Figure 18 and non-equilibrium values can be quite marked. For example, a blend with ASA-3 was tested at 52 pS/m at 1°C originally, but retested at 107 pS/m at 2°C 24 hours later. The same blend shows 200 pS/m conductivity at 24°C. The conductivity



* Typical equilibrium conductivities of test Jet A plus ASA-3.

Figure 18. Fuel Conductivity Vs. Temperature*

(Equilibrium Values)
(Jet A + ASA-3)

values shown in Data Summary Sheets in the appendices to this report represent the actual measurements at the time of testing since it is felt that these values more accurately reflect the response of the foam to the fuel. In interpreting the test data in terms of conductivity criteria to be used for fuel quality control purposes, the equilibrium values in Figure 18 should be used.

SECTION VI

DISCUSSION OF TEST RESULTS

Experimental data reported in the previous section on static charge generation and spark discharge in filling a tank packed with reticulated polyurethane foam with jet fuel must be analyzed with respect to the factors that play a role in the charging/discharging mechanism. These are:

- the charging tendency of different foams and their tendency to retain separated charge
- the effect of localized fuel velocities through foam on charging and discharging
- the quantity and distribution of charge in flowing fuel as it affects foam charging and discharging
- the pro-static activity and conductivity of fuel as it affects foam charging and discharging
- the spark frequency and energy of discharge with different foams, fuels and inlet conditions
- the role of charge collectors in promoting discharges

1. CHARGE GENERATION AND RETENTION OF FOAMS

The dielectric properties of each of the five polyurethane foams are similar, the dielectric constant of 3 to 4 being 50% higher than hydrocarbon fuel while the conductivity of the polymer (1400 to 8600 pS/m) is about 1000 times greater than fuel. These values represent properties of the bulk polymer itself rather than the surface on which charges separate; differences in these properties among the foams have little significance. That the surface properties

of the foams vary widely can be seen in both the laboratory and rig tests conducted to measure charging tendency under flow conditions.

Laboratory charging tendency data (Table 20) obtained are expressed as $\mu\text{C}/\text{m}^3$ of fuel/g of foam. In the MST test identically sized foam samples are exposed to flowing fuel under standard velocities. The data show that blue foam generates 2 to 3 times more charge than the orange or red foams of equivalent porosity.

Rig charging tests provide a more realistic measure of charging tendency of foam since much higher flow rates and velocities are attained. In Table 20, the laboratory MST data are compared with two different rig tests. The Foam Charging rig data represent the currents measured off the test section containing about 36 g of foam through which uncharged clay treated fuel is flowing at $.00315 \text{ m}^3/\text{s}$. The Drum Test and Bladder Cell data represent the currents measured from the Drum or Cell as uncharged clay treated fuel enters the drum at a flow rate of $.00347 \text{ m}^3/\text{s}$. By all three test criteria, the blue foam is much more prone to generate charge than red foam.

Charge retention of separated charge on the foam surface is best illustrated by the field strength readings during filling and after draining fuel from the drum. The lower portion of Table 20 lists the maximum field meter readings observed at 90% full and the residual fuel meter readings of the foam after draining fuel and preparing for a subsequent test about 10 minutes later. The blue foam appears to retain ten times or more charge than the red and to develop a higher maximum field on filling with uncharged fuel. In addition, blue foam always developed negative charge regardless

TABLE 20

**SUMMARY OF FOAM CHARGING TENDENCY
LAB VS RIG TESTS
(Uncharged Clay Treated Fuel)**

	<u>Red</u>	<u>Blue</u>
MST Lab Data, $\mu\text{C}/\text{m}^3/\text{g}$	38	112
Foam Charging Rig Data $\mu\text{C}/\text{m}^3$ (Run No.)	1 (13)	-175 (31)
Bladder Cell Rig Data		
High Velocity Inlet Cell Current $\mu\text{C}/\text{m}^3$ (Run No.)	16 (2024)	-198 (3022)
Low Velocity (Piccolo) Inlet Cell Current $\mu\text{C}/\text{m}^3$ (Run No.)	-19 (2022)	-55 (3003)
Drum Test Rig Data (High Velocity Inlet)		
Drum Current $\mu\text{C}/\text{m}^3$ (Run No.)	~ 1 (533-537)	36-40 (616-618)
Max. Field KV/m	-300	-500
Residual Field KV/m	-5	-50

of the polarity of the charge on the input fuel. Thus, in terms of both charge generation and charge retention, the surface properties of blue foam are significantly different than red foam.

2. LOCALIZED CHARGE/DISCHARGE FACTORS

Since it is evident that charge separation takes place on the foam surface as fuel flows through the open pore structure, it follows that the quantity of charge separated will depend to some extent on the local velocity of this fuel. The jet of fuel is slowed by the pore structure and charged fuel tends to accumulate in localized "pockets" or zones near the inlets. The resulting voltage developed by this zone can lead to breakdown and discharge either to a grounded object like the inlet or the tank wall or to another zone of foam or fuel of different potential. A discharge, i.e. a spark that can be sensed by a radio antenna, provides some indication of the development and collapse of these high voltage zones. The radio signal is a better measure of localized charge/discharge phenomena than current signals from the inlet or drum unless the amount of charge transferred in each spark is enough to cause a "spike" in the current signals.

a. Inlet Velocity/Charge Distribution

By distributing the fuel into the foam through multiple orifices (the piccolo inlet) instead of just one orifice, velocities are reduced and localized zones of charged fuel are minimized in charge density. The advantage of this distribution mode can be seen by comparing spark frequencies between the multiple and the single orifice as in Figure 19 which summarizes drum test data in blue foam

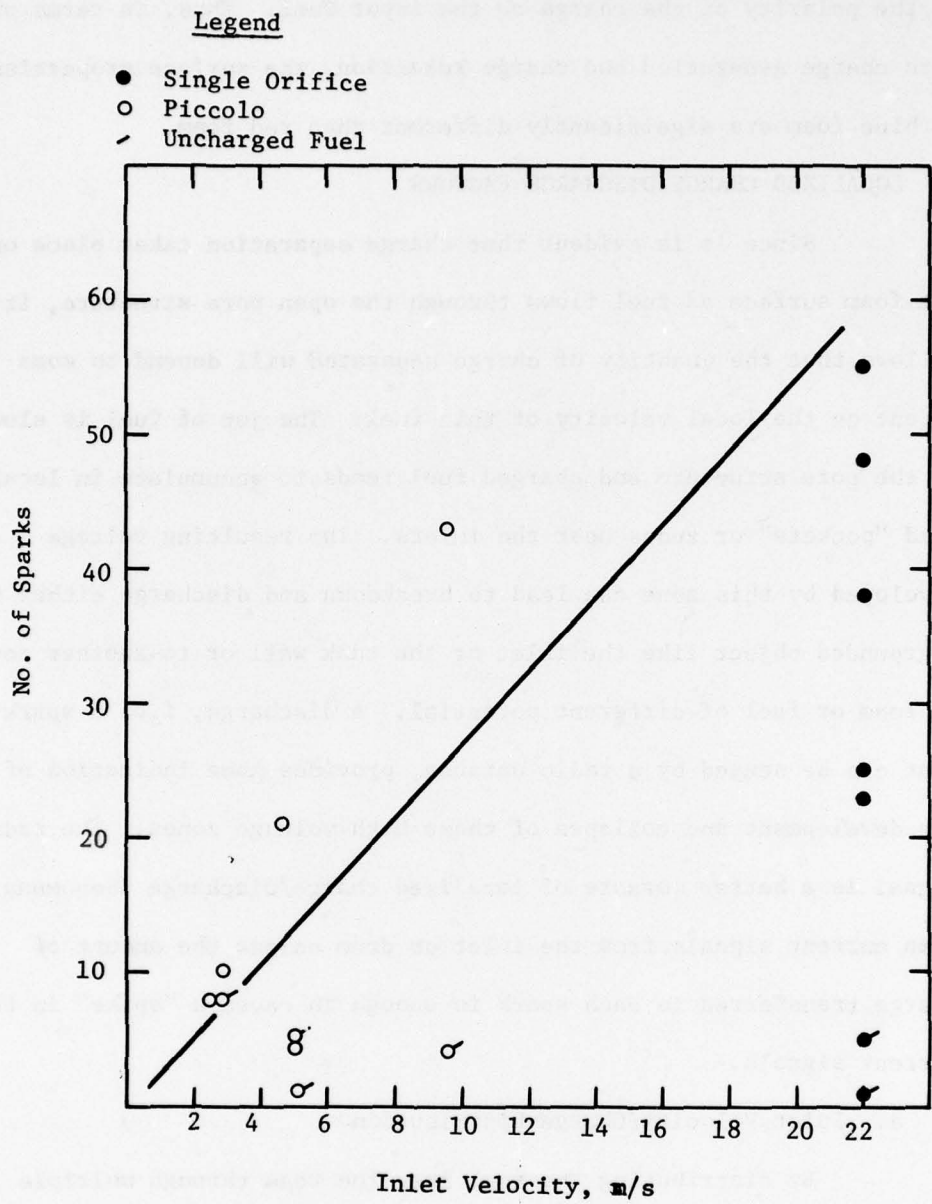


Figure 19. Spark Frequency vs. Inlet Velocity

Clay Treated Fuel
Blue Foam - Drum Rig Tests

with non-additive (clay treated) fuel. Spark counts plotted against the exit velocity of fuel at the inlet orifice show a significant reduction when multiple orifices distribute the fuel.

Drum test data on two different piccolo inlets are plotted in Figure 15. The P-1 piccolo distributed fuel through ten holes sized to produce the same exit velocity as the single orifice. The reduction in spark frequency was dramatic suggesting that distribution of charged fuel is a more important factor than exit velocity itself. It is noteworthy that even when uncharged fuel is distributed into blue foam a few sparks are observed. With red foam, as seen in Figure 20, the difference between the multiple and the single orifice is more dramatic because sparks are detected with the piccolo only at extreme input charge levels, $>2000 \mu\text{C}/\text{m}^3$.

The concept of localized "pockets" where discharges occur explains why more sparks are observed in the Drum than in the Bladder Cell, particularly with a piccolo inlet. The floor area and volume of the two test tanks are noted in Table 21. With a single velocity inlet, the floor area is not critical but the foam volume is. In Bladder Cell tests, the same quantity of charge is jetting into 60% more foam so a larger number of discharge "zones" should be anticipated. The spark frequency data appear to bear this out because many more discharge signals are observed with the same type of fuel in cell tests than in drum tests as noted in Figure 21.

With a multiple orifice inlet on the other hand, the foam-covered floor area on which charge fuel is distributed plays a more significant role than the volume of the foam. The cell contains

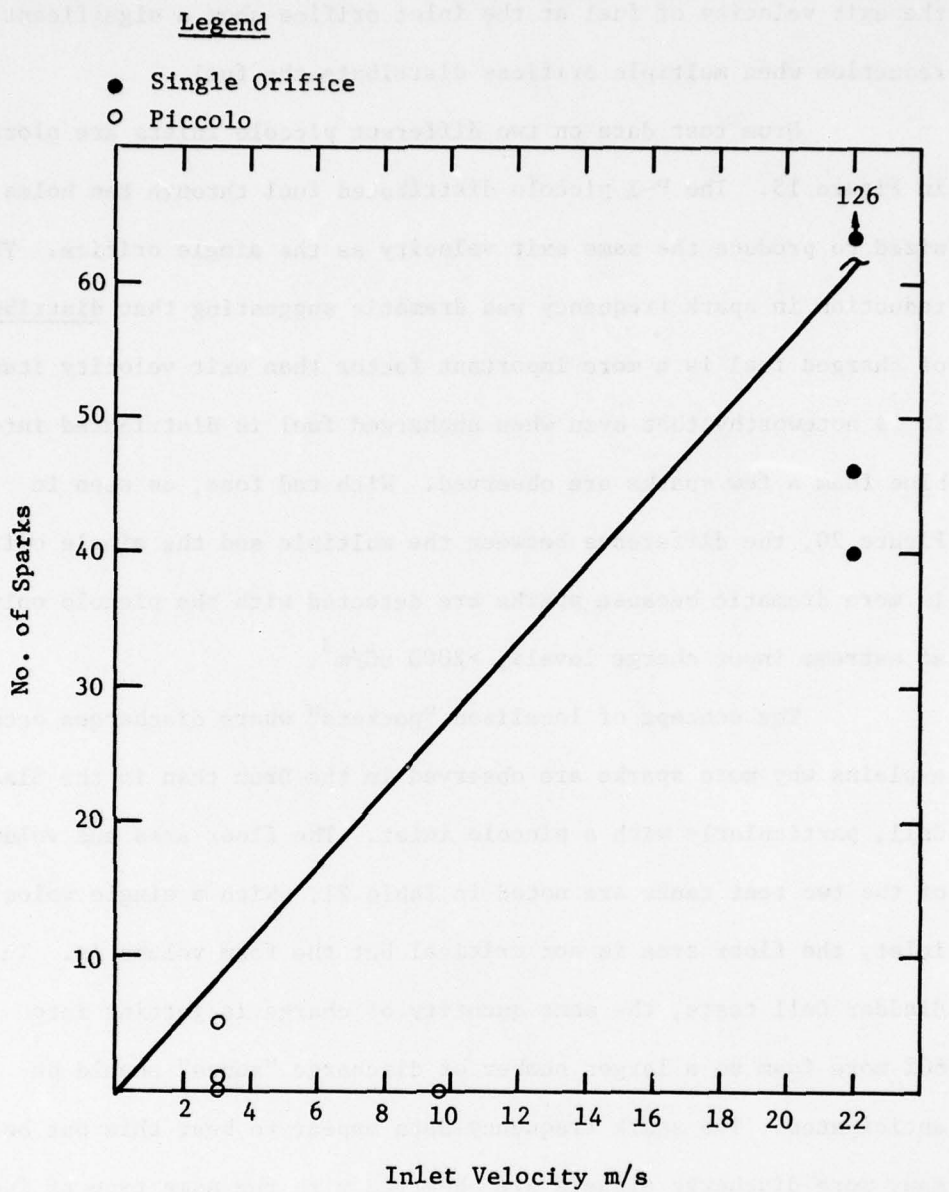


Figure 20. Spark Frequency vs. Inlet Velocity

Clay Treated Fuel
Red Foam - Bladder Cell Tests

TABLE 21
GEOMETRICAL FACTORS IN TEST DRUM VS BLADDER CELL

	<u>Drum</u>	<u>Cell</u>	<u>Critical Inlet</u>
Volume of Foam m ³	0.185	0.303	
Floor Area m ²	0.245	0.543	
<u>Ratio Cell/Drum</u>			
Ratio of Volume		1.64	Single
Ratio of Floor Area		2.22	Multiple

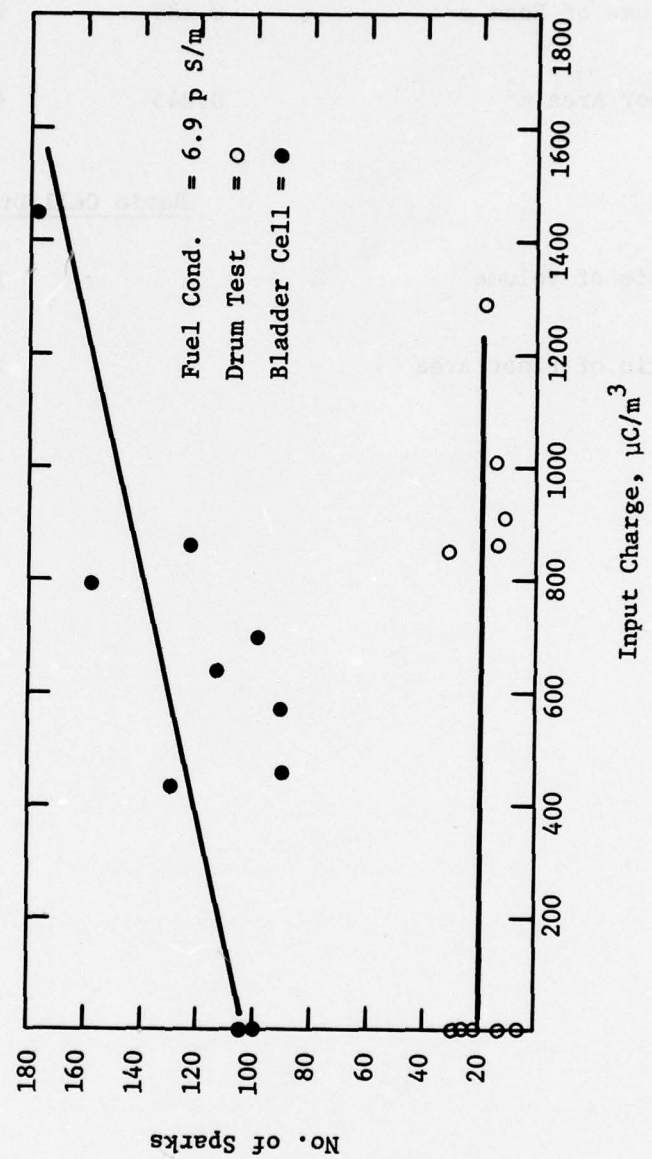


Figure 21. Spark Frequency: Bladder vs. Drum Single Orifice - Blue Foam

over twice as much floor area as the drum which reduces the number of localized discharge zones that will develop in the foam. The difference is dramatically shown by Figure 22 which compares spark frequency with the same piccolo inlet and similar fuel in both drum and cell tests. The smaller floor area drum is shown to be much more critical.

The importance of this observation to a fuel inlet design would suggest that the fuel should be introduced to the floor (or wall) of the tank which provides the greatest area on which charged fuel can distribute itself before flowing upward through the foam. The number of orifices in the inlet should be a maximum consistent with the tank floor area and a spacing of about 4-5 cm; the orifice size should provide not more than 3 m/s exit velocity at maximum flow rate.

b. Input Charge Level

The quantity and the polarity of the charge carried by the fuel as it enters the foam **also influences** the development of localized charge/discharge zones. Data on spark counts vs. input charge density (negative polarity) with clay treated fuel of low conductivity entering foam through the high velocity single orifice are plotted in Figure 23. It is apparent that discharge frequencies increase as fuel charge rises. The blue foam is much more active in producing discharge zones than the red foam and, in fact, creates charge/discharge zones with completely uncharged fuel. On the other hand, the threshold for red foam spark formation appears to be at an input charge density of about $300 \mu\text{C}/\text{m}^3$.

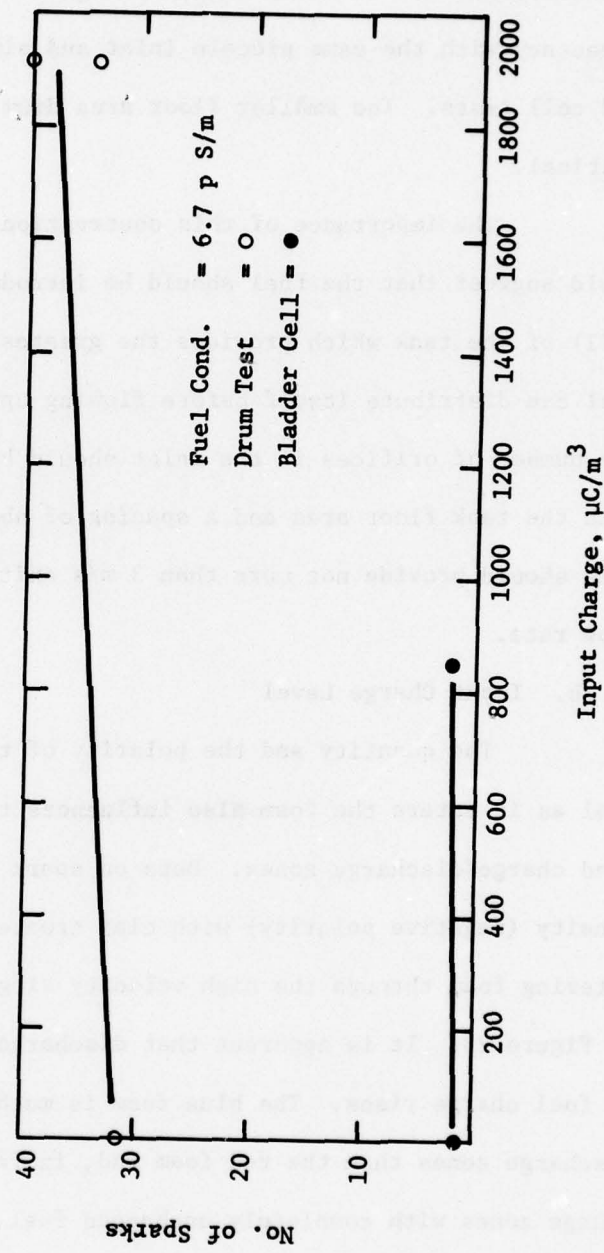


Figure 22. Spark Frequency: Bladder vs. Drum Piccolo 2 - Blue Foam

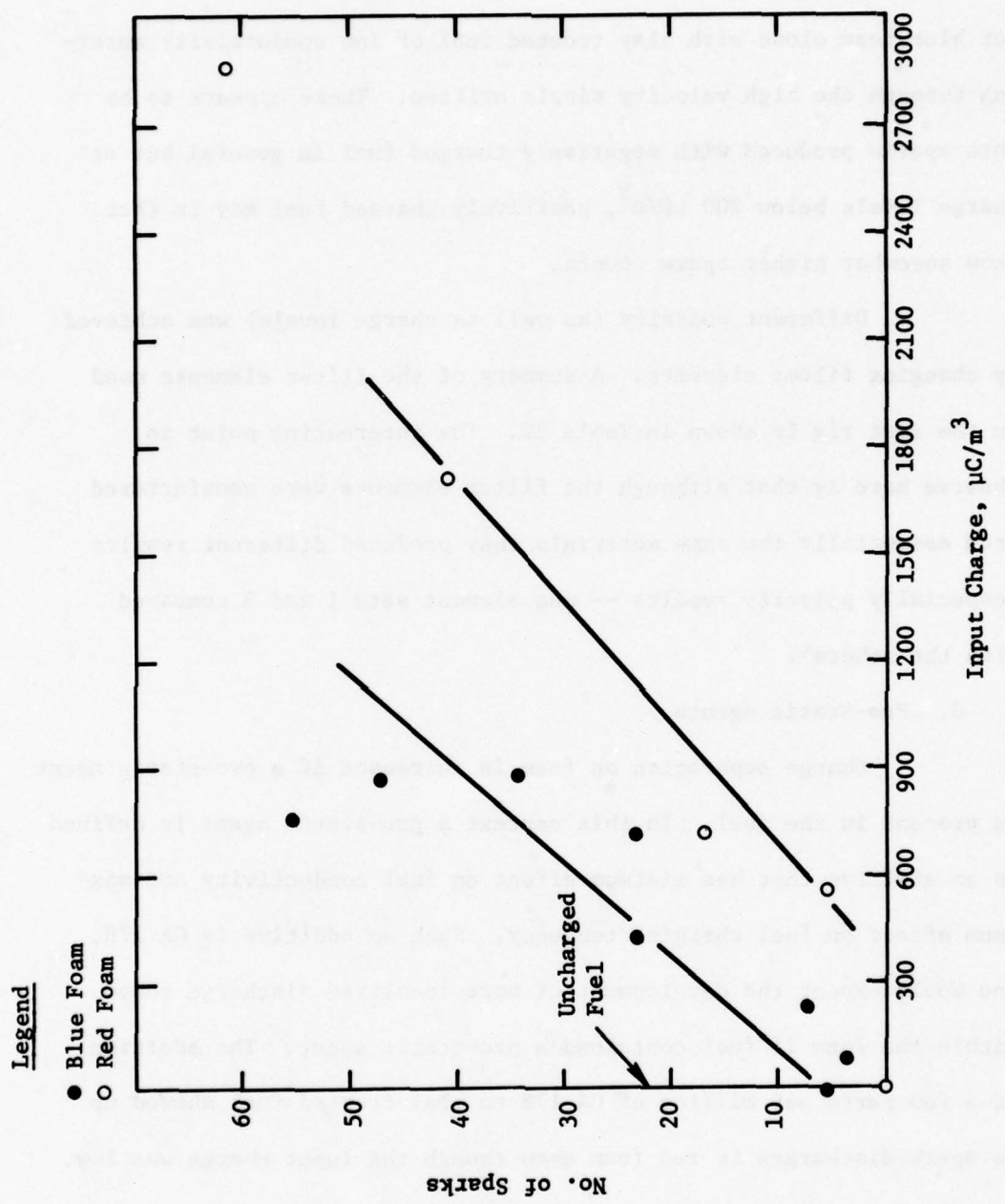


Figure 23. Spark Frequency vs. Input Charge Level

Drum Tests on Clay Treated Fuel
 Blue vs. Red Foam
 High Velocity Inlet

c. Input Charge Polarity

The effect of charge polarity is illustrated in Figure 12 for blue foam alone with clay treated fuel of low conductivity entering through the high velocity single orifice. There appears to be more sparks produced with negatively charged fuel in general but at charge levels below $200 \mu\text{C}/\text{m}^3$, positively charged fuel may in fact show somewhat higher spark counts.

Different polarity (as well as charge levels) was achieved by changing filter elements. A summary of the filter elements used in the test rig is shown in Table 22. The interesting point to observe here is that although the filter elements were manufactured from essentially the same materials they produced different results (especially polarity results -- see element sets 1 and 3 compared with the others).

d. Pro-Static Agents

Charge separation on foam is increased if a pro-static agent is present in the fuel. In this context a pro-static agent is defined as an additive that has minimum effect on fuel conductivity and maximum effect on fuel charging tendency. Such an additive is GA 178. One would expect the development of more localized discharge zones within the foam if fuel contained a pro-static agent. The addition of a few parts per million of GA 178 to clay treated fuel showed up as spark discharges in red foam even though the input charge was low. GA 178 produced positively charged fuel. It is noteworthy that fuel conductivity showed little change when the GA 178 was added. When GA 178 was added to fuel containing ASA-3 which always produced

TABLE 22
FILTER SUMMARY (1)
ELEMENT SET UTILIZATION (2)

Set No.	Installation Condition	Test Runs		Observed Fuel Charge Polarity
		Drum	Bladder	
1	Old (used) (3)	1-530, 542-552, 600-624	3093, 3094	positive
2	New	531-541, 553-583, 588-594	2029-2031	negative
3	Old (new) (4)	584-587	3043-3054	positive
4	New	595-599, 6016-6094	1000-1013, 3000-3023, 3026-3031	negative
5	New		2000-2004	negative
6	New		2032-2044, 3024-3025 3032-3037	negative
7	New		2045-2060, 3038-3042 3055-3092	negative

- (1) Bendix "Go-No-Go" Gage, Part No. 041210-M2. The gage holds up to five filter cartridges.
- (2) During our charged fuel testing, we always operated with five cartridges.
- (2) The elements are constructed of plastic, metal, and paper. The filter media consists primarily of paper material.
- (3) Had been used for testing on a previous program. They were about 2 years old.
- (4) These elements were about 2 years old, but had never been used before. Each cartridge was in a sealed plastic bag. (The bags, of course, were removed prior to insertion in the Bendix gage.)

negatively charged fuel, the negative charge was drastically reduced.

There is evidence that blue foam itself contains a pro-static agent that is extracted by the fuel and increases fuel charging tendency. The evidence is seen in laboratory MST charging tendency tests comparing fuels as well as rig tests. Laboratory tests showed fuel to have 3-4 times higher charging tendency after exposure to blue foam (see Table 15). The blue foam agent produced negatively charged fuel. Aside from reversing fuel charge polarity, it increases fuel conductivity within a few runs from 2 to 15 pS/m.

Corrosion inhibitor and anti-icing agent which are normal additives in JP-4 act as minor pro-static agents. The Bladder Cell tests provided an opportunity to assess these effects because the base fuel containing these additives was successively clay treated, doped with ASA-3, then redoped with corrosion inhibitor and anti-icing agent in the course of testing. The effect of CI/AIA was generally to increase the charge output of the filter and also to influence the number of spark discharges. In Table 23, spark frequencies are compared for the various combinations of foam type and inlet type tested. It is evident that spark discharges increase when CI/AIA are present either with base fuel or fuel containing low levels of ASA-3.

e. Role of Charge Collector

The role of a metal charge collector within the foam-filled fuel tank has been uncertain. The foam itself obviously becomes charged when exposed to flowing fuel and may not require the supplementary aid of an unbonded conductive object to concentrate

TABLE 23

EFFECT OF CORROSION INHIBITOR/AIA
ON SPARK FREQUENCY
(Bladder Cell Tests)

Cond. pS/m	Foam Type	Inlet*	Range of Spark Counts Observed			
			Clay-Treated Fuel		Clay-Treated Fuel +ASA-3	
			with CI/AIA <u>1.4</u>	without CI/AIA <u>2.5</u>	with CI/AIA <u>6.8</u>	without CI/AIA <u>6.8</u>
Red	S	40-126	0-4	-	5-24	0
Red	P-2	0	-	-	0-2	-
Blue	S	-	-	-	28-176	2
Blue	P-2	39-60	39-60	-	2-4	-

* S = Single orifice, high velocity inlet (21 m/s velocity)
P-2 = Multiple orifice, low velocity inlet (10 m/s velocity)

charge. However, the aircraft tanks which have experienced ignitions have sometimes contained unbonded small metal clamps for holding pipes or wire bundles and so the question remains about their participation in the discharge process.

Evaluation of the charge collector role was limited to drum filling tests. An actual marriage clamp from an A-10 aircraft tank was employed, attached to the inlet itself, resulting in a gap of about 3-4 mm across the rubber protective sheath. No effects were seen in a tank of charged fuel not containing foam. With red foam, the clamp collected enough charge from rising charged fuel to create a discharge on several occasions. However, the data on conductive vs. non-conductive fuel suggest that the fuel itself rather than the red foam became the primary source of charge to the clamp. With blue foam, on the other hand, the activity of the foam in collecting charge seemed to overpower fuel in providing a charge source for the metal clamp. For example, with completely uncharged fuel rising through blue foam, the presence of an unbonded metal clamp produced a discharge.

Even though the data obtained on metal charge collectors in foam, filled tanks were somewhat limited, it seems reasonable to define their role as secondary to the foam itself which is the primary charge collector present.

3. ROLE OF CONDUCTIVITY IMPROVER

The development of a localized zone of high potential within the foam structure is to some extent dependent on the conductivity of the fuel. If the conductivity is high, charge relaxation processes

outpace charge generation rates and charge accumulation does not cause voltage levels high enough to initiate breakdown and discharge. Unfortunately, most additives that increase fuel conductivity also act as pro-static agents so that charge generation rates within the foam also increase. It is not at all clear without experimental data how fuel conductivity can be related to spark discharges since each foam responds differently to the pro-static tendencies of conductivity additive.

When filling non-foam containing tanks with fuel containing traces of a pro-static agent such as conductivity improver it is possible to create a more hazardous condition within the tank if a charge separating surface such as a filter is close to the tank so that charge relaxation in the filling hose is not sufficient to offset increased charge generation. For this reason, minimum conductivity levels are invariably specified in handling systems. When the charge separating surface such as foam is within the tank, the minimum conductivity level is bound to be higher.

a. Threshold Conductivity with Uncharged Fuel

In the Test Rig employed to test foam in either a Drum or Bladder Cell, the filter is close to the tank so that only about 0.2 seconds of residence time is available for charge relaxation processes to occur with high rates of flow. Thus a very large fraction of the charge in the fuel generated by the filter is actually delivered into foam despite the high conductivity that would be created by the additive. However, it was the practice also to bypass the filter during the testing of anti-static additive. In this configuration,

the charging tendency of anti-static additive within the foam became the primary factor affecting development of localized charge/discharge zones.

As expected, the blue foam proved to be much more potent than red foam when anti-static additive in uncharged fuel was the only source of charge generation. For example, in Drum Tests using the high velocity inlet, red foam ceased to produce sparks when the ASA-3 level in uncharged fuel was only 5.5 pS/m conductivity while with blue foam, uncharged fuel still produced sparks at an ASA-3 level equivalent to 260 pS/m conductivity.

b. Threshold Conductivity with Charged Fuel

Since it is normal practice to filter fuel immediately prior to aircraft fueling, the tests using charged fuel are more realistic for assessing the threshold conductivity level for eliminating spark discharges. Spark frequency data as a function of fuel conductivity are shown in Figures 10 and 13 for Drum Tests and Figures 16 and 17 for Bladder Cell Tests.

The threshold conductivity data for spark elimination are summarized in Table 24. The significant difference between red and blue foams extends from the high velocity single orifice inlet to the multiple orifice (piccolo) inlets. However, the inlet configuration is so important that it dictates the safe level of anti-static additive. Thus the low velocity (3 m/s) piccolo is superior to the medium velocity (10 m/s) piccolo and either of these is in turn superior to the single orifice inlet. With the low velocity piccolo, it may be possible to avoid anti-static additive altogether

TABLE 24
 THRESHOLD CONDUCTIVITY VALUES OF FUEL
 FOR SPARK ELIMINATION
 (Fuel with CI/AIA + ASA-3)

Foam Type	Test Rig	Single Orifice	Conductivity, pS/m*			
			Inlet Type		Piccolo No. & Exit Velocity	
			P-2	P-4		
Red	Drum	33	<u>10 m/s</u>			
	Bladder Cell	33	10	<10**		
<hr/>						
Blue	Drum	>260	>70	-		
	Bladder Cell	>300	250	33		

*Conductivities at testing temperature of 0-10°C.

**Fuel without ASA-3 caused sparks at input charge density >2000 $\mu\text{C}/\text{m}^3$.

with red foam and utilize a normal concentration of ASA-3 (say 50 ps/m minimum conductivity) with blue foam.

The spark energy measurements that accompanied some of the Bladder Cell tests (and are summarized in Table 19) were made with both non-additive fuel and with various levels of ASA-3. There was no indication that additive level influenced discharge energy. However, both foam type and inlet type did affect spark energies as discussed in Section VI-5 below.

4. METALLIC FOAM

The aluminum mesh ("Explosafe") which had been provided by Vulcan Industrial Packaging Ltd. of Canada was fit into our Drum Rig and tested using clay treated fuel (Section V-6-d).

Field strength measurements during this testing suggested that the metal mesh was acting as a ground to a significant extent (hence, the low field strengths, Table 17, Section V-6-d). As a device for "bleeding" charge the mesh worked well.

The major drawback encountered with the aluminum mesh concerned its propensity to form charge collectors. This occurred when very small pieces of the mesh broke off the main body during removal from the drum. The result was several small metal chips acting as unbonded charge collectors floating around in the drum during filling. When these chips, which became charged as the result of exposure to charged fuel, contacted a grounded object such as our inlet, discharge occurred. In an aircraft tank packed with aluminum mesh, a few small pieces of broken mesh would not present a problem except for the possibility of clogging a filter. However, fuel transfer operations or defueling

could move the metal chips into another tank or a refueler vehicle and create the potential hazard of static discharge. Because of the pronounced tendency to develop charge collectors, the aluminum mesh material was not considered a technical solution to the static electrification problems.

5. RELATIONSHIP OF SPARK ENERGY TO INPUT CHARGE WITHIN FOAM

Foam can be considered to be a filter through which low conductivity fluid flows and thereby generates electric charge. While it is not possible to apply the equations developed by Huber and Sonin (8) for theoretical charge generation because the foam is such a complicated type of filter, their general relationships make possible some comparisons.

The charging characteristics of the filter depend on flow conditions, filter properties and fluid properties. Flow conditions between a single orifice and a multiple orifice differ drastically. Both the amount of foam (i.e. filter) involved and the fluid velocity are affected. With a high velocity jet, it has been estimated visually that about 50% of the fluid bounces back and does not contribute to charging by foam. On the other hand, with a 19 hole piccolo, only 5% of the foam volume is exposed per orifice but at each opening 100% of the fluid penetrates the foam. There is, therefore, a 10-fold difference in the amount of foam involved in localized charge generation between one inlet and another. With a downward facing orifice - the usual piccolo installation mode - the jet of fuel bounces off the floor, disperses and enters the foam at still lower velocity than it exits from the orifice. Fluid velocity into the foam is 20-50%

as high with the piccolo inlet compared with the single orifice.

Combining these two factors suggests that charging of fluid by foam should be only 2-5% as high with a piccolo type inlet.

Foam (i.e. filter) properties are a second factor in the equation. Blue foam has been shown to have a charging tendency 10-100 times greater than red foam. To a large extent, therefore, blue foam tends to offset the advantage of the multiple orifice inlet.

Spark energy measurements support this analysis of foam charging characteristics vis-a-vis inlet type. In the following table the spark energies are summarized for foam and inlet:

Foam Type	Spark Energy, nC (charge transfer)		
	Single Orifice	Piccolo-2	Piccolo-4
Red	2-10	*	*
Blue	50-600	0.1-10	0-2

*Too low to measure

The piccolo inlet is shown to produce sparks in blue foam with only about 2% as much energy as the single orifice, consistent with the estimate of foam volumes involved. At the same time, blue foam produces at least 10 times more energy in sparks than red foam and causes the blue foam-piccolo combination to be roughly equivalent to the red foam-single orifice combination.

SECTION VII

CONCLUSIONS

The interactions between foam type, fuel quality, and inlet fueling velocity significantly affect charge generation and static discharge. The synergistic effects of these variables on charge generation can, if not properly considered, lead to potentially serious static electrification problems.

The conclusions presented below, supported by our experimental results, point out several foam/fuel/inlet interactions and identify certain conditions where the static problems could possibly be minimized.

- Polyurethane open-pore foam provides a surface for static charge generation and retention when installed in an aircraft tank.
- Blue polyether foam is a much more active material for charge generation and retention than red polyester foam.
- Transient localized pockets or zones of high charge develop in the foam and discharge as sparks depending critically on fuel properties and velocity of the fuel jet into the foam.
- A multiple orifice low velocity inlet (i.e. piccolo) eliminates sparks in red foam except at unrealistically high input charge levels and reduces spark energies in blue foam to low values with fuel containing only corrosion inhibitor and anti-icing additives.
- A multiple orifice inlet produces fewer sparks if the entering fuel spreads over a large tank floor (or wall surface) at exit velocities not greater than 3 m/s.

- With a single orifice (high velocity) inlet, fuel conductivity additive is needed to eliminate sparks in red foam; threshold conductivity is 30 pS/m. With blue foam, sparks cannot be eliminated even at impractically high conductivity levels, i.e. greater than 500 pS/m.
- With a multiple orifice (piccolo) inlet, fuel conductivity additive is not needed to eliminate sparks in red foam unless input charge is extremely high. With blue foam, the threshold fuel conductivity for no sparks is 250 pS/m for a 10 m/s velocity piccolo but only 30 pS/m for a 3 m/s velocity piccolo. With non-additive fuel, sparks in blue foam appear to be very low in energy.
- Spark energy (charge transfer) measurements made with an oscilloscope on the inlet show blue foam discharges are 10-100 times greater in energy than red foam discharges. In a multiple orifice (piccolo) inlet only 1/10 to 1/100 as much charge is transferred in a spark compared with a single (high velocity) orifice inlet. The spark energy levels appear to be incendive for the single orifice and appear to be non-incendive for the multiple orifices.
- A bladder liner shows no significant difference in static charge generation or retention compared with an empty drum. Initial charge relaxation was equivalent to charged fuel in the metal drum but the rate of decay of field strength became slower at low voltage levels.
- Substitution of an expanded metal mesh for reticulated foam produced much lower field strengths with both single and multiple orifice inlets. However, the development of broken fragments of aluminum mesh which

acted as charge collectors mitigates against use of metal instead of plastic foam.

It is important to point out that this project was limited in scope and that these conclusions and the data from which they were derived are specific to the test materials and facilities used during this project. Although an attempt was made to realistically simulate actual aircraft refueling operations the direct extension of these limited data to full scale aircraft facilities should be discouraged. Further work is required to adequately define the effects of scale-up (tank geometry, internal plumbing configurations, foam volume, inlet location, fuel quality, etc.). Section IX of this report addresses the need for such additional work.

SECTION VIII

SUGGESTED CRITERIA FOR FUEL SYSTEM DESIGN AND FUEL QUALITY

The experimental program in small-scale test tanks packed with reticulated foam produced results suggesting that criteria in fuel systems design and fuel quality parameters can be established to reduce the potential hazard from static electrification in aircraft fueling. The following specific items are suggested by the data developed in this work:

- Multiple orifice (*piccolo*) fuel inlets with a maximum exit velocity of 3 m/s

Test results in both a 55-gallon drum and a 90-gallon bladder cell demonstrated that spark discharges were completely eliminated or reduced in frequency and energy by distributing fuel entering a tank packed with foam through a multi-holed inlet located in the bottom of the vessel. The orifices tested were spaced on 5 cm centers and their number was related to the size of the tank floor area. For the two test vehicles, 19 holes were used. This so called "piccolo" inlet can be a single pipe or several pipes attached to a common header but should be located in the lowest portion of the tank so that in most practical circumstances the pipes would be immersed in residual undrained fuel.

The size of each orifice proved to be critical since the exit velocity of fuel jetting into the foam determines the tendency for spark discharges to occur. An orifice sized to limit the velocity of fuel from each hole under maximum flow conditions to 3 m/s is a desirable limit. The orifices should be directed downward toward the tank

lining rather than upward into foam. The holes drilled in pipe as orifices should retain a sharp edge in order to dissipate charge as corona.

- Minimum conductivity of 50 pS/m in fuel for unmodified aircraft containing orange, yellow or red foam

Unmodified aircraft containing a single orifice fuel inlet permitting fuel to jet into foam at high velocities, e.g. 15-25 m/s, risk spark discharges within the foam unless the conductivity of the fuel is maintained at a certain minimum level. With ASA-3 as a conductivity additive, this minimum level proved to be about 50 pS/m conductivity in small-scale test tanks when the foam was the polyester type, colored orange, yellow or red.

The data generated with polyester foam suggest that a trade-off exists, i.e. conductivity additive in fuel or replacement of single orifice inlets by a multiple orifice (piccolo) inlet. Since modification of thousands of aircraft, each of which contains several foam-filled tanks, is a formidable and time-consuming program, the risk of spark discharges in these aircraft can be reduced by establishing minimum conductivity levels in fuel as delivered, which means at the particular temperature of fueling. The minimum value of 50 pS/m has been the standard in commercial fueling for the past 15 years and has demonstrated its usefulness by an excellent safety record. It has generally been attained by adding 0.5 to 0.75 ppm of ASA-3 additive to fuel in the refinery or marketing terminal and monitoring the fuel conductivity with a field type conductivity instrument.

- Polyether (blue) foam requires both inlet modifications and minimum conductivity levels in fuel

Polyether type blue polyurethane foam is an experimental material with certain advantages over polyester foam which have focused attention on its use. However, the test programs have clearly demonstrated its greater tendency to generate charge and cause spark discharges. So great is this sparking hazard of blue foam that a safe conductivity level for fuel could not be established except with the multiple orifice (piccolo) type inlet. Hence, unlike the case of aircraft with red foam, a tradeoff between fuel conductivity level and inlet modification does not seem possible with blue foam except as a function of piccolo design. Thus, until single orifice, high velocity aircraft inlets are modified with a properly designed inlet, the blue foam should not be installed regardless of its advantages over the polyester type material.

- Minimum conductivity levels of fuel in aircraft with modified inlets depend on the type of foam used in tanks

While it is clear that use of a multiple orifice (piccolo) fuel inlet is desirable to replace the single orifice fuel inlet and to reduce the potential hazard of static electrification and discharge when fueling aircraft, the concurrent requirement for a minimum conductivity level in fuel depends on the type of foam chosen for tank packing. The small-scale data generated in this program suggest that no minimum conductivity level is required in fuel if only polyester foam of the orange, yellow or red type is used. However, if it is decided to install polyether blue foam in all or some

aircraft, a minimum conductivity level in fuel appears to be necessary. That level depends on the type of piccolo inlet designed. If the exit velocity of the inlet is held to a maximum of 3 m/s by sizing the holes properly, a minimum conductivity level of 50 pS/m at the temperature of delivery appears to be adequate. However, if the inlet is designed with an exit velocity up to 10 m/s, the minimum conductivity level of fuel would have to be higher, i.e. about 250 pS/m at the temperature of fueling.

SECTION IX

ADDITIONAL WORK NEEDS

Considerable progress has been made with a difficult problem and we feel that this work has expanded the state-of-the-art of static electricity hazards in foam-filled aircraft. However, it is clear that in spite of this progress certain technical questions remain unanswered. This section of the report addresses the need for additional work to help fill some of the technical gaps remaining.

• Incendivity Studies

Test results under this contract establish clearly that static discharges are occurring within the reticulated foam inside the drum under a variety of conditions. Nothing is known of the energy level of these sparks except by inference from the radio signals and oscilloscopes which detect them.

At the same time, it was known from a companion program carried out by Fairchild-Republic (under Contract No. F 33657-73-C-0500) in a test rig that mocks-up a full-scale A-10 aircraft tank that visual sparks between foam and fuel or between foam and inlet could be seen and photographed. The visibility of these internal discharges strongly implies that their energy content is sufficient to ignite flammable fuel/air mixtures but as in the case of the Exxon work, the test rig was always filled with inert gas and the evidence of spark incendivity must be inferred.

The conditions for spark discharge to occur appear to be critically dependent on fuel inlet velocity into the foam and the presence of pro-static activity in the fuel. The current project

(and the work at Fairchild) suggests that a low velocity inlet will eliminate discharges. Both Exxon and Fairchild have determined that below some concentration (i.e. conductivity) of anti-static additive in fuel static discharges may still be detected. From the magnitude of radio signals, under these circumstances, low spark energies could be inferred.

These findings suggest that an additive alone may not be the optimum solution and that the possibility of further static discharges in foam cannot be discounted. In order to complete the present work in the most significant manner, a direct technique for measuring the incendivity of spark discharges that do occur in foam under various conditions would be useful for selecting the best solution to insure that ignition of foam filled aircraft during fueling may be prevented in the future.

- Additional Conductivity Additives

Time constraints on the project permitted the evaluation of only one conductivity additive (ASA-3). In order to assure the selection of the optimum additive from a performance as well as a fuel handling standpoint, one or more additional conductivity additives should be evaluated in spark discharge tests.

- Fuel System Design Details

The results of this study suggest that criteria in fuel system design can be established to reduce the potential hazard from static electrification in aircraft fueling. The detailed fuel system design modifications that would be required need additional study. Factors such as the optimization of inlet location are best

determined by the airframe designers. Once these design modifications have been made, full scale static electrification study would be desirable to corroborate ignition type tests and design modifications.

The only types of inlets examined in this program were orifices where the hole size is fixed and the velocity obviously depends on flow rate. Other types of inlets are used in aircraft, however, in which hole size increases with flow rate. A so-called "shower head" nozzle is an example of such a device. The performance of such an inlet in charge generation within foam cannot be predicted from fixed orifice studies and should be studied separately.

• Full Scale Static Electrification Tests

Data obtained in the two Exxon test tanks which differ in volume by a factor of two compared with Fairchild's data in a tank ten times as large suggest that scale up to larger size increases the magnitude of both charge generation and discharge. Full scale testing would be a prudent step for insuring that the system and fuel changes suggested by this work are indeed adequate for protecting actual aircraft in service.

APPENDIX A
ABSTRACTS OF PERTINENT
LITERATURE REFERENCES

LITERATURE ON STATIC ELECTRICITY IN
HYDROCARBONS AND PLASTICS

J. C. Gibbings and G. S. Saluja "Electrostatic Streaming Current and Potential in a Liquid Flowing Through Insulating Pipes"

Electrostatische Anfladung Dechema-Monographion Nr 1370-1409 Buna 72
40 Vortiage Der 2 Internationalen Tagung Über Electrostatische Anfladung,
Frankfurt/Main, March 1973

Experiments were performed by passing kerosene through a P.T.F.E. pipe. Streaming current in the liquid was observed as a function of time and of Reynolds number for both laminar and turbulent flow. Measurements in turbulent flow show that charging of the wall occurs in batches and this related to previous evidence that ions separate into layers of various types. Exponential decay curves for turbulent flow indicate that streaming current tends to zero at infinite time. The equality of the potential of the liquid for laminar flow with turbulent flow suggests that the mechanism controlling the limit of charge deposit upon the wall is the same for both regions.

S. K. Wu and W. D. Rees "Static Electricity and the Safe Handling of Small Plastic Containers"

Electrostatische Anfladung Dechima-Monographion Nr 1370-1409 Buna 72
40 Vortiage Der 2 Internationalen Tagung Über Electrostatische Anfladung,
Frankfurt/Main, March 1973

Static associated with frictional rubbing of polyethylene container smaller than 75 l is more hazardous than that produced by filling the container with charged liquid. No insulated conductive object should exist in the vicinity of the container during filling and handling. An earthed metal object can be inserted safely into a container filled with liquid to dissipate charges. Containers should not be used in low relative humidity conditions, i.e., less than 30% but can be used if the relative humidity is in excess of 45%.

Yu. I. Vasilenok; B. A. Konoplev; V. N. Lagunova; N. S. Kozlov; V. A. Serzhania;
N. Ya. Yurashevich; A. P. Zezyuleja "Cation-Active Surfactants Consisting of
Naphthenic Acids as Antistatics for Plastics"

Vesti Akad. Navuk B. SSR, Ser. Khim Navuk 1975 (4), 87-92

Antistatic properties of polymers were improved by addition of quaternary ammonium salts of naphthenic acids. High- and low-density polyethylene (I), polypropylene, block polystyrene and poly(Me methacrylate), surface-treated with various cation-active surfactants, showed a decrease in specific surface resistivity from $>4.2 \times 10^{15}$ to $10^8-10^{10} \Omega$. A maximum antistatic effect was obtained with trihydroxyethylnaphthenylammonium chloride. Surface resistivity of polymers decreased with increasing concentration of the antistatic agent solution and with relative humidity of the air. The antistatic activity of surfactants decreased with increasing length of the alkyl radical of the examined salts. Thus, the surface resistivity of dimethylnaphthenylcetylammnonium stearate and dimethylnaphthenylbenzylammnonium stearate was $>4.2 \times 10^{15}$ and $6.3 \times 10^{11}-8.1 \times 10^{14} \Omega$, respectively. Different anions of the salts had no significant effect on their antistatic activity. Mechanical properties of polymers, except of I, did not change with decreasing surface resistivity.

V. N. Verevkin; V. I. Gorshkov; V. N. Zacheteiskii; L. L. Ilvovskii;
A. I. Kazubov "Fire Danger from Static-Electrical Charges in a Tank with
Pontoon of Polyurethane Foam"

Transp. Khranenie Nefti Nefteprod. 1973 (10), 24-7

Static electricity charges did not form on a polyurethane foam pontoon moved at ≤ 6 m/hr. during the filling and emptying of a storage tank with gasoline. The static electricity charges formed in the air-gasoline vapor mixture in the gap between the pontoon cover and liquid surface did not exceed the permissible level.

J. B. Agnew "Static Electricity Generation By Flowing Hydrocarbon Liquids"

National Chemical Engineering Conference, 2nd Proceeding, Surfers Paradise,
Queensland, Australia, July 10-12, 1974

This is a general review article. The mechanism of static generation is outlined and some common hazardous situations are discussed. A portable demonstration rig has been developed to illustrate the rapid build-up of static charge during the pumping of kerosine. This can be used to illustrate some of the important hazards encountered in industry.

B. C. O'Neill and T. R. Foord "Contact and Tribo Charging of Polymer Surfaces"

4th Conference on Static Electrification, Institute of Physics,
London, May 1975

Charge produced by rubbing metal probes on a polypropylene surface was usually negative. Under vacuum this charge was stable and could only be reduced by a high electric field, i.e., 5 KV on a probe 2 mm from the surface. Positive charges could sometimes be produced but were not as stable as negative charges.

E. A. Baum and T. J. Lewis "Controlled Charging of Insulating Surfaces"

4th Conference on Static Electrification, Institute of Physics,
London, May 1975

Polyethylene terephthalate (PET) films could be charged with a Nernst filament by the applied potential. When relative humidity of air was reduced from 70 to 20%, charge density of positive ions dropped 36%, negative ions only 2%. Heat is believed to influence the ability of surfaces to retain charge. By depositing well-defined patches of opposite sign, the kinetics of charge movement and neutralization can be studied. A decay mechanism based on neutralization by thermally generated carriers within the polymer is proposed. The dependence of the conductivity of PET on its degree of crystallinity is determined. For polypropylene and polycarbonate $\sigma = \frac{\epsilon}{d} V_{AB}$ where σ = charge

V_{AB} = applied voltage, ϵ is dielectric constant and d = thickness.

APPENDIX B
FOAM CHARGE GENERATING TESTS
RAW DATA

TABLE B.1
FOAM CHARGE GENERATING TESTS - RED FOAM
Test Fuel: Jet A ($C_u = 1.65 \text{ pS/m} @ 27^\circ\text{C}$)

Run No.	Flow Rate ⁽¹⁾ $\text{m}^3/\text{sec} \times 10^{-3}$	Fuel Charge Density ⁽²⁾ $\mu\text{C}/\text{m}^3$	Foam Test Section Charge Density $\mu\text{C}/\text{m}^3$	Max. Field St. KV/m
1	1.26	-	-1.67	+2.2
5	1.26	-	-0.08	+1.2
6	1.26	-	-0.08	+1.2
Conductivity Check = 1.15 @ 20°C				
7	1.58	-	-0.89	+1.4
8	1.89	-	-0.85	+1.4
9	2.21	-	-0.90	+2.0
10	2.52	-	-0.87	+2.4
11	2.84	-	-0.99	+2.6
12	3.15	-	-0.95	+2.4
Conductivity Check = 1.4 @ 27.8°C				
13	3.35	-	-0.97	+2.4
14	1.26	-	-1.43	-40.0
15	1.26	-	-1.43	-90.0
16	3.15	-	-	-
17	2.52	-	-1.59	-80.0
18	2.52	-	-1.59	-150.0
Conductivity Check = 1.55 @ 25.6°C				
19	1.26	+115.1	+7.94	-
20	1.26	+111.1	+8.73	+20.0
21	3.15	+71.4	+3.17	+38.0
22	1.26	+103.2	+7.94	+42.0
23	1.26	+108.5	+8.35	+62.0
24	2.52	+75.4	+5.16	+90.0
25	1.26/0.63	+126.8	+2.78	+12.0
26	1.26/0.63	+130.0	+2.78	+9.5
Conductivity Check = 1.32 @ 28.9°C				
27	1.26/0.63	+134.8	+1.59	+3.8
28	3.15/1.58	+113.9	+1.59	+25.0
29	2.52/1.26	+130.9	+2.38	+70.0
Conductivity Check = 1.38 @ 30.6°C				

(1) When two numbers are shown, this indicates mixed flow (charged + uncharged fuel). The second number indicates flow rate of uncharged fuel, the first number is the total system flow rate.

(2) Fuel charge represents the current density measured from the filter but of opposite polarity. Where the value is blank, the filter was bypassed.

TABLE B.2
FOAM CHARGE GENERATING TESTS - RED FOAM

Test Fuel: Jet A + CI + AIA ($C_u = 1.72 \text{ pS/m} @ 19.5^\circ\text{C}$)

Run No.	Flow Rate ⁽¹⁾ $\text{m}^3/\text{sec} \times 10^{-3}$	Fuel ⁽²⁾		Foam Test Section $\mu\text{C}/\text{m}^3$	Max. Field St. kV/m
		Charge Density $\mu\text{C}/\text{m}^3$	Charge Density $\mu\text{C}/\text{m}^3$		
74	1.26/1.26	-	+0.48	-0.03	
75	3.15/3.15	-	+0.29	+0.35	
76	1.26/1.26	-	+0.16	+0.14	
77	1.26/1.26	-	+0.24	-10.0	
<hr/> Conductivity Check = 1.64 @ 25°C					
78	2.52/2.52	-	+0.04	-11.0	
79	1.26	+71.4	+6.34	+5.0	
80	2.85	+45.6	+2.1	+13.0	
81	2.52	+43.7	+3.97	+18.5	

Test Fuel: Jet A + CI + AIA + ASA-3 ($C_u = 15.5 \text{ pS/m} @ 24^\circ\text{C}$)

95	1.26/1.26	-	+6.3	-0.09
96	3.15/3.15	-	+34.9	-0.10
97	1.26/1.26	-	+5.7	-2.60
98	2.52/2.52	-	-55.6	-9.20
99	1.26	+206.3	+31.7	-0.13
100	3.15	+127.0	+17.5	+0.20
101	1.26	+182.5	+20.6	-2.60
102	2.52	+154.8	-9.5	+4.0

Test Fuel: Jet A + CI + AIA + ASA-3 ($C_u = 106.2 \text{ pS/m} @ 24.5^\circ\text{C}$)

103	1.26/1.26	-	+71.4	-
104	3.15/3.15	-	+38.1	-
105	1.26/1.26	-	+71.4	-0.10
106	2.52/2.52	-	+31.7	-0.27
107	1.26	-79.4	+59.5	-
108	3.15	-254.0	+22.2	-0.12
109	1.26	-95.2	+63.5	-0.25
110	2.52	-218.3	+23.8	-0.50

- (1) When two numbers are shown, this indicates mixed flow (charged + uncharged fuel). The second number indicates flow rate of uncharged fuel; the first number is the total system flow rate.
- (2) Fuel charge represents the current density measured from the filter but of opposite polarity. Where the value is blank, the filter was bypassed.

TABLE B.3
FOAM CHARGE GENERATING TESTS - BLUE FOAM (Coarse Pore)
Test Fuel: Jet A ($C_u = 1.64 \text{ pS/m} @ 25^\circ\text{C}$)

Run No.	Flow Rate ⁽¹⁾ $\text{m}^3/\text{sec} \times 10^{-3}$	Fuel (2)	Foam Test Section	Max. Field St. KV/m
		Charge Density $\mu\text{C}/\text{m}^3$	Charge Density $\mu\text{C}/\text{m}^3$	
50	1.26/1.26	-	+73.0	-6.5
51	3.15/3.15	-	+285.7	-65.0
52	1.26/1.26	-	+206.3	-70.0
53	2.52/2.52	-	+238.1	-180.0
54	1.26	+87.3	+253.97	-19.0
55	3.15	+52.4	+390.5	-65.0
56	1.26	+83.3	+269.8	-60.0
57	2.52	+67.5	+396.8	-135.0
58	2.62/1.31	+95.2	+407.1	-65.0
59	2.52/1.26	+92.1	+396.8	-95.0

Test Fuel: Jet A + CI + AIA ($C_u = 1.64 \text{ pS/m} @ 22.5^\circ\text{C}$)				
82	2.64/2.64	-	+355.7	-41.0
83	2.52/2.52	-	+238.1	-36.0
84	2.52/2.52	-	+237.2	-33.0
85	2.52	+6.5	+396.8	-50.0
86	2.52	+17.9	+515.9	-65.0

Conductivity Check = 1.49 @ 17°C

Test Fuel: Jet A + CI + AIA + ASA-3 ($C_u = 12 \text{ pS/m} @ 18^\circ\text{C}$)

87	1.26/1.26	-	+35.7	-0.03
88	2.52/2.52	-	+31.7	-0.03
89	1.26/1.26	-	+39.7	-0.02
90	2.52/2.52	-	+23.8	-0.6
91	1.26	+75.4	+35.7	-
92	3.15	+34.9	+23.8	-0.07
93	1.26	+95.2	+39.7	-3.5
94	2.52	+93.3	+29.8	+0.9

- (1) When two numbers are shown, this indicates mixed flow (charged + uncharged fuel). The second number indicates flow rate of uncharged fuel; the first number is the total system flow rate.
- (2) Fuel charge represents the current density measured from the filter but of opposite polarity. Where the value is blank, the filter was bypassed.

TABLE B.4
FOAM CHARGE GENERATING TESTS - BLUE FOAM (Fine Pore)

Test Fuel: Jet A ($C_u = 1.26 \text{ pS/m} @ 22^\circ\text{C}$)

Run No.	Flow Rate ⁽¹⁾ $\text{m}^3/\text{sec} \times 10^{-3}$	Fuel ⁽²⁾ $\mu\text{C}/\text{m}^3$	Foam Test Section Charge Density $\mu\text{C}/\text{m}^3$	Max. Field St. KV/m
30	1.26/1.26	-	+71.4	-9.9
31	3.15/3.15	-	+174.6	-60.0
32	1.26/1.26	-	+111.1	-55.0
33	1.26/1.26	-	+119.0	-85.0
34	2.52/2.52	-	+130.9	-110.0
<hr/>				
Conductivity Check = 1.35 @ 26°C				
35	1.26	+111.1	+198.4	-14.0
36	2.95	+72.6	+231.1	-48.0
37	1.26	+107.9	+199.2	-45.0
38	3.15/1.58	+96.2	+238.1	-60.0
39	2.52/1.26	+111.1	+210.3	-140.0
<hr/>				
Conductivity Check = 1.15 @ 27°C				
SP-1	1.26/1.26	-	-0.55	+0.39
SP-2	1.26/1.26	-	+0.12	-13.0
<hr/>				
Conductivity Check = 1.52 @ 27°C				

Test Fuel: Jet A + CI + AIA + ASA-3 ($C_u = 117.7 \text{ pS/m} @ 30^\circ\text{C}$)

111	1.26/1.26	-	+202.4	-
112	3.15/3.15	-	+46.0	-0.18
113	1.26/1.26	-	+134.9	-0.27
114	2.52/2.52	-	+63.5	-50.0
115	1.26	-63.5	+142.9	-
116	3.15	-155.6	+38.1	-0.24
117	1.26	-55.6	+134.9	-0.33
118	2.52	-131.0	+55.6	-0.70

- (1) When two numbers are shown, this indicates mixed flow (charged + uncharged fuel). The second number indicates flow rate of uncharged fuel; the first number is the total system flow rate.
- (2) Fuel charge represents the current density measured from the filter but of opposite polarity. Where the value is blank, the filter was bypassed.

TABLE B.5
FOAM CHARGE GENERATING TESTS - YELLOW FOAM
Test Fuel: Jet A ($C_u = 1.52 \text{ pS/m} @ 27.5^\circ\text{C}$)

Run No.	Flow Rate ⁽¹⁾ $\text{m}^3/\text{sec} \times 10^{-3}$	Fuel ⁽²⁾	Foam Test Section	Max. Field St. KV/m
		Charge Density $\mu\text{C}/\text{m}^3$	Charge Density $\mu\text{C}/\text{m}^3$	
60	1.26/1.26	-	-3.0	+0.5
61	3.15/3.15	-	-1.75	+2.3
62	1.26/1.26	-	-3.1	-15.0
63	2.52/2.52	-	-19.8	-27.0
64	1.26	+95.2	+3.6	+10.0
65	3.15	+60.3	+0.76	+25.0
66	1.26	+87.3	+3.17	+25.0
67	2.52	+63.5	+0.79	+96.0
68	3.15/1.58	+101.3	-0.32	+15.0
69	2.52/1.26	+79.4	-0.4	+40.0
Conductivity Check = $1.49 @ 25.5^\circ\text{C}$ —				
R-1	1.26/1.26	-	-1.03	+0.3
R-2	3.15/3.15	-	-0.92	+1.9

- (1) When two numbers are shown, this indicates mixed flow (charged + uncharged fuel). The second number indicates flow rate of uncharged fuel; the first number is the total system flow rate.
- (2) Fuel charge represents the current density measured from the filter but of opposite polarity. Where the value is blank, the filter was bypassed.

TABLE B.6
FOAM CHARGE GENERATING TESTS - ORANGE FOAM
Test Fuel: Jet A ($Cu = 1.52 \mu S/m @ 27^\circ C$)

Run No.	Flow Rate ⁽¹⁾ $m^3/sec \times 10^{-3}$	Fuel ⁽²⁾ $\mu C/m^3$	Foam Test Section Charge Density $\mu C/m^3$	Max. Field St. KV/m
40	1.26/1.26	-	-2.14	+1.0
41	3.15/3.15	-	-1.75	+3.9
42	1.26/1.26	-	-3.25	-26.0
43	2.52/2.52	-	-2.18	-23.5
<hr/> Conductivity Check = 2.18 @ 33°C				
44	1.26	+126.98	+7.94	+12.0
45	3.15	+82.5	+2.54	+27.0
46	1.26	+119.1	+5.55	+20.0
47	2.52	+89.3	+3.17	+70.0
48	3.15/1.58	+107.6	+0.95	+19.0
49	2.52/1.26	+119.0	+0.79	+27.0
<hr/> Conductivity Check = 2.35 @ 34°C				
Test Fuel: Jet A ($Cu = 1.49 \mu S/m @ 25.5^\circ C$) ⁽³⁾				
70	3.15/3.15	-	+0.16	+1.0
71	2.52/2.52	-	+0.56	-39.0
72	3.15	+61.9	+2.54	+24.0
73	2.52	+59.5	+3.17	+50.0
<hr/> Conductivity Check = 1.44 @ 26°C				

- (1) When two numbers are shown, this indicates mixed flow (charged + uncharged fuel). The second number indicates flow rate of uncharged fuel; the first number is the total system flow rate.
- (2) Fuel charge represents the current density measured from the filter but of opposite polarity. Where the value is blank, the filter was bypassed.
- (3) This test series was done using used orange foam supplied by the Air Force.

APPENDIX C
DRUM CHARGING/SPARKING TESTS
BASE CASE STUDIES

(PRECEDING PAGE BLANK)

TABLE C.1
DRUM CHARGING/SPARKING TESTS - BASE CASE (EMPTY DRUM)
JET A ($C_u = 1.03 \text{ pS/m}$ @ 23°C)

Run No.	Element Set	Flow Rate $\text{m}^3/\text{s} \times 10^{-3}$	Fuel Test Inlet:	Fuel(1)	Inlet Charge	Drum Charge	Field(2) Strength	Total No. Radio Disch. Signals	Remarks
				Charge Density $\mu\text{C}/\text{m}^3$	Density $\mu\text{C}/\text{m}^3$	Density $\mu\text{C}/\text{m}^3$	KV/m		
201	1	3.15	Low Velocity	+28.6	+7.1	—	+2.6	—	
202	1	3.15	Low Velocity	+25.4	+2.5	+25.4	+12.5	—	
203	1	3.15	Low Velocity	+25.4	+2.5	+23.8	+12	—	
204	1	3.15	Low Velocity	+25.4	+3.2	+23.2	+10	—	
205	1	3.15	Low Velocity	-22.2	-3.8	-9.5	-24	—	
206	1	3.15	Low Velocity	-12.7	-1.9	-5.1	-8	—	
207	1	3.15	Low Velocity	-7.9	-0.9	-7	-4.7	—	
208	1	3.15	Low Velocity	+2.5	+0.3	+2.2	+8	—	
209	1	3.15	Low Velocity	+3.2	+0.3	+2.5	+7.5	—	
210	1	3.15	Low Velocity	+4.3	+0.5	+4.1	+6.5	—	
211	1	3.15	Low Velocity	+4.3	+0.6	+4.3	+7.5	—	
212	1	3.15	Added ~8.5 ppm GA-178 to fuel	+4.6	+1.1	+3.8	+7.2	—	
213	1	3.15	Clay filtered out 1/2 of GA-178	+508	+85.7	—	+140	12	
214	1	3.15	Clay filtered out 1/2 of GA-178	+619	+82.5	+413	+87	11	
215	1	3.15	Clay filtered out 1/2 of GA-178	+260	+26	+191	+70	7	

Cold ambient temperatures
{ and fuel water content were
suspected of having some
effect on electrical measurements, hence the polarity
reversals.

(1) Fuel charge represents the current density measured from the filter but of opposite polarity. Where the value is blank, the filter was bypassed.
 (2) Field Strength observed at about 90% full.
 (3) Exit velocity is about 3 m/s at maximum flow rate.

TABLE C.2

DRUM CHARGING/SPARKING TESTS - BASE CASE (EMPTY DRUM)
JET A WITH ~ 4 PPM GA 178 ($C_u = 1.78 \text{ PS/m} @ 12^\circ\text{C}$)

Run No.	Element Set	Flow Rate $\text{m}^3/\text{s} \times 10^{-3}$	Fuel (1) Test Inlet = Low Velocity	Inlet		Drum Charge Density $\mu\text{C/m}^3$	Field (2) Strength KV/m	Total No. Radio Disch. Signals	Remarks
				Charge Density $\mu\text{C/m}^3$	Charge Density $\mu\text{C/m}^3$				
301	1	3.15	+222	+16	+159	+65	-	-	w/chg. collector present
302	1	3.15	+191	+16	+159	+60	-	-	w/chg. collector present
303	1	3.15	+191	+16	+159	+65	-	-	w/chg. collector present
304	1	3.15	--	-0.6	+3.0	+1.7	-	-	w/chg. collector present
305	1	3.15	--	-0.4	+2.9	+1.5	-	-	w/chg. collector present
306	1	3.15	+206	+27	+159	+60	-	-	w/chg. collector present
307	1	3.15	+181	+19	+159	+61	-	-	w/chg. collector present
308	1	3.15	+175	+21	+159	+60	-	-	w/chg. collector present
309	1	3.15	+168	+17	+159	+50	-	-	w/chg. collector present
310	1	3.15	+162	+17	+143	+50	-	-	w/chg. collector present
311	1	3.15	+159	+17	+143	+50	-	-	w/chg. collector present
312	1	3.15	+159	+17	+143	+50	-	-	w/chg. collector present
<hr/>									
313	1	0.63	+294	+38	+164	+12	-	-	
314	1	0.63	+265	+35	+144	+12	-	-	
315	1	1.26	+187	+21	+135	+27	-	-	
316	1	1.89	+157	+14	+132	+8.5	-	-	
317	1	2.52	+132	+10	+119	+140	-	-	
<hr/>									
318	1	1.89	+130	+10	+116	+100	-	-	w/chg. collector present
319	1	1.89	+122	+15	+103	+70	-	-	w/chg. collector present
320	1	1.89	+119	+13	+101	+70	-	-	w/chg. collector present
321	1	1.89	+122	+11	+106	+92	-	-	w/chg. collector present
322	1	1.89	+122	+12	+103	+85	-	-	w/chg. collector present

Footnotes to Table C.2:

- (1) Fuel charge represents the current density measured from the filter but of opposite polarity.
Where the value is blank, the filter was bypassed.
- (2) Field Strength observed at about 90% full.
- (3) Exit velocity is about 3 m/s at maximum flow rate.
- (4) Exit velocity is about 21 m/s at maximum flow rate.

TABLE C.3
DRUM CHARGING/SPARKING TESTS - BASE CASE (DRUM + BLADDER)
JET A + 4 PPM GA 178

Run No.	Element Set	Flow Rate $\frac{\text{m}^3/\text{s}}{\text{x } 10^{-3}}$	$\frac{\mu\text{C}/\text{m}^3}{\text{Test Inlet = High Velocity}}$	Fuel (1)	Inlet Charge	Drum Charge	Field (2)	Total No. Radio Disch.	Remarks
				µC/m ³	Density	Density	Strength KV/m	Signals	
<u>"drop tube" type) (3)</u>									
401	1	1.89	+163	+16	+132	+47	-	12.5	14.5
402	1	1.89	+152	+16	+116	+12.5	-	13.5	15
403	1	1.89	+154	+16	+116	+100	-	14.5	16.5
<u>Conductivity Check = 3.1 @ 14.5°C</u>									
404	1	1.89	+153	+21	+116	+90	-	15	17.5
405	1	1.89	+183	+27	+132	+90	-	16	18.5
406	1	1.89	+193	+24	+138	+70	-	16.5	19
407	1	1.89	+201	+8	+53	+15	-	16	17
<u>Clay Filtered 1/2 of Fuel Volume</u>									
407R	1	1.89	+135	+15	+106	+60	-	17.5	19
<u>Conductivity Check = 3.3 @ 19°C</u>									
<u>Installed Low Velocity Inlet (Splash Plate) (4)</u>									
408	1	3.15	+61	+13	+51	+40	-	15	15
409	1	3.15	+67	+8.6	+54	+34	-	16.5	14
410	1	3.15	+67	+13	+54	+45	-	w/chg. collector present	
411	1	3.15	+68	+13	+57	+45	-	w/chg. collector present	
412	1	3.15	+70	+10	+57	+45	-	w/chg. collector present	
413	1	3.15	+69	+10	+57	+45	-	w/chg. collector present	

Footnotes to Table C.3:

- (1) Fuel charge represents the current density measured from the filter but of opposite polarity.
Where the value is blank, the filter was bypassed.
- (2) Field Strength observed at about 90% full.
- (3) Exit velocity is about 15 m/s at maximum flow rate.
- (4) Exit velocity is about 3 m/s at maximum flow rate.
- (5) A = ambient temperature; L = liquid (fuel) temperature.

APPENDIX D

DRUM CHARGING/SPARKING TESTS

RED FOAM - BASE FUEL

TABLE D.1
 DRUM CHARGING/SPARKING TESTS - RED FOAM
 Test Fuel: Jet A (+2 ppm GA 178)

Run No.	Element Set	Flow Rate $\text{m}^3/\text{s} \times 10^{-3}$	Fuel Test Inlet:	Inlet Charge (1) $\mu\text{C}/\text{m}^3$	Drum Charge (2) $\mu\text{C}/\text{m}^3$	Field (3) $\mu\text{C}/\text{m}^3$	Total No. Radio Disch.	Remarks	Signals
				+20	+3	+19	-10	-	
501	1	2.52		+20	+2.4	+18	-3.7	-	
502	1	2.52		+20	+2.4	+20	+2.1	-	
503	1	2.52		+20	+2.4				
			Conductivity Check =	2.64 @ 21°C					
504	1	2.52		+20	+2.6	+18	-7	-	
505	1	2.52		+19	+3	+17	+4.2	-	
506	1	2.52		+19	+3	+18	-7	-	
			Conductivity Check =	2.12 @ 14°C					
507	1	2.52		+16	+3	+18	-2.3	-	
508	1	2.52		+38	+6	+34	-2.3	-	
509	1	2.52		+57	+10	+51	-1.0	-	
510	1	2.52		+62	+10	+56	+1.2	-	
511	1	2.52		+65	+10	+60	+1.2	-	
511A	1	2.52		+99	-	+198	+1.2	10	
512	1	2.52		+91	-79	+198	+4.5	26	
513	1	2.52		+107	-95	+198	+4.5	27	
			Conductivity Check =	1.12 @ 13°C					
514	1	2.52		+105	-52	+159	+6.2	8	
515	1	2.52		+98	-48	+159	+6.0	12	
516	1	2.52		+86	-48	+139	+5.2	10	
517	1	2.52		+87	-52	+151	+5.2	7	
518	1	2.52		---	-83	+99	+5.0	20	

Footnotes to Table D.1:

- (1) Fuel charge represents the current density measured from the filter but of opposite polarity. Where the value is blank, the filter was bypassed.
- (2) All current readings were made about 8 seconds after flow started.
- (3) Field Strength observed at about 90% full when the fuel reached the top of the foam.
- (4) Exit velocity was about 15 m/s at .00252 m³/s flow rate.

TABLE D.2

DRUM CHARGING/SPARKING TESTS - RED FOAM

Test Fuel: Jet A (+ 4.5 ppm GA 178 - Cu = 1.12 pS/m @ 13°C)

Run No.	Element Set	Flow Rate $\text{m}^3/\text{s} \times 10^{-3}$	Fuel (1)			Inlet (2)			Drum (3)			Total No. Radio Disch. Signals	Remarks
			Charge Density $\mu\text{C}/\text{m}^3$	Density $\mu\text{C}/\text{m}^3$	$\mu\text{C}/\text{m}^3$	Charge Density $\mu\text{C}/\text{m}^3$	Density $\mu\text{C}/\text{m}^3$	$\mu\text{C}/\text{m}^3$	Field Strength KV/m	Field Strength KV/m	Field Strength KV/m		
Test Inlet: High Velocity E11 (4)													
519	1	2.52	+87	-28		+119	+52		-	-	-	{ Started with low flow then, after inlet was covered, flow was increased. }	
520	1	2.52	+81	-24		+107	+51		-	-	-		
521	1	2.52	+80	-28		+119	+50		-	-	-		
522	1	2.52	+79	-24		+119	+51		-	-	-		
Combined Leads from Drum and Inlet													
523	1	2.52	+85	---		+88	+48		-	-	-		
524	1	2.52	+87	---		+91	+46		-	-	-		
525	1	2.52	+92	---		+96	+44		-	-	-		
526	1	2.52	+85	---		+87	+41		-	-	-		
527	1	2.52	+87	---		+90	+41		-	-	-		
Conductivity Check = 1.75 @ 17°C													
Charge Collector Present (5)													
528	1	2.52	+97	---		+97	+35		-	-	-		
Charge Collector Present + Brass Plate													
529	1	2.52	+96	---		+101	+18		-	-	-		
Charge Collector Present + Brass Plate													
530	1	2.52	+96	---		+97	+28		-	-	-		

(1) Fuel charge represents the current density measured from the filter but of opposite polarity.
 Where the value is blank, the filter was bypassed.

(2) All current readings were made about 8 seconds after flow started.

(3) Field Strength observed at about 90% full when the fuel reached the top of the foam.

(4) Exit Velocity was about 15 m/s at .00252 m^3/s flow rate.

(5) The charge collector was a metal clamp that was fastened to the inlet. It was electrically isolated from the inlet with a rubber gasket.

TABLE D.3

DRUM CHARGING/SPARKING TESTS - RED FOAM

Test Fuel: Jet A (Cu = 3.73 pS/m @ 4°C)

Run No.	Element Set	Flow Rate (1) m ³ /s x 10 ⁻³	Inlet: High Velocity E11(5)	Fuel (2)			Fuel (3)			Drum (4)			Total No. Radio Disch. Signals		Remarks	
				Charge	Charge	Density	Density	Field Strength	Field Strength	kV/m	kV/m	A	L	Temp °C (6)		
531	2	3.47	-1729	-317	-375	-300	-	-	-	-	-	3	6			
532	2	3.47	-1441	-288	-375	-300	-	-	-	-	-	3	7			
533	2	3.47/3.47	-	-8	+0.8	-290	-	-	-	-	-	5.5	4.5			
534	2	3.47/3.47	-	-8	+1.2	-310	2	-	-	-	-	4	5.5			
535	2	3.47/3.47	-	+6	-3	-290	4	-	-	-	-	5	6			
536	2	2.52	-	+12	-12	-300	-	-	-	-	-	5	7			
537	2	3.15/3.15	-	+3	+0.4	-300	-	-	-	-	-	5	7			
538	2	3.47/3.47	-	-1	+1	-320	1	-	-	-	-	5	8			
539	2	3.47	-1627	-218	-80	-290	-	-	-	-	-	5	8			
540	2	3.47/2.60	-1048	-8	-4	-300	6	-	-	-	-	6	9			
541	2	3.47/1.74	-1278	-20	-12	-300	-	-	-	-	-	5	9.5			
542	1	3.47	+22	-3	+22	-200	-	-	-	-	-	1	1			
543	1	3.47	-4	-5	+8	-300	-	-	-	-	-	1	1			
544	1	3.47	-8	-3	+10	-300	-	-	-	-	-	1	2			
545	1	3.47	+4	-4	+15	-300	-	-	-	-	-	1	2			

Footnotes to Table D.3:

- (1) When two numbers are shown this indicates mixed flow (charged + uncharged fuel). The second number identifies the uncharged fuel flow rate; the first number is the total system flow rate.
- (2) Fuel charge represents the current density measured from the filter but of opposite polarity. Where the value is blank, the filter was bypassed.
- (3) All current readings were made about 8 seconds after flow started.
- (4) Field Strength observed at about 90% full when the fuel reached the top of the foam.
- (5) Exit velocity was about 15 m/s at .00252 m³/s flow rate.
- (6) A = ambient temperature; L = liquid (fuel) temperature.

TABLE D.4

DRUM CHARGING/SPARKING TESTS - RED FOAM

Test Fuel: Jet A (Cu = 1.94 pS/m @ 3°C)

Run No.	Element Set	Flow Rate (1) m ³ /s x 10 ⁻³	Fuel Charge (2) μC/m ³	Inlet (3) Charge Density μC/m ³		Drum Strength KV/m	Field (4) μC/m ³	Total No. Radio Disch. Signals	Remarks	
				Test Inlet:	High Velocity E11 (5)				A	Temp °C
546	1	3.47/3.47	-	-4	+10	-300	-	-	1	3
547	1	3.47/3.47	-	-4	+9	-300	-	-	1	4
548	1	3.47/1.74	+12	-2	+16	-280	-	-2.8	-1.7	
549	1	3.47/2.60	+3	-2	+14	-300	-	-1.1	-1.1	
550	1	3.47	+9	-4	+20	-280	-	0.6	0	
		<u>Moved Charge Collector Up ~ 6 Inches on Inlet</u>								
551	1	3.47	+8	-3	+17	-280	½	+1.1	1.1	
552	1	3.47	+7	-2	+18	-280	1	1.7	1.7	
		<u>Charge Collector Removed</u>								
553	2	3.47/3.47	-	+1	+6	-200	-	6.1	12.2	
554	2	3.47	-2880	-173	-202	-130	62	6.1	11.7	
555	2	3.47	-1729	-288	-576	-200	36	6.1	11.7	

TABLE D.4 (Continued)

DRUM CHARGING/SPARKING TESTS - RED FOAM

Test Fuel: Jet A ($C_u = 1.94 \text{ pS/m}$ @ 3°C)

Run No.	Element Set	Flow Rate $\text{m}^3/\text{s} \times 10^{-3}$	Fuel (2)		Inlet (3)		Drum (3)		Field Strength KV/m	Total No. Radio Disch. Signals	Remarks
			Charge $\mu\text{C/m}^3$	Density $\mu\text{C/m}^3$	Charge $\mu\text{C/m}^3$	Density $\mu\text{C/m}^3$	A	L			
556	2	3.47/3.47	-	-	-4	-43	-300	6			
557	2	3.47/2.52	-721	-231	-288	-200	17			6.1	11.7
558	2	3.47/2.52	-576	-87	-317	-500 (6)	4			-3.3	-3.3
		Conductivity Check = 1.3 @ -2.2°C								-3.3	-2.8

- (1) When two numbers are shown, this indicates mixed flow (charged + uncharged fuel). The second number identifies the uncharged fuel flow rate; the first number is the total system flow rate.
- (2) Fuel charge represents the current density measured from the filter but of opposite polarity. Where the value is blank, the filter was bypassed.
- (3) All current readings were made about 8 seconds after flow started.
- (4) Field Strength observed at about 90% full when the fuel reached the top of the foam.
- (5) Exit velocity was 21 m/s at maximum flow rate.
- (6) The field meter used for this study was limited in the maximum value it could sense (500 KV/m or more. Thus, a reading of 500 KV/m could indicate that the field strength was 500 KV/m or more.

APPENDIX E
DRUM CHARGING/SPARKING TESTS
RED FOAM - ASA-3 EFFECTS

TABLE E.1
DRUM CHARGING/SPARKING TESTS - RED FOAM

Test Fuel: Jet A + ASA-3

Run No.	Element Set	Flow Rate $\text{m}^3/\text{s} \times 10^{-3}$	Fuel Charge $\mu\text{C}/\text{m}^3$	Inlet (1) Charge Density $\mu\text{C}/\text{m}^3$	Drum (2) Charge Density $\mu\text{C}/\text{m}^3$	Field (3) Strength kV/m	Total No. Radio Disch. Signals	Remarks	
								A	L
<u>Test Inlet: High Velocity E11 (4)</u>									
559	2	0.01 ppm ASA-3 Added	(4 pS/m @ 5°C)						
		3.47	-865	-202	-288	-180	40	1.7	7.2
560	2	3.47	-576	-58	-288	-270	3	1.7	7.2
561	2	3.47	-519	-115	-288	-250	3	1.7	6.1
562	2	3.47	-432	-52	-245	-270	-	1.7	6.7
<u>Conductivity Check = 2.3 @ 5.6°C</u>									
<u>2nd Step Increase in ASA-3 (C.U. = 9.2 @ 15°C)</u>									
563	2	3.47	-1153	-231	-375	-19	4	5	15
564	2	3.47	-432	-87	-202	-50	-	5.5	18
565	2	3.47	-404	-61	-202	-70	-	5.5	18
<u>Conductivity Check = 5.74 @ 12°C</u>									
<u>Installed Charge Collector on Inlet (~ 6" up on Inlet)</u>									
566	2	3.47	-346	-87	-144	+60	43	5	11
567	2	3.47	-288	-40	-144	-70	-	6	11.5
568	2	3.47	-259	-38	-144	-60	-	6	12
<u>Removed Charge Collector</u>									
569	2	3.47	-567	-115	-144	+150	49	11	10
<u>Conductivity Check = 5.45 @ 11°C</u>									
570	2	3.47	-288	-72	-144	-40	-	12	10.5
<u>Uncharged Fuel</u>									
571	2	3.47	-	+3	-144	-50	-	11.5	11.2
<u>0.01 ppm more ASA-3 --- Conductivity Check = 9.76 @ 17°C</u>									

Footnotes to Table E.1:

- (1) Fuel charge represents the current density measured from the filter but of opposite polarity.
Where the value is blank, the filter was bypassed.
- (2) All current readings were made about 8 seconds after flow started.
- (3) Field Strength observed at about 90% full when fuel reached the top of the foam.
- (4) Exit velocity was 20 m/s @ .00347 m³/s flow rate.
- (5) A = ambient temperature; L = liquid (fuel) temperature.

TABLE E.2
DRUM CHARGING/SPARKING TESTS - RED FOAM
Test Fuel: Jet A + ASA-3

Run No.	Element Set	Flow Rate $m^3/s \times 10^{-3}$	Fuel (2) Charge Density $\mu C/m^3$	Inlet (3) Charge Density $\mu C/m^3$	Drum (3) Charge Density $\mu C/m^3$	Field (4) Strength KV/m	Total No. Radio Disch. Signals	Remarks Temp °C (6)
<u>Test Inlet: High Velocity E11 (5)</u>								
572	2	3.47	-375	-58	-115	+26	35	A 11.5 10
573	2	3.15	-288	-52	-115	-45	-	L 15.5 10 15.5
<u>Installed Charge Collector</u>								
574	2	3.47	-259	-35	-115	-45	-	10 15.5
<u>Removed Charge Collector</u>								
<u>Uncharged Fueh After 1 1/2 Hours Layoff</u>								
575	2	3.47/3.47	-	+29	-	-28	-	8.5 15
<u>Conductivity Check = 8.9 @ 13°C</u>								
576	2	3.47	-288	-58	-87	+40	21	8.5 14.5
<u>Step Increase in ASA-3 Total Conc. = .024 ppm (Cu = 17.2 PS/m @ 19°C)</u>								
<u>Filters Untouched Overnight</u>								
577	2	3.47	-403	-144	+25	21	8	21
578	2	3.47	-288	-52	-87	-30	-	8.5 21
<u>Installed Charge Collector on Inlet</u>								
579	2	3.47	-259	-43	-72	+69	-	9 20
<u>Removed Charge Co-lector</u>								
<u>Step Increase in ASA-3 Total Conc. = .025 ppm (Cu = 43 PS/m @ 21°C)</u>								
580	2	3.47	-634	-127	-6	-	14	22
581	2	3.47	-539	-63	-63	-5	-	12 22
<u>Installed Charge Collector on Inlet</u>								
582	2	3.47	-461	-63	-46	-6	-	13 22
<u>Conductivity Check = 32.7 @ 18°C</u>								
<u>Removed Charge Collector</u>								

Footnotes to Table E.2:

- (1) When two numbers are shown, this indicates mixed flow (charged + uncharged fuel). The second number identifies the uncharged fuel flow rate; the first number is the total system flow rate.
- (2) Fuel charge represents the current density measured from the filter but of opposite polarity. Where the value is blank, the filter was bypassed.
- (3) All current readings were made about 8 seconds after flow started.
- (4) Field Strength observed at about 90% full when fuel reached the top of the foam.
- (5) Exit velocity was about 20 m/s @ .00347 m³/s flow rate.
- (6) A = ambient temperature; L = liquid (fuel) temperature.

TABLE E.3
DRUM CHARGING/SPARKING TESTS - RED FOAM

Test Fuel: Jet A + ASA-3

Run No.	Element Set	Flow Rate $\text{m}^3/\text{s} \times 10^{-3}$	Fuel (1) Charge Density $\mu\text{C}/\text{m}^3$	Inlet (2)		Field (3) Strength KV/m	Total No. Radio Disch. Signals	Remarks $\frac{\text{Temp } ^\circ\text{C} (5)}{\text{A } \text{L}}$						
				Charge Density $\mu\text{C}/\text{m}^3$	Charge Density $\mu\text{C}/\text{m}^3$									
Test Inlet: High Velocity E11(4)														
Over the Weekend - Fuel/System Untouched														
583	2	3.47	-231	-43	-14	-20	-	5 4						
Conductivity Check = 20 @ 5°C														
584	3	3.47	+576	+144	+202	+7	Installed Filter Element Set #3	5.5 5.5						
585	3	3.47	+576	+115	+202	+12								
586	3	3.47	Step Increase in ASA-3 (0.28 ppm total)	(0.28 ppm total) C.U. = 74.6 @ 13°C	+43	-2								
587	3	3.47	+461	+72	+55	-2								
588	2	3.47	+576	+89	+202	-3	Reinstalled Filter Element Set #2							
589	2	3.47	Conductivity Check = 68.9 @ 11°C	-20	-3	-3	5.5 13.5							
590	2	3.47	-231	-20	-3	-3	5.5 13.5							
591	2	3.47	-202	-	-13	Installed Charge Collector on Inlet, Near Nozzle	5.5 13							
592	2	3.47	-202	-43	+23	-5	5 13							
593	2	3.47	-202	-43	+14	-4	5.5 13							
594	2	3.47	Removed Charge Collector	-72	-29	-10	5.5 9.5							
				-432	-69	-29	5.5 10							
						-10								

Footnotes to Table E.3:

- (1) Fuel charge represents the current density measured from the filter but of opposite polarity.
Where the value is blank, the filter was bypassed.
- (2) All current readings were made about 8 seconds after flow started.
- (3) Field Strength observed at about 90% full when fuel reached the top of the foam.
- (4) Exit velocity was about 20 m/s @ .00347 m³/s flow rate.
- (5) A = ambient temperature; L = liquid (fuel) temperature.

TABLE E.4
DRUM CHARGING/SPARKING TESTS - RED (WATER SATURATED) FOAM (1)

Run No.	Element Set	Flow Rate $\text{m}^3/\text{s} \times 10^{-3}$	Test Fuel: Jet A + ASA-3		Fuel (2)		Inlet (3)		Drum (3)		Field (4)		Total No. Radio Disch.		Remarks		
					Charge	Charge Density	Charge Density	Strength	KV/m	Signals							
					$\mu\text{C}/\text{m}^3$	$\mu\text{C}/\text{m}^3$	$\mu\text{C}/\text{m}^3$	$\mu\text{C}/\text{m}^3$	$\mu\text{C}/\text{m}^3$	$\mu\text{C}/\text{m}^3$							
			Test	Inlet:	High Velocity	E11(6)											
595	4	3.47			-4467	-14		-14		-1		-			$\frac{\text{A}}{-3}$	$\frac{\text{L}}{-3}$	
596	4	3.47			-3890	-14		-9		-2		-			$\frac{\text{A}}{-3}$	$\frac{\text{L}}{-3}$	
597	4	3.47			-	+6		-3		-2		-			$\frac{\text{A}}{-2}$	$\frac{\text{L}}{-2}$	
			Conductivity Check = 143.5 @ -1.5°C												$\frac{\text{A}}{-2}$	$\frac{\text{L}}{-1.5}$	
598	4	3.47			-4323	-29		-3		-2		-			$\frac{\text{A}}{0}$	$\frac{\text{L}}{0}$	
599	4	3.47			-3458	-17		-3		-1		-			$\frac{\text{A}}{0.5}$	$\frac{\text{L}}{1.5}$	
															$\frac{\text{A}}{0}$	$\frac{\text{L}}{1.5}$	

- (1) The test fuel was exposed to blue foam directly prior to this test series.
- (2) Fuel charge represents the current density measured from the filter but of opposite polarity. Where the value is blank, the filter was bypassed.
- (3) All current readings were made about 8 seconds after flow started.
- (4) Field Strength observed at about 90% full when fuel reached the top of the foam.
- (5) A = ambient temperature; L = liquid (fuel) temperature.
- (6) Exit velocity was about 20 m/s (0.0347 m^3/s) flow rate.

APPENDIX F
DRUM CHARGING/SPARKING TESTS
BLUE FOAM - BASE FUEL

TABLE F.1

DRUM CHARGING/SPARKING TESTS - BLUE FOAM
 Test Fuel: Jet A + 2 ppm GA 178

Run No.	Element Set	Flow Rate $\text{m}^3/\text{s} \times 10^{-3}$	Fuel(1) Charge Density $\mu\text{C}/\text{m}^3$	Inlet(2)		Drum(2)		Total No. Radio Disch. Signals	Remarks
				Charge Density $\mu\text{C}/\text{m}^3$	Charge Density $\mu\text{C}/\text{m}^3$	Field(3) Strength kV/m	Field(3) Strength kV/m		
<u>Test Inlet: High Velocity Ell(4)</u>									
600	1	2.52	+71	-	+48	-500	43	Combined Leads	
601	1	2.52	+24	-	+40	-500	77	From Inlet & Drum	
602	1	2.52	-130	-	-29	-500	52	Combined Leads	
<u>Conductivity = 2.1 @ 14°C</u>									
603	1	2.52	-242	-	-28	-500	50	From Inlet & Drum	
604	1	2.52	-278	+183	-198	-500	23		
605	1	2.52	-337	+238	-277	-500	30		
<u>Uncharged Fuel</u>									
606	1	2.52	-	+397	-397	-500	36	<u>A</u>	
607	1	2.52	-	-14	+40	-500	7	12	26
608	1	2.52	-	-12	+26	-500	2	12	25
609	1	2.52	-	-12	+28	-500	4	11	24
<u>Conductivity Check = 2.18 @ 18°C</u>									
610	1	2.52	+119	+20	+79	-500	11	10	10
611	1	2.52	-	-12	+36	-500	4	10	11
612	1	2.52	+198	+28	+159	-500	6	11	12

Footnotes to Table F.1:

- (1) Fuel charge represents the current density measured from the filter but of opposite polarity.
Where the value is blank, the filter was bypassed.
- (2) All current readings were made about 8 seconds after flow started.
- (3) Field Strength observed at about 90% full when fuel reached the top of the foam. The field meter used for this study was limited in the maximum value it could sense (500 KV/m). Thus, a reading of 500 KV/m could indicate that the field strength was 500 KV/m or more.
- (4) Exit velocity was 15 m/s @ .00252 flow rate.
- (5) A = ambient temperature; L = liquid (fuel) temperature.

TABLE F.2
DRUM CHARGING/SPARKING TESTS - BLUE FOAM
Test Fuel: Jet A (Clay Treated; Cu = 2.2 pS/m @ 18°C)

Run No.	Element Set	Flow Rate(1) $\text{m}^3/\text{s} \times 10^{-3}$	Charge Density $\mu\text{C}/\text{m}^3$	Fuel(2)	Inlet(3)	Drum(3)	Field(4) Strength kV/m	Total No. Radio Disch. Signals	Remarks	
									$\mu\text{C}/\text{m}^3$	$\mu\text{C}/\text{m}^3$
613	1	2.52	+198	Charge Collector Present	+20	+159	-500	5	A	L
				Charge Collector Removed					11	12
614	1	2.52	+198		+20	+159	-500	5	11	13
615	1	2.52	+198		+16	+159	-500	13	11	13
				Uncharged Fuel Runs						
616	1	2.52	-		-12	+36	-500	1	12	13
617	1	3.47/3.47	-		-12	+40	-500	-		
618	1	3.47/3.47	-		-12	+40	-500	-		
619	1	2.52/1.26	+198		-20	+115	-500	1		
620	1	2.52/1.26	+238		+5	+119	-500	7		
621	1	2.52/1.89	+238		-10	+60	-500	10		
622	1	2.52/0.63	+212		+12	+159	-500	14		
623	1	3.47	+309		+24	+278	-500	-	2	2
624	1	3.47	+278		+20	+258	-500	-	4	3

(1) When two numbers are shown, this indicates mixed flow (charged + uncharged fuel). The second number identifies the uncharged fuel flow rate; the first number is the total system flow rate.

(2) Fuel charge represents the current density measured from the filter but of opposite polarity. Where the value is blank, the filter was bypassed.

(3) All current readings were made about 8 seconds after flow started.

(4) Field Strength observed at about 90% full when fuel reached the top of the foam. The field meter used for this study was limited in the maximum value it could sense (500 KV/m). Thus, a reading of 500 KV/m could indicate that the field strength was 500 KV/m or more.

(5) Exit velocity was 15 m/s @ .00252 m^3/s ; 20 m/s @ .00347 m^3/s flow rates.

(6) A = ambient temperature; L = liquid (fuel) temperature.

TABLE F.3
DRUM CHARGING/SPARKING TESTS - BLUE FOAM
Test Fuel: Jet A (Cu = 2.2 pS/m @ 18°C)

Run No.	Element Set	Flow Rate $\text{m}^3/\text{s} \times 10^{-3}$	Fuel(1) Charge Density $\mu\text{C}/\text{m}^3$	Inlet(2)		Field(3) Strength KV/m	Total No. Radio Disch. Signals	Remarks $\frac{\text{Temp } ^\circ\text{C}(4)}{\text{A } \text{L}}$
				Charge Density $\mu\text{C}/\text{m}^3$	Field(2) Strength $\mu\text{C}/\text{m}^3$			
<u>Test Inlet: Short Pipe w/orifice (5)</u>								
625	2	3.47	-	-6	+20	-500	-	
626	2	3.47	-	-6	+20	-500	3	1 2.5
627	2	3.47	-	-6	+17	-500	-	1.5 2.5
628	2	2.52	-	-6	+14	-500	-	1.5 3
629	2	3.47	-14	-9	+9	-500	1	3 3.5
630	2	3.47	-14	-9	+14	-500	2	3 5
<u>No Charge Collector for Runs 625 thru 651</u>								
631	2	3.47	-	-1.4	+19	-500	1	3.5 4.5
632	2	3.47	-	-1.4	+23	-500	-	2 4
633	2	3.47	-	-1.4	+16	-500	-	2 5
634	2	3.47	+14	+4	+32	-500	-	2 5
635	2	3.47	+32	+12	+32	-500	-	2.5 5
636	2	3.47	+35	+6	+40	-500	1	3 6
<u>Conductivity Check = 1.4 @ 5°C</u>								
637	1	3.47	+72	+6	+58	-500	22	-2.5 -1
638	1	3.47	+63	+29	+72	-500	14	-2 -1
639	1	3.47	+63	+29	+87	-500	12	-1.5 0
<u>Conductivity Check = 1.25 @ -0.5°C</u>								

Footnotes to Table F.3:

- (1) Fuel charge represents the current density measured from the filter but of opposite polarity.
Where the value is blank, the filter was bypassed.
- (2) All current readings were made about 8 seconds after flow started.
- (3) Field Strength observed at about 90% full when fuel reached the top of the foam. The field meter used for this study was limited in the maximum value it could sense (500 KV/m). Thus, a reading of 500 KV/m could indicate that the field strength was 500 KV/m or more.
- (4) A = ambient temperature; L = liquid (fuel) temperature.
- (5) Exit velocity was about 20 m/s @ .00347 m^3/s flow rate.

TABLE F.4
DRUM CHARGING/SPARKING TESTS - BLUE FOAM
Test Fuel: Jet A ($Cu = 1.3$ pS/m @ $-5^{\circ}C$)

Run No.	Element Set	Flow Rate $m^3/s \times 10^{-3}$	Fuel(1) Charge Density $\mu C/m^3$	Inlet(2) Charge Density $\mu C/m^3$	Drum (3) Field Strength KV/m	Total No. Radio Disch. Signals	Remarks	
							A Temp $^{\circ}C$ (4)	L $\frac{1}{A}$
Test Inlet: High Velocity E11(5)								
640	1	3.47	-	-6	+23	-500	3	-1
641	1	3.47	-	-3	+20	-500	3	-1
642	1	3.47	-	-3	+20	-500	2	-1
643	4	3.47	-86	-7	-14	-500	3	1.5
644	4	3.47	-230	-40	-87	-500	7	1.5
645	4	3.47	-346	-43	-144	-500	25	2
646	4	3.47	-720	-72	-173	-500	23	3.5
647	4	3.47	-749	-72	-202	-500	55	4
Conductivity Check = 8.0 @ $3^{\circ}C$								
Fuel Clay Treated to Cond. = 0.5 pS/m @ $14.5^{\circ}C$								
648	4	3.47	-	-6	+6	-500	5	-2
649	4	3.47	-864	+29	-432	-500	48	-1
650	4	3.47	-864	+43	-432	-500	38	0
651	4	3.47	-	+6	-12	-500	5	1
652	4	3.47	-	-	+6	-500	-	3
653	4	3.47	Charge Collector Installed	-12	+14	-500	1	5.5
654	4	3.47	Removed Charge Collector	-3	+9	-500	1	4

Footnotes to Table F.4:

- (1) Fuel charge represents the current density measured from the filter but of opposite polarity.
Where the value is blank, the filter was bypassed.
- (2) All current readings were made about 8 seconds after flow started.
- (3) Field Strength observed at about 90% full when fuel reached the top of the foam. The field meter used for this study was limited in the maximum value it could sense (500 KV/m). Thus, a reading of 500 KV/m could indicate that the field strength was 500 KV/m or more.
- (4) A = ambient temperature; L = liquid (fuel) temperature.
- (5) Exit velocity was 20 m/s @ .00347 m^3/s flow rate.

APPENDIX G
DRUM CHARGING/SPARKING TESTS
BLUE FOAM - ASA-3 EFFECTS

TABLE G.1
DRUM CHARGING/SPARKING TESTS - BLUE FOAM - ASA-3 EFFECTS
Test Fuel: Jet A + ASA-3

Run No.	Element Set	Flow Rate $\text{m}^3/\text{s} \times 10^{-3}$	Charge Density $\mu\text{C}/\text{m}^3$	Inlet(2) Charge Density $\mu\text{C}/\text{m}^3$	Drum(2) Charge Density $\mu\text{C}/\text{m}^3$	Field(3) Strength KV/m	Total No. Radio Disch. Signals	Remarks	
								$\text{C}(4)$	
ASA-3 Increment #1 (.00115 ppm)									
655	4	3.47	-864	-100	-230	-500	12	$\frac{\text{A}}{4.5}$	$\frac{\text{L}}{13}$
Conductivity Check = 2.9 @ 14°C									
656	4	3.47	-864	-69	-576	-500	13	2	0
657	4	3.47	-	-3	+12	-500	44	2	1
658	4	3.47	-	-6	+14	-500	27	2.5	3
ASA-3 Increment #2 (.02 ppm) - Conductivity = 3.9 @ 10°C									
659	4	3.47	-864	-100	-230	-500	11	3	14
ASA-3 Increment #2A (.030 ppm) - Conductivity = 4 @ 11.5°C									
660	4	3.47	-	-7	+6	-500	10	4	18
661	4	3.47	-720	-77	-172	-500	Pens Not Functioning	4	15
ASA-3 Increment #2B (.035 ppm) - Conductivity = 4.9 @ 14°C									
662	4	3.47	-720	-77	-172	-500	11	4.5	14.5
663	4	3.47	-1008	-100	-172	-500	18	4	18
664	4	3.47	-	-7	+12	-500	20	5	16
665	4	3.47	-	-9	+14	-500	19	5	15.5
ASA-3 Increment #3 (.045 ppm) - Conductivity = 6.6 @ 17°C									
666	4	3.47	-1297	-100	-130	-250	18	5	23.5
667	4	3.47	-	-10	+14	-270	15	5.5	20

TABLE G.1 (continued)

DRUM CHARGING/SPARKING TESTS - BLUE FOAM - ASA-3 EFFECTS

Test Fuel: Jet A + ASA-3

Run No.	Element Set	Flow Rate $\text{m}^3/\text{s} \times 10^{-3}$	Charge Density $\mu\text{C}/\text{m}^3$	Fuel (1) Inlet (2) Charge Density $\mu\text{C}/\text{m}^3$	Drum (2) Charge Density $\mu\text{C}/\text{m}^3$	Field (3) Strength kV/m	Total No. Radio Disch. Signals	Remarks	
								$\frac{\text{A}}{6}$	$\frac{\text{L}}{20}$
668	4	3.47	-864	-72	-172	-300	15		
669	4	ASA-3 Increment #4	(.067 ppm)						
		3.47	-865	-72	-101	-500	32	9.5	9
		Conductivity Check = 7.2 @ 9°C							
670	4	3.47	-	-14	+14	-500	28	7	9
671	4	3.47	-	-14	+14	-500	21	6.5	9
		ASA-3 Increment #5	(.090 ppm)	Conductivity = 9.2 @ 14°C					
672	4	3.47	-1009	-72	-101	-500	15	6.5	18
673	4	3.47	-	-14	+14	-500	7	7	16.5
674	4	3.47	-	-14	+14	-500	28	7.5	16
		ASA-3 Increment #6	(.135 ppm)	Conductivity = 13.8 @ 15°C					
675	4	3.47	-1441	-72	-58	-270	16	8	21
676	4	3.47	-	-43	+43	-180	37	8.5	18
677	4	3.47	-1153	-58	-58	-300	69	9	17
		ASA-3 Increment #7	(.27 ppm)	Conductivity = 20.7 @ 15°C					
678	4	3.47	-2017	-87	+58	-150	58	8	18
679	4	3.47	-	-144	+144	-150	109	8	18
		ASA-3 Increment #8	(.54 ppm)	Conductivity = 39 @ 18°C					
680	4	3.47	-2161	-58	+404	-28	97	6.5	22.5

TABLE G.1 (continued)

DRUM CHARGING/SPARKING TESTS - BLUE FOAM - ASA-3 EFFECTS
Test Fuel: Jet A + ASA-3

Run No.	Element Set	Flow Rate $\text{m}^3/\text{s} \times 10^{-3}$	Fuel(1) Charge Density $\mu\text{C}/\text{m}^3$	Inlet(2) Charge Density $\mu\text{C}/\text{m}^3$	Drum(2) Field(3) Strength KV/m	Total No. Radio Disch. Signals	Remarks	
							Temp °C(4)	
681	4	3.47	-	-721	+576	-20	100	
682	4	2.52	-	-794	+397	-10	61	
								L
							7	20.5
							7	19
683	4	ASA-3 Increment #9 (.89 ppm)	-2882	-4223	+288	-23	122	-3.5
684	4	3.47	-	-2882	+576	-60	94	-2.5
685	4	1.89	-	-794	+688	+23	41	0
							-2	0
686	4	ASA-3 Increment #10 (1.24 ppm)	-1440	+144	-23	41	-1	1
687	4	3.47	-2882	-1440	Conductivity = 88.9 @ 7°C			
688	4	3.47	-	-1153	+144	-18	69	-5
689	4	1.89	-	-529	+159	-6	46	0
						-7	32	8
							+5.5	7
690	4	ASA-3 Increment #11 (1.59 ppm)	-1729	-231	Conductivity = 120 @ 7°C			
691	4	3.47	-	-144	+144	-6	26	-0.5
692	4	2.52	-	-43	-130	+15	14	9
							-1	8
693	4	ASA-3 Increment #12 (1.94 ppm)	-2305	-144	Conductivity = 166 @ 9°C			
694	4	3.47	-	+87	+144	-5	35	-2.5
695	4	3.47	-	-58	-202	-6	44	14
					+144	-8	19	2
							2	0

TABLE G.1 (continued)

DRUM CHARGING/SPARKING TESTS - BLUE FOAM - ASA-3 EFFECTS
Test Fuel: Jet A + ASA-3

Run No.	Element Set	Flow Rate $\text{m}^3/\text{s} \times 10^{-3}$	Fuel(1) Charge Density $\mu\text{C}/\text{m}^3$	Inlet(2) Charge Density $\mu\text{C}/\text{m}^3$	Drum(3) Strength KV/m	Total No. Radio Disch. Signals	Remarks	
							A	L
Test Inlet: High Velocity E11(5)								
696	4	3.47	-5764	-432	+144	-6	31	
697	4	3.47	-2882	-865	+259	+23	83	
698	4	3.47	-	-721	+144	+36	58	
ASA-3 Increment #13 (2.29 ppm)								
699	4	3.47	-2305	-231	+144	-0.7	53	-0.5
Conductivity Check = 183.7 @ 5.5°C								
6000	4	3.47	-	-202	+202	-5	18	
6001	4	3.47	-2882	-173	+115	-0.4	44	
ASA-3 Increment #14 (2.64 ppm)								
6002	4	3.47	-2882	-288	-173	-1.2	47	-3
Conductivity Check = 218.1 @ 25°C								
6003	4	3.47	-	-144	+144	-6	6	-2
6004	4	3.47	-2882	+1440	-144	-10	45	-
6005	4	3.47	-	+29	-58	-10	13	0.5
ASA-3 Increment #15 (2.99 ppm)								
6006	4	3.47	-2882	-144	-87	-6	25	1
Conductivity Check = 258.3 @ 6.5°C								
6007	4	3.47	-	-58	+58	-6	6	2
6008	4	3.47	-	+17	-29	-5	7	0.5
							2	10

TABLE G.1 (continued)

DRUM CHARGING/SPARKING TESTS - BLUE FOAM - ASA-3 EFFECTS
Test Fuel: Jet A + ASA-3

Run No.	Element Set	Flow Rate $\text{m}^3/\text{s} \times 10^{-3}$	Fuel(1)		Inlet(2)		Drum(3)		Total No. Radio Disch. Signals	Remarks
			Charge $\mu\text{C}/\text{m}^3$	Density $\mu\text{C}/\text{m}^3$	Charge $\mu\text{C}/\text{m}^3$	Density $\mu\text{C}/\text{m}^3$	Field Strength KV/m			
Test Inlet: High Velocity E11 (59)										
6009	4	2.52	-1786	+40	-198	-0.4	36	$\frac{A}{3.5}$	$\frac{L}{8.5}$	
6010	4	2.52	-	-20	-20	-1	6	4	9	
6011	4	1.26	-48	-79	+48	-0.1	-	4	9.5	
6012	4	1.89	-1058	+16	-27	-0.4	7	4	11	
6013	4	1.89	-	+16	-16	-0.4	1	5	11.5	
6014	4	1.89	-	+16	-16	-0.4	3	5	12	
6015	4	1.26	-	+10	-87	-0.1	-	5	13	

(1) Fuel charge represents current density measured from the filter but of opposite polarity.
Where the value is blank, the filter was bypassed.

(2) All current readings were made about 8 seconds after flow started.

(3) Field Strength observed at about 90% full when fuel reached the top of the foam. The field meter used for this study was limited in the maximum value it could sense (500 KV/m). Thus, a reading of 500 KV/m could indicate that the field strength was 500 KV/m or more.

(4) A = ambient temperature; L = liquid (fuel) temperature.

(5) Exit velocity was about 20 m/s @ .00347 m^3/s flow rate.

APPENDIX H
DRUM CHARGING/SPARKING TESTS
INLET STUDIES

TABLE H.1
DRUM CHARGING/SPARKING TESTS - BLUE FOAM
INLET STUDIES

Run No.	Element Set	Flow Rate $\text{m}^3/\text{s} \times 10^{-3}$	Test Fuel: Jet A + ASA-3						Remarks	
			Fuel (1)		Inlet (2)		Drum (3)			
			Charge	Density $\mu\text{C}/\text{m}^3$	Charge	Density $\mu\text{C}/\text{m}^3$	Field (3) Strength KV/m	Temp $^{\circ}\text{C}(4)$		
6016	4	3.47	-5764	+231	-231	-231	-1.4	3	2 0	
6017	4	3.47	-2305	+231	-231	-231	-1.2	1	2 1	
			Conductivity Check = 192.3 @ 2°C							
6018	4	3.66	-2882	+202	-231	-231	-7	3	-1 -2.5	
6019	4	3.66	-4323	+202	-231	-231	-2	-	0 -3	
6020	4	3.66	-2882	+173	-231	-231	-3	3	3 6	
			Clay Filtered Out Some ASA-3							
6021	4	3.66	-	+202	-216	-216	-2	-	2.5 5.5	
6022	4	3.66	-6284	+191	-191	-191	-5	1	3 -1	
			Conductivity Check = 132 @ 1°C							
6023	4	3.66	-6284	+273	-273	-273	-5	1	5 1.5	
6024	4	3.66	-	+191	-191	-191	-3.2	1	5 2	
			Inverted "Jets" in Piccolo -- Now Facing "Up" into Foam							
6025	4	3.66	-6284	+55	-55	-55	-13	1	5 3	
			Clay Filtered out more ASA-3							
6026	4	3.66	-	+86	-68	-68	-5	-	5 3.5	
6027	4	3.66	-5464	+191	-301	-301	-13	-	5 4	
			Conductivity Check = 89 @ 6°C							
6028	4	3.66	-6831	-683	-355	-355	-20	3	1.5 8.5	
			Clay Filtered out more ASA-3							
6029	4	3.66	-	+137	-137	-137	-15	-	2 6.5	
6030	4	3.66	-6284	-164	-355	-355	-20	1	4 6.5	
6031	4	3.66	-8743	-546	-328	-328	-60	1	0.5 -1.5	
6032	4	3.66	-	+137	-137	-137	-90	1	1 1	

TABLE H.1 (continued)

DRUM CHARGING/SPARKING TESTS - BLUE FOAM
INLET STUDIES

Run No.	Element Set	Flow Rate $\text{m}^3/\text{s} \times 10^{-3}$	Test Fuel: Jet A + ASA-3						Remarks $\frac{\text{Temp } ^\circ\text{C}(4)}{\text{A/L}}$	
			Fuel (1)		Inlet (2)		Drum (2)			
			Charge Density $\mu\text{C}/\text{m}^3$	Density $\mu\text{C}/\text{m}^3$	Charge Density $\mu\text{C}/\text{m}^3$	Density $\mu\text{C}/\text{m}^3$	Field (3) Strength KV/m	Total No. Radio Disch. Signals		
6033	4	3.53	-4098	+109	-301	-70	-	-	$\frac{\text{A}}{1}$ $\frac{\text{L}}{0}$	
	Installed New Piccolo (#2)		-19 holes	(10 m/s velocity)	-	-	-	-		
6034	4	3.66	-6831	-465	-246	-13	7	3.5	2.5	
6035	4	3.66	-7377	-410	-246	-13	7	3.5	3	
6036	4	3.66	-	+63	-68	-12	-	3.5	3	
6037	4	3.66	-6010	-218	-137	-10	2	6	2.5	
	Conductivity Check = 94.7 @ 5°C									
6038	4	3.66	-	+54.6	-68	-7	-	4.5	3	
6039	4	3.66	-6010	-164	-137	-12	1	5	3.5	
6040	4	2.84	-4929	-88	-88	-3	2	5	4.5	
6041	4	2.21	-4525	+32	-50	-3	-	4	5	
6042	4	3.66	-5737	-164	-109	-10	-	.5	1	
	Conductivity Check = 91.8 @ 10°C									
6043	4	3.66	-5738	-164	-137	-11	1	1	1.5	
6044	4	3.66	-5464	-137	-109	-11	-	1	2	
6045	4	3.66	-6557	-273	-205	-13	-	2.5	8.5	
	4th ASA-3 Reduction + 8 Gals. Addition of Fuel (Jet A + ASA-3)									
6046	4	3.66	-6010	-191	-177	-11	5	3.5	6	
6047	4	3.66	-5464	-273	-164	-13	-	3	7	

TABLE H.1 (continued)

DRUM CHARGING/SPARKING TESTS - BLUE FOAM
INLET STUDIES

Run No.	Element Set	Test Fuel: Jet A + ASA-3						Remarks	
		Fuel (1)		Inlet (2)		Drum (3)			
		Charge	Charge	Density	Density	Field Strength	Total No. Radio Disch.		
				$\mu\text{C}/\text{m}^3$	$\mu\text{C}/\text{m}^3$	KV/m	Signals		
6048	4	3.66	-4918	-218	-164	-13	-	$\frac{\text{A}}{3.5} \frac{\text{L}}{7}$	
		Test Inlet: Piccolo #2 (10 m/s velocity)							
		Conductivity Check = 71.8 @ 7°C							
6049	4	3.66	-6830	-464	-382	-23	-	-2.5 -1	
		5th ASA-3 Reduction							
6050	4	3.66	-6284	-409	-363	-23	-	+0.5 0	
6051	4	3.66	-5737	-464	-355	-25	3	1 0.5	
6052	4	3.66	-6011	-546	-410	-30	2	1.5 1.5	
		6th ASA-3 Reduction							
6053	4	3.66	-5191	-355	-245	-23	3	3 9.5	
		Conductivity Check = 51.7 @ 8°C							
6054	4	3.66	-4918	-355	-300	-23	4	4 9	
6055	4	3.78	-	+49	-68	-18	-	5 9	
		7th ASA-3 Reduction							
6056	4	3.66	-4918	-273	-191	-28	3	5 16	
6057	4	3.66	-4371	-355	-327	-25	5	5 12	
		Temp. Reduction After #7 Reduction							
6058	4	3.66	-6557	-792	-738	-90	4	3 0	
		Conductivity Check = 38.5 @ 1°C							
6059	4	3.66	-5191	-519	-464	-90	-	4 1.0	
		8th ASA-3 Reduction							

TABLE H.1 (continued)

DRUM CHARGING/SPARKING TESTS - BLUE FOAM
INLET STUDIES

Run No.	Element Set	Flow Rate $\text{m}^3/\text{s} \times 10^{-3}$	$\mu\text{C}/\text{m}^3$	Test Fuel: Jet A + ASA-3				Total No. Radio Disch. Signals	Remarks $\frac{\text{Temp } ^\circ\text{C}(4)}{\text{A}}$ $\frac{\text{L}}{3.5}$		
				Fuel (1)		Fuel (2)					
				Charge	Charge	Density $\mu\text{C}/\text{m}^3$	Density $\mu\text{C}/\text{m}^3$				
6060	4	3.66	-4644	-601	-355	-220	1	$\frac{\text{A}}{3.5}$	$\frac{\text{L}}{8}$		
6061	4	3.66	Conductivity Check = 27 @ 7°C	-546	-546	-100	1	6	7		
6062	4	3.78	-4644	+41	-68	-50	-	7	7.5		
6063	4	3.66	-	-	-437	-90	2	7	8		
6064	4	3.66	9th ASA-3 Reduction	-409	-437	-409	-150	2	7		
6065	4	3.66	Test Inlet: Piccolo #2 (10 m/s velocity)	-4371	-437	-409	-150	2	7		
6066	4	3.66	Conductivity Check = 32.7 @ 13°C	-683	-1229	-500	12	6	12.5		
6067	4	2.52	-3825	-628	-1092	-500	10	6	12		
6068	4	3.0	-3571	-476	-634	-500	-	6	13		
6069	4	3.66	-3000	-500	-733	-500	2	6.5	13		
6070	4	3.66	-2596	-437	-683	-500	10	7	12.5		
6071	4	3.66	-	+6	-41	-500	6	7	12.5		
6072	4	3.66	Conductivity Check = 14.9 @ 10°C	-41	-41	-500	8	7	13		
6073	4	3.78	-2592	-505	-1229	-500	2	0.5	-2		
6074	4	2.52	-	-123	+95	-500	8	1.5	-1		
			-3373	-595	-1111	-500	-	3	0		

TABLE H.1 (continued)

DRUM CHARGING/SPARKING TESTS - BLUE FOAM
INLET STUDIES

Test Fuel: Jet A + ASA-3

Run No.	Element Set	Flow Rate $\text{m}^3/\text{s} \times 10^{-3}$	Charge $\mu\text{C}/\text{m}^3$	Fuel (1)		Inlet (2)		Drum (2)		Total No. Radio Disch. Signals	Remarks $\frac{\text{Temp } ^\circ\text{C}}{\text{A } \frac{\text{L}}{6}}$
				Charge $\mu\text{C}/\text{m}^3$	Density $\mu\text{C}/\text{m}^3$	Charge $\mu\text{C}/\text{m}^3$	Density $\mu\text{C}/\text{m}^3$	Strength kV/m			
6075	4	3.66	-2787	-628	-1229	-500	14				
		Conductivity Check = 13.2 @ 8°C									
		12th ASA-3 Reduction									
6076	4	3.66	-3142	-573	-1174	-500	1	0	-1.5		
		Conductivity Check = 8.3 @ 1.5°C									
6077	4	3.66	-2868	-546	-1174	-500	2	0.5	-0.5		
6078	4	2.84	-3169	-563	-1197	-500	6	1.5	+0.5		
6079	4	3.78	-	-105	+105	-500	1	2	2		
		13th ASA-3 Reduction									
6080	4	2.52	-2579	-476	-992	-500	1	2	3		
6081	4	3.47	-	-202	+173	-500	3	2	3		
6082	4	2.52	-2380	-476	-992	-500	1	2	3		
6083	4	2.21	-1809	-317	-542	-500	-	2.5	4		
		Conductivity Check = 9.0 @ 5.5°C									
6084	4	3.66	-2459	-464	-956	-500	17	4	1		
		Conductivity Check = 13.2 @ 8°C									
6085	4	3.66	-2459	-546	-1229	-500	19	6.5	3.5		
6086	4	3.78	-	-132	+132	-500	7	7	4		
6087	4	2.52	-1786	-436	-793	-500	16	7	5		
6088	4	1.89	-2010	-317	-582	-500	2	7.5	7		
6089	4	1.26	-1984	-198	-396	-300	-	8	7.5		
		Partially Replaced Fuel w/"Clean" Jet A (~ 40 gals); Cu (pS/m) = 2.09 @ 71°C									

TABLE H.1 (continued)

DRUM CHARGING/SPARKING TESTS - BLUE FOAM
INLET STUDIES

Run No.	Element Set	Flow Rate $\text{m}^3/\text{s} \times 10^{-3}$	Fuel (1) Charge Density $\mu\text{C}/\text{m}^3$	Test Fuel: Jet A + ASA-3		Total No. Radio Disch. Signals	Remarks $\frac{\text{Temp } ^\circ\text{C}(4)}{\frac{\text{A}}{2} - \frac{\text{L}}{0}}$
				Inlet (2) Drum (2)	Field (3) Strength KV/m		
				Charge Density $\mu\text{C}/\text{m}^3$	Field Strength $\mu\text{C}/\text{m}^3$		
6090	4	3.66	-1639	-383 @ 2°C	-765	-500	34
		Conductivity Check = 6.3	-1366	-328	-820	-500	
6091	4	3.66	-	-159	-106	-500	40
6092	4	3.78	-	-1164	-265	-500	32
6093	4	1.59	-	-265	-265	-500	4
6094	4	1.26	-1111	-222	-71	-500	4.5
						-	5
							4.5

- (1) Fuel charge represents the current density measured from the filter but of opposite polarity. Where the value is blank, the filter was bypassed.
- (2) All current readings were made about 8 seconds after flow started.
- (3) Field Strength observed at about 90% full when fuel reached the top of the foam. The field meter used **for** this study was limited in the maximum value it could sense (500 KV/m). Thus, a reading of 500 KV/m could indicate that the field strength was 500 KV/m or more.
- (4) A = ambient temperature; L = liquid (fuel) temperature.

TABLE H.2
DRUM CHARGING/SPARKING TESTS - BLUE FOAM
INLET STUDIES

Test Fuel: Jet A (Clay treated) ($C_u = 1.2 \text{ pS/m} @ 6^\circ\text{C}$)

Run No.	Element Set	Flow Rate $\frac{\text{m}^3/\text{s}}{10^{-3}}$	Fuel Charge $\mu\text{C}/\text{m}^3$	Fuel (1)		Inlet (2)		Drum (2)		Total No. Radio Disch. Signals	Remarks $\frac{\text{Temp } ^\circ\text{C}(4)}{\text{A } \text{L}}$
				Test Inlet:	Piccolo #2	Density $\mu\text{C}/\text{m}^3$	Charge $\mu\text{C}/\text{m}^3$	Density $\mu\text{C}/\text{m}^3$	Field (3) KV/m		
					(10 m/s velocity)						
6095	4	3.66	-820	-109	-601	-500	-500	-500	-500	62	$\frac{5.5}{6.5}$
6096	4	3.66	Conductivity Check = 1.2 @ 6°C	+27	-14	-500	-500	-500	-500	4	$\frac{5.5}{5.5}$
6097	4	1.89	-	-90	-502	-500	-500	-500	-500	4	$\frac{5.5}{7.5}$
6098	4	1.26	-952	-87	-476	-500	-500	-500	-500	8	$\frac{5.5}{8.5}$
6099	4	1.89	-	+23	-23	-500	-500	-500	-500	1	$\frac{5}{9}$
6100	4	1.26	-	+32	-64	-500	-500	-500	-500	10	$\frac{4}{8.5}$
<hr/>											
<hr/>											
Installed Piccolo #3 (4.8 m/s velocity)											
6101	4	3.66	-546	-164	-246	-500	-500	-500	-500	22	$\frac{0.5}{-1}$
6102	4	3.78	-	-41	+55	-500	-500	-500	-500	5	$\frac{1.5}{0}$
6103	4	2.52	-437	-119	-238	-500	-500	-500	-500	8	$\frac{2}{1.5}$
6104	4	1.89	-397	-106	-230	-500	-500	-500	-500	1	$\frac{2}{2}$

- (1) Fuel charge represents the current density measured from the filter but of opposite polarity. Where the value is blank, the filter was bypassed.
- (2) All current readings were made about 8 seconds after flow started.
- (3) Field Strength observed at about 90% full, when fuel reached the top of the foam. The field meter used for this study was limited in the maximum value it could sense (500 KV/m). Thus, a reading of 500 KV/m could indicate that the field strength was 500 KV/m or more.
- (4) A = ambient temperature; L = liquid (fuel) temperature.

APPENDIX I
DRUM CHARGING/SPARKING TESTS
ALUMINUM MESH

TABLE I.1
DRUM CHARGING/SPARKING TESTS - ALUMINUM MESH
Test Fuel: Jet A (Clay treated) (Cu = .98 PS/m @ -1°C)

Run No.	Element Set	Flow Rate $\text{m}^3/\text{s} \times 10^{-3}$	Fuel Test Inlet: Piccolo #3	Fuel Charge(1)	Inlet Charge(2)	Drum Charge(3)	Total No.	$\frac{\text{Temp } ^\circ\text{C}(4)}{\text{A } \text{L}}$
				Density $\mu\text{C}/\text{m}^3$	Density $\mu\text{C}/\text{m}^3$	Strength KV/m	Radio Disch. Signals	
700	4	3.66	-410	-410	-	-6	-	$\frac{-2}{-1}$
			Conductivity Check = 1.84 @ -1°C					
701	4	3.66	-301	-328	-	-20	-	-1.5
702	4	3.78	-	-16	-	-5	-	-1.5
			Removed Piccolo Inlet - Installed High Velocity E11					-0.5
703	4	3.34	-359	-359	-	-130	-	-0.5
704	4	3.34	-270	-270	-	-200	-	0
705	4	3.34	-239	-270	-	-200	-	+0.5
706	4	3.34	-	-18	-	-180	-	1.5
			Conductivity Check = 1.6 @ 2°C					0

- (1) Fuel charge represents current density measured from the filter but of opposite polarity. Where the value is blank, the filter was bypassed.
- (2) All current readings were made about 8 seconds after flow started.
- (3) Field Strength observed at about 90% full, when fuel reached the top of the aluminum mesh.
- (4) A = ambient temperature; L = liquid (fuel) temperature.

TABLE I.2
DRUM CHARGING/SPARKING TESTS - ALUMINUM MESH
Test Fuel: Jet A (Clay treated) ($Cu = 1.6 \mu S/m @ 2^\circ C$)

Run No.	Element Set	Flow Rate $m^3/s \times 10^{-3}$	Fuel Test Inlet: High Velocity Ell	Fuel Charge (1)	Inlet Charge (2)	Drum Charge (2)	Field (3) Strength	Total No. Radio Disch. Signals	Remarks $\frac{Temp. ^\circ C(4)}{A \quad L}$
				Density $\mu C/m^3$	Density $\mu C/m^3$	Density $\mu C/m^3$	KV/m		
Removed Explosafe From Drum - Empty Drum Runs for Comparison									
707	4	3.34	-329	-144	-135	-500	6(5)	0	2
708	4	3.34	-240	-270	-200	6	0.5	2	
709	4	3.34	-240	-270	↑	-500	7	0.5	2
710	4	3.34	-	-	Inlet	Splashing	5	0.5	2
711	4	1.89	-	-	Touching	-3.9	-	0.5	1.5
712	4	1.89	-	-	Drum	-11	-	0.5	3
713	4	1.89	-317	-26	-260	-200	-	0.5	4
714	4	1.89	-260	-26	-260	-200	-	0.5	5
Conductivity Check = 1.72 @ 5°C									
Installed Piccolo #3 (5 m/s velocity)									
715	4	3.66	-219	-49	-137	-150	2	0.5	-2.5
716	4	3.66	-164	-33	-109	-150	-	1	-2
717	4	3.78	-	+5.3	-13.2	-26	-	1	-1
718	4	3.78	-	+4.8	-10.6	-20	-	1.5	-0.5
Conductivity Check = 2.07 @ 0°C									

- (1) Fuel charge represents current density measured from the filter but of opposite polarity. Where the value is blank, the filter was bypassed.
- (2) All current readings were made about 8 seconds after flow started.
- (3) Field Strength observed at about 90% full, when fuel reached the top of the aluminum mesh. The field meter used for this study was limited in the maximum value it could sense (500 KV/m). Thus, a reading of 500 KV/m could indicate that the field strength was 500 KV/m or more.
- (4) A = ambient temperature; L = liquid (fuel) temperature.
- (5) Aluminum chips which broke off from the main mesh body were left behind upon removal. These acted as unbonded charge collectors floating in the tank.

AD-A061 450

EXXON RESEARCH AND ENGINEERING CO LINDEN N J
STATIC ELECTRICITY HAZARDS IN AIRCRAFT FUEL SYSTEMS.(U)
AUG 78 W G DUKEK, J M FERRARO, W F TAYLOR F33615-77-C-2046
EXXON/GRUS.1PEB.78 AFAPL-TR-78-56 NL

F/G 21/4

UNCLASSIFIED

3 OF 3

AD
A061450



END
DATE
FILED
1-79
DDC

APPENDIX J
BLADDER CELL TESTS
BASE CASE

(PRECEDING PAGE BLANK)

TABLE J.1(1)
BLADDER CELL TESTS - BASE CASE

Run No.	Filter Set No.	ASA-3 Conc. (ppm)	C.U. $\mu\text{S}/\text{m}^{\circ}\text{C}$	Fuel (2) C.D. $\mu\text{C}/\text{m}^3$	Inlet (3) C.D. $\mu\text{C}/\text{m}^3$	Field (4) Strength KV/m	No. of Radio Discharge Signals	
							Inlet	Field
1000	#4	-	2.4/2	-437	-82	-301	-100	-
1001	#4	-		-273	-55	-219	-100	-
1002	#4	-		-	8	-16	-12	-
1003	#4	-	1.35/7	-396	-	-396	-500	8
1004	#4	-		-273	-41	-219	-500	-
1005	#4	-		-	8	-16	-28	1
1006	#4	-		-273	-41	-219	-500	1
1007	#4	-	1.52/2	-296	-38	-191	-500	2
1008	#4	-		-219	-33	-164	-500	-
1009	#4	-		-	10	-16	-23	-
1010	#4	-		-232	-36	-164	-500	3
1011	#4	-		-383	-41	-328	-500	3
1012	#4	-		-	11	-24	-28	-
1013	#4	-		-	1	-8	-23	-

(1) All tests at maximum flow rates, .00366 m^3/s for piccolo inlets, .00347 m^3/s for high velocity inlets.

(2) Fuel charge represents the current density measured from the filter but of opposite polarity. Where the value is blank, the filter was bypassed.

(3) All current readings were made about 8 seconds after flow started.

(4) Field Strength observed at about 90% full. The field meter used for this study was limited in the maximum value it could sense (500 KV/m). Thus, a reading of 500 KV/m could indicate that the field strength was 500 KV/m or more.

APPENDIX K
BLADDER CELL TESTS
RED FOAM

TABLE K.1(1)

BLADDER CELL TESTS
RED FOAM

Run No.	Filter Set No.	ASA-3 Conc. (ppm)	C.U. PS/m/ $^{\circ}$ C	Fuel (2)		Inlet (3)		Drum (3)		Field (4)		No. of Radio Discharge Signals	Inlet
				C.D. μ C/m ³	μ C/m ³	C.D. μ C/m ³	μ C/m ³	C.D. μ C/m ³	μ C/m ³	C.D. μ C/m ³	μ C/m ³		
2000	#5		3.2/11	-71	-6	-60	-53	-	-	-	-	PIC 4	
2001				-137	-11	-123	-180	-	-	-	-	PIC 4	
2002	New Fuel		1.35/6.5	-191	-36	-150	-150	-	-	-	-	PIC 4	
2003				-232	-38	-161	-180	-	-	-	-	PIC 4	
2004	#4			-	13	-21	-150	-	-	-	-	PIC 4	
2005	#4			-2049	-464	-1093	-250	5	-	-	-	PIC 4	
2006	#4			-1175	-273	-546	-250	1	-	-	-	PIC 4	
2007	#4			-798	-246	-437	-250	-	-	-	-	PIC 4	
2008	#4			-1441	-127	-865	-500	126	-	-	-	HI-VEL	
2009	#4			-865	-58	-634	-500	46	-	-	-	HI-VEL	
2010	#4			-865	-	-692	-250	40	(Visual)	-	-	HI-VEL	
2011	#4			-865	-43	-576	-300	-	-	-	-	HI-VEL	
2012	#4			-865	-	-548	-300	1	-	-	-	HI-VEL	
2013	#4		3.3/11	-1557	-191	-519	-170	-	-	-	-	PIC 2	
2014	#4			-1011	-164	-396	-200	-	-	-	-	PIC 2	
2015	#4			-	225	-32	-180	-	-	-	-	PIC 2	
2016	#4			-929	-137	-355	-200	-	-	-	-	PIC 2	
2017	#4			-861	-	-464	-200	-	-	-	-	PIC 2	
2018	#4		4.7/6.5	-1148	-123	-355	-130	-	-	-	-	PIC 2	
2019	#4		6.8/8	-874	-137	-273	-70	-	-	-	-	PIC 2	
2020	#4			-	4	27	-60	-	-	-	-	HI-VEL	
2021	#4			-1093	-164	-437	-220	-	-	-	-	HI-VEL	
2022	#4			-	106	-19	-180	-	-	-	-	HI-VEL	
2023	#4			-930	-137	-342	-220	-	-	-	-	HI-VEL	
2024	#4		7.3/9.5	-	-	16	-16	-	-	-	-	HI-VEL	
2025	#4			-588	-	-202	-27	-	-	-	-	HI-VEL	
2026	#4			-618	-	-	-	1	-	-	-	HI-VEL	
2027	#2			-500	-	-101	-18	6	-	-	-	HI-VEL	
2028	#2			-367	-	-95	-18	8	-	-	-	HI-VEL	

TABLE K.1(1) (continued)

BLADDER CELL TESTS
RED FOAM

Filter Set No.	ASA-3 Conc. (ppm)	C.U. ps/m/ $^{\circ}$ C	Fuel (2) C.D. μ C/m 3	Inlet (3) C.D. μ C/m 3	Drum (3) C.D. μ C/m 3	Field (4) Strength KV/m	No. of Radio Discharge Signals	Inlet
Run No.	.0115			-331	-	-86	-18	1.8
Scope Testing	#2	9.6/13	-317	-	-86	-18	5	HI-VEL
Stopped	#2		-529	-	-	-18	-	HI-VEL
2029	#2		-353	-	-82	-19	-	HI-VEL
2030	#2		-853	-	-97	-25	-	HI-VEL
2031	#2		-911	-	-191	-25	-	HI-VEL
2032	#6		-1118	-	-	-64	-	HI-VEL
2033	#6		-676	-	-317	-54	-	HI-VEL
2034	#6		-411	-	-191	-37	-	PIC 2
2035	#6		-355	-	-178	-60	-	PIC 2
2036	#6		-273	-41	-109	-28	-	PIC 2
2037	#2	6.8/13.5	-1230	-164	-328	-28	-	PIC 2
2038	#2	.023	-833	-123	-287	-30	-	PIC 2
2039	#2		-519	-	-355	-3.6	-	PIC 2
2040	#6	.0345	8.7/16.5	-492	-	-312	-3.6	HI-VEL
2041	#6		-451	-	-295	-3.6	1	HI-VEL
2042	#6		-345	-	-259	-4	4	HI-VEL
2043	#6		-605	-	-547	-4	-	HI-VEL
2044	#6		-628	-	-385	-4	2	HI-VEL
2045	#7		-1153	-	-547	-40	-	HI-VEL
2046	#7		-1008	-	-461	-30	-	HI-VEL
2047	#7		-691	-	-317	-25	-	HI-VEL
2048	#7	12.4/10.5 Clay Trt'd \rightarrow 6.8/15 (1/3 Volume)	-738	-101	-219	-45	-	PIC-2
2049	#7		-792	-104	-232	-50	-	HI-VEL
2050	#7		-	25	-38	-41	-	PIC-2
2051	#7	9.6/15.5	-634	-81	-173	-30	-	HI-VEL
2052	#7		-605	-67	-144	-20	2	HI-VEL
2053	#7		-	5	-14	-17	-	HI-VEL
2054	#7		-	-	-	-	-	HI-VEL
2055	#7		-	-	-	-	-	HI-VEL
2056	#7		-634	-90	-187	-30	-	HI-VEL
2057	#7		-778	-81	-58	-2.5	-	HI-VEL
2058	#7	.184	33.8/13	-1153	-81	-52	-3.0	HI-VEL
2059	#7		-	0	-9	-.6	-	HI-VEL
2060	#7							

Footnotes to Table K.1:

- (1) All tests at maximum flow rates, .00366 m^3/s for piccolo inlets, .00347 m^3/s for high velocity inlet.
- (2) Fuel charge represents the current density measured from the filter but of opposite polarity. Where the value is blank, the filter was bypassed.
- (3) All current readings were made about 8 seconds after flow started.
- (4) Field Strength observed at about 90% full, when fuel reached the top of the foam.

APPENDIX L
BLADDER CELL TESTS
BLUE FOAM

TABLE L.1(1)
BLADDER CELL TESTS
BLUE FOAM

Run No.	Filter Set No.	ASA-3 Conc. (ppm)	C.U. pS/m/°C	Fuel(2) C.D. $\mu\text{C}/\text{m}^3$	Inlet(3) C.D. $\mu\text{C}/\text{m}^3$	Drum(3) O.D. $\mu\text{C}/\text{m}^3$	Field(4) Strength KV/m		No. of Radio Discharge Signals	Inlet
							Fuel(2) $\mu\text{C}/\text{m}^3$	Inlet(3) $\mu\text{C}/\text{m}^3$		
3000	#4	-	4.4/11	-1639	-410	-738	-500	-500	8	PIC 4
3001	#4			-1092	-167	-505	-500	-500	-	PIC 4
3002	#4			-738	-109	-383	-500	-500	1	PIC 4
3003	#4			-	55	-55	-500	-500	-	PIC 4
3004	#4			3.3/11	-738	-87	-355	-500	2	PIC 4
3005	#4			-656	-137	-219	-500	-500	16	PIC 2
3006	#4			-656	-137	-191	-500	-500	24	PIC 2
3007	#4			-	-27	21	-500	-500	30	PIC 2
3008	#4			-	-29	32	-500	-500	29	PIC 2
3009	#4	.0115	6.8/8	-847	-109	-300	-500	-500	4	PIC 2
3010	#4			-	16	-19	-500	-500	1	PIC 2
3011	#4			6.8/8	-1441	-	-216	-250	176	HI-VEL
3012	#4				-865	-	-216	+500	122	HI-VEL
3013	#4				-778	-	-	+500	159	HI-VEL
3014	#4				-800	-	-178	-270	4	HI-VEL
3015	#4				-714	-	-238	-300	99	HI-VEL
3016	#4				-635	-	-198	-500	112	HI-VEL
3017	#4				-575	-	-198	-500	90	HI-VEL
3018	#4				-456	-	-159	-220	89	HI-VEL
3019	#4				-496	-	-159	-220	97	HI-VEL
3020	#4				-456	-	-159	-220	98	HI-VEL
3021	#4				-	-	-79	-275	99	HI-VEL
3022	#4				-	-	-198	-220	102	HI-VEL
3023	#4				-	-	-115	-220	130	HI-VEL
3024	#6				-432	-	-115	-150	-	PIC 2
3025	#6				-683	-85	-232	-300	-	PIC 2
3026	#4				-738	-78	-232	-300	-	PIC 2
3027	#4				-1366	-96	-191	-500	1	PIC 2
3028	#4				-710	-71	-164	-500	-	PIC 2
					(Clay Trt'd)	2.56/18	-847	-328	51	PIC 2

TABLE L.1(1) (continued)
 BLADDER CELL TESTS
 BLUE FOAM

Run No.	Filter Set No.	ASA-3 Conc. (ppm)	C.V. pS/m ³	Fuel (2) C.D. μ C/m ³	Inlet (3) C.D. μ C/m ³	Drum (3) O.D. μ C/m ³	Field (4) Strength KV/m	No. of Radio Discharge Signals		Inlet
								189	6.8/13	
3029	#4	(Clay Trt'd) 2.56/18	-4.91	-	-246	-500	60	PIC 2		
3030	#4		-3.83	-	-191	-500	39	PIC 4		
3031	#4		-4.37	-	-204	-300	-	PIC 4		
3032	#6		-11.74	-	-404	-500	15	PIC 4		
3033	#6		-7.65	-	-355	-500	35	PIC 4		
3034	#6		-6.01	-68	-	-500	1	PIC 4		
3035	#6		-5.19	-	-300	-500	1	PIC 4		
3036	#6		-6.01	-	-410	-7	32	PIC 4		
3037	#6		-4.78	-	-328	-7	22	PIC 4		
Add CI/AIA	3039	#7	-6.34	-	-273	-120	2	HI-VEL		
	3040	#7	-5.18	-	-216	-120	-	HI-VEL		
	3041	#7	-17.29	-	-346	-130	1	HI-VEL		
	3042	#7	-13.25	-	-374	-150	22	HI-VEL		
	3043	#3	-10.06	-	-317	-150	21	HI-VEL		
	3044	#3	-2.30	-	-57	-130	32	HI-VEL		
	3045	#3	-	-	-29	-150	56	HI-VEL		
	3046	#3	-	-	-29	-150	111	HI-VEL		
	3047	#3	-	-	-17	-150	92	HI-VEL		
Time	3048	#3	-	-	-35	-150	62	HI-VEL		
Exposure Photos Taken	3049	#3	-	-	-12	-180	64	HI-VEL		
	3050	#3	-	-	0	-180	92	HI-VEL		
	3051	#3	9.9/21	+173	+173	-180	103	HI-VEL		
	3052	#3	-	+86	-51	-180	132	HI-VEL		
	3053	#3	-	-	-17	-250	102	HI-VEL		
	3054	#3	-	+123	-	-230	1	PIC 2		
	3055	#7	-	-	-14	-230	-	PIC 2		
	3056	#7	-819	-	-240	-230	1	PIC 2		
	3057	#7	9.9/21	-710	-191	-250	2	PIC 2		
			-	-	-27	-250	-	PIC 2		
					19					

TABLE L.1(1) (continued)
 BLADDER CELL TESTS
 BLUE FOAM

Run No.	Filter Set No.	ASA-3		Fuel (2)		Inlet (3)		Field (4)		No. of Radio Discharge Signals	Inlet
		Conc. (ppm)	C.U. $\mu\text{S}/\text{m}^2/\text{°C}$	C.D. $\mu\text{C}/\text{m}^3$	D.O. $\mu\text{C}/\text{m}^3$	Drum (3) $\mu\text{C}/\text{m}^3$	Strength KV/m				
3058	#7	184	33.8/13	-1182	-75	-32	+60	105	HI-VEL		
3059	#7			-	29	-29	+100	143	HI-VEL		
3060		PENS NOT ON					+100	17	HI-VEL		
3061	#7			-922	-	-144	+120				
3062	#7		25.3/15.5	-874	-79	-72	+130	18	HI-VEL		
3063	#7			-929	-82	-30	-25				
3064	#7			-	22	-25	-20				
3065	#7			-847	68	-36	-25				
3066	#7			-956	-55	-55	-6				
3067	#7			-929	-66	-49	-6				
3068	#7			25.3/15.5	-	27	-27				
3069	#7			65/11	-683	-4	-19	-5			
3070	#7				-1913	-109	-41	-2			
3071	#7				-1093	-16	-14	-5			
3072	#7				-1230	-55	-22	-5			
3073	#7					11	-11	-4	2		
3074	#7						-11	-4	-		
3075	#7	.893	65/11	-			-11	-4	-		
3076	#7		126.7/11.5	-1148	96	-30	-3				
3077	#7			-1639	41	-27	-3				
3078	#7			-	16	-14	-2.6				
3079	#7			-1913	3	-3	-3				
3080	#7		126.7/11.5	-1913	-6	-22	-3.8				
3081	#7	1.15	180/7	-1093	25	-27	-4				
3082	#7			-1776	18	-27	-4				
3083	#7			-	19	-16	-1.5				
3084	#7		180/7	-	16	-11	-1.5				
3085	#7	1.53	250/11.5	-1366	-	-27	-1.5				
3086	#7			-1366	-	-25	-1.7				

TABLE L.1(1) (continued)
BLADDER CELL TESTS
BLUE FOAM

Run No.	Filter Set No.	ASA-3 Conc. (ppm)	C.U. PS/m/ $^{\circ}$ C	Fuel (2)		Inlet (3) C.D. μ C/m 3	Drum (3) O.D. μ C/m 3	Field (4) Strength KV/m	No. of Radio Discharge Signals	Inlet
				C.D. μ C/m 3	O.D. μ C/m 3					
3087	#7	1.53	250/11	-	14	-8	-0.9	-	PIC 2	
3088	#7	4 ppm	293	-1366	30	-33	-1.8	-	PIC 2	
3089	#7	GA 178		-683	30	-33	-1.5	-	PIC 2	
		+ ASA-3		-374	-3	-	-0.4	19	HI-VEL	
3090	#7			-	3	3	-0.4	-	HI-VEL	
3091	#7			-230	-	-	-0.3	1	HI-VEL	
3092	#7			-59	-	-	-0.3	1	HI-VEL	
3093	#1			-57	-	-	-0.4	-	HI-VEL	
3094	#1								HI-VEL	

(1) All tests at maximum flow rate, .00366 m 3 /s for piccolo inlets, .00347 m 3 /s for high velocity inlet.

(2) Fuel charge represents the current density measured from the filter but of opposite polarity. Where the value is blank, the filter was bypassed.

(3) All current readings were made about 8 seconds after flow started.

(4) Field Strength observed at about 90% full when fuel reached the top of the foam. The field meter used for this study was limited in the maximum value it could sense (500 KV/m). Thus, a reading of 500 KV/m could indicate that the field strength was 500 KV/m or more.

REFERENCES

1. "Generation and Dissipation of Electrostatic Charge During Aircraft Fueling - a Selected Literature Survey", CRC Report No. 466, May 1974, Coordinating Research Council, 30 Rockefeller Plaza, New York, New York 10020.
2. Leonard, J. T. and Affens, W. A., "Electrostatic Charging of JP-4 Fuel on Polyurethane Foam" NRL Report 8204, Naval Research Laboratory, Washington, D.C., March 1978.
3. Leonard, J. T. and Carhart, H. W., "Electrical Discharges from a Fuel Surface" 1967 Static Electrification Conference.
4. Gibson, N. and Lloyd, F. C., "Incendivity of Discharges from Electrostatically Charged Plastics", J. Appl. Phys. 1965, Vol. 6, page 1619.
5. Unpublished memorandum: Exxon Research and Engineering Company.
6. Dukek, W. G. and Bachman, K. C., "Static Electricity in Fueling of Superjets", Exxon Research and Engineering Company publication, January 1972.
7. "Electrostatic Charging in Foam-Filled Tanks," Shell International Chemical Company, Ltd., Shell Report No. TB/M/1, January 1978.
8. Huber, Peter W. and Sonin, A. A., "Theory for Electrical Charging in Liquid Hydrocarbon Filtration" Journal of Colloid and Interface Science, V61, No. 1, August 1977.